Aus dem Universitätsklinikum Münster
Institut für Molekulare Tumorbiologie
Direktoren: Univ.-Prof. Dr. Frank Rosenbauer,
Univ.-Prof. Dr. Michael Meisterernst

Characterisation of a putative Diffuse Large B-Cell Lymphoma-associated silencing element within the *NKIRAS1* gene

INAUGURAL – DISSERTATION
zur
Erlangung des doctor medicinae

der Medizinischen Fakultät
der Westfälischen Wilhelms-Universität Münster

vorgelegt von Brüstle, Johanna Kristin
aus Washington D.C., USA

Münster, 2020

Gedruckt mit Genehmigung der Medizinischen Fakultät der Westfälischen Wilhelms-Universität Münster

Dekan: Univ.-Prof. Dr. med. Frank Ulrich Müller
1. Berichterstatter: Univ.-Prof. Dr. Frank Rosenbauer
2. Berichterstatter: Univ.-Prof. Dr. Wolfgang Hartmann
Tag der mündlichen Prüfung: 05.11.2020

Aus dem Universitätsklinikum Münster
Institut für Molekulare Tumorbiologe
Direktoren: Univ.-Prof. Dr. Frank Rosenbauer,
Univ.-Prof. Dr. Michael Meisterernst
Referent: Univ.-Prof. Dr. Frank Rosenbauer
Korreferent: Univ.-Prof. Dr. Wolfgang Hartmann

Abstract

Characterisation of a putative Diffuse Large B-Cell Lymphoma-associated silencing element within the *NKIRAS1* gene

Brüstle, Johanna Kristin

Diffuse large B-cell lymphoma (DLBCL), the most common form of non-Hodgkin lymphoma, is a very aggressive type of tumour with a five-year survival rate of only 65 %. To further investigate the molecular pathogenesis of this malignant lymphoma, predicted regulatory elements that are commonly mutated in DLBCL patients were examined. Particular focus was put on a putative silencer element within the first intron of the *NKIRAS1* gene. *NKIRAS1* encodes κB-Ras1, an inhibitor of the NF-κB pathway, which is known to be highly important for DLBCL lymphomagenesis. Specifically, in activated B-cell (ABC) DLBCL cells multiple dysregulations of the NF-κB pathway have been described. Using a luciferase assay, a position-dependent silencing function of this putative silencer element could be confirmed. The negative regulatory effect was furthermore found to vary between different cell lines. Insertion of a single nucleotide polymorphism (SNP), repeatedly found within the putative silencer element in patients but also in healthy individuals showed no change in the silencing effect. In the germinal centre B-cell (GCB) DLBCL cell line OCI-ly1 a CRISPR-Cas9 mediated knockout of a 46 base pair segment within the putative silencer element had no effect on transcription levels of the two adjacent genes *NKIRAS1* and *RPL15* nor on cell proliferation, questioning thereby the silencer element's impact on the NF-κB pathway.
Taken together, these data identify a new silencing element within the first intron of *NKIRAS1.* Further studies are required to identify the target genes regulated by this silencer element and to evaluate its role in the pathogenesis of DLBCL.

Tag der mündlichen Prüfung: 05.11.2020

Declaration

Ich gebe hiermit die Erklärung ab, dass ich die Dissertation mit dem Titel “Characterisation of a putative Diffuse Large B-Cell Lymphoma-associated silencing element within the NKIRAS1 gene” im Institut für Molekulare Tumorbiologe unter der Anleitung von Univ.-Prof. Dr. Frank Rosenbauer

1. selbständig angefertigt,
2. nur unter Benutzung der im Literaturverzeichnis angegebenen Arbeiten angefertigt und sonst kein anderes gedrucktes oder ungedrucktes Material verwendet,
3. keine unerlaubte fremde Hilfe in Anspruch genommen,
4. sie weder in der gegenwärtigen noch in einer anderen Fassung einer in- oder ausländischen Fakultät als Dissertation, Semesterarbeit, Prüfungsarbeit, oder zur Erlangung eines akademischen Grades, vorgelegt habe.

Münster, 06.05.2020
Ort, Datum

J. Brasse
Name/Unterschrift

Abbreviations

°C	degree Celsius
3'	3-prime
3C	chromosome conformation capture
3D	three dimensional
4C	circular chromosome conformation capture
5'	5-prime
5C	chromosome conformation capture carbon copy
ABC	activated B-cell
AG	Arbeitsgruppe (working group)
AID	activation-induced cytidine deaminase
Amp	ampere
ANOVA	analysis of variance
AMP	adenosine monophosphate
ATAC-Seq	assay for transposase-accessible chromatin with high-throughput sequencing
ATG	adenine, thymine, guanine (start codon)
ATP	adenosine triphosphate
BAFF	B-cell activating factor
BCL2/6	B-cell lymphoma 2/6
BCR	B-cell receptor
BLIMP1	B-lymphocyte-induced maturation protein-1
bp	base pair
C	cytosine
c-IAP1/2	cellular inhibitor of apoptosis protein 1/2
C-terminal	carboxy-terminal
CARD11	caspase recruitment domain family member 11
Cas9	CRISPR-associated endonuclease 9
CBM	complex of CARD11/BCL10/MALT1
CD...	cluster of differentiation...
cDNA	complementary deoxyribonucleic acid
ChIP-Seq	chromatin immunoprecipitation DNA sequencing
Cis	lat: cis (on this site)
cm	centimetre
CO_2	carbon dioxide
CRE-Seq	cis-regulatory element analysis by sequencing
CREB	cyclic AMP response element-binding protein
CRISPR	clustered regularly interspaced short palindromic repeats
crRNA	CRISPR RNA
CTCF	11-zinc finger protein
CTG	CellTiter-Glo
DLBCL	diffuse large B-cell lymphoma
DMSO	dimethyl sulfoxide
DNA	deoxyribonucleic acid
DNAse I	deoxyribonuclease 1

DPBS	Dulbecco’s phosphate-buffered saline
E coli	Escherichia coli
e.g.	exempli gratia (for example)
EDTA	ethylenediaminetetraacetic acid
ESMO	European Society for Medical Oncology
et al.	et alii (and others)
ETS	E26 transformation specific
FACS	fluorescence-activated cell sorting
FBS	fetal bovine serum
FDG	fluorodeoxyglucose
FDG-PET/CT	fluorodeoxyglucose-positron emission tomography/computed tomography
FLIP	FLICE-like inhibitory protein
fwd	forward
g	acceleration of gravity
G1-phase	gap-1 phase
GAPDH	glyceraldehyde-3-phosphate dehydrogenase
GCB	germinal centre B-cell
gDNA	genomic DNA
GDP	guanosine diphosphate
GFP	green fluorescent protein
GTP	guanosine triphosphate
GTPase	guanosine triphosphatase
H3K27ac	acetylation of lysine 27 on histone 3
H3K27me3	trimethylation of lysine 27 on histone 3
H3K4me1	methylation of lysine 4 on histone 3
H3K4me3	trimethylation of lysine 4 on histone 3
H3K9ac	acetylation of lysine 9 on histone 3
HBL-1	human diffuse large B-cell lymphoma
HCV	hepatitis c virus
HiC	high-throughput chromosome conformation capture
HOXB13	homeobox B13
HSP90	heat shock protein 90
i.e.	id est (that is)
IgH	immunoglobulin heavy chain
IKK	inhibitor of κB kinases
IL-1R	interleukin1 receptor
IMDM	iscove's modified Dulbecco’s medium
IPI	international prognostic index
IRAK1/4	interleukin-1 receptor-associated kinase 1/4
IRF4	interferon regulatory factor 4
IκB	inhibitor of κB
JAK/STAT3	januskinase/signal transducers and activators of transcription
kb	kilobase
KCl	potassium chloride
Ki67	Kiel-67 (proliferation marker)
KLD	kinase, ligation, DpnI

l	litre
LB	lysogeny broth
LDH	lactate dehydrogenase
MALT1	mucosa-associated lymphoid tissue lymphoma translocation protein 1
mAmp	milliampere
mg	milligram
Mg^{2+}	magnesium
min	minute
miRNA	microRNA
ml	millilitre
mM	millimolar
mm	millimetre
mRNA	messenger ribonucleic acid
MYC	v-myc avian myelocytomatosis viral oncogene homolog
MYD88	myeloid differentiation primary response 88
n	size of a subsample
N2	nitrogen
NEMO	NF-kappa-B essential modulator
NFKBIZ	NFKB inhibitor zeta
NFκB	nuclear factor 'kappa-light-chain-enhancer' of activated B-cells
ng	nanogram
NHL	non-Hodgkin lymphoma
NIK	NFκB inducing kinase
NKIRAS	NF-kappa-B inhibitor-interacting Ras-like protein
NKX3.1	homeobox protein Nkx-3.1
nl	nanolitre
nm	nanometre
NP-40	nonyl phenoxypolyethoxylethanol 40
o/n	overnight
O_2	oxygen
OCI-ly1	Ontario Cancer Institute, cell line ly1
OCI-ly3	Ontario Cancer Institute, cell line ly3
ODN	oligodeoxynucleotides
oligos	oligonucleotides
ORF	open reading frame
P	p-value (statistical probability)
PAM	protospacer adjacent motif
PAMPS	pathogen-associated molecular patterns
PAX5	paired box 5
PBS	phosphate-buffered saline
PCR	polymerase chain reaction
pH	potentia Hydrogenii
Poly-A	polyadenylation
PPi	pyrophosphate
pRL-TK	HSV-thymidine kinase promoter
PTEN	phosphatase and tensin homolog

PTPN6/SHP1	tyrosine-protein phosphatase non-receptor type 6/ Src homology region 2 domain-containing phosphatase-1
qPCR	quantitative polymerase chain reaction
R-CHOP	rituximab, cyclophosphamide, hydroxydaunorubicin, oncovin, prednisolone
Ras	rat sarcoma
Rel	oncogene Rel, avian reticuloendotheliosis
RelA/B	v-Rel avian reticuloendotheliosis viral oncogene homolog A/B
rev	reverse
RFX6	regulatory factor X6
RNA	ribonucleic acid
RPL15	ribosomal protein L15
rpm	rotations per minute
RPMI	Roswell Park Memorial Institute
RT-qPCR	reverse transcriptase quantitative polymerase chain reaction
SCFßTRCP	Skp1-Cullin1-F-box protein ubiquitin ligase complex with beta-transducin repeat containing E3 ubiquitin protein ligase
SCP1	S. cerevisiae CalPonin
SD	standard deviation
SDHD	succinate dehydrogenase
SG	suicide gene
sgRNA	single-guide RNA
SNP	single nucleotide polymorphism
SNV	single nucleotide variant
SOB	super optimal broth
STARR-Seq	self-transcribing active regulatory region sequencing
STAT3	signal transducer and activator of transcription 3
SW	square wave
SYBR	synergy brands
T	thymine
TAD	topologically associated domain
TAE	TRIS-acetate-EDTA
TCR	T-cell receptor
TERT1	telomerase reverse transcriptase
TFD	transcription factor decoy
TLR	toll-like receptor
Tn5	transposase 5
TNFR	tumour necrosis factor receptor
TOPMed	Trans-Omics for Precision Medicine program
TP53	tumour protein p53
tracrRNA	trans-activating crRNA
TRAF2/TRAF3	TNF receptor associated factor 2/3
Tris	Tris(hydroxymethyl)-aminomethane
UV	ultraviolet
V	volt
W	watt
WHO	World Health Organisation

κB	'kappa-light-chain-enhancer' of activated B-cells
µl	microlitre
µM	micromolar

Table of contents

1 Introduction

1.1 Diffuse large B-cell lymphoma

Diffuse large B-cell lymphoma (DLBCL) is the most common form of non-Hodgkin lymphoma (NHL), representing 25 %–35 % of all adult NHLs in developed countries (112). It is a malignant, fast growing and very aggressive type of lymphoma with an incidence of 3.8/100.000 newly diagnosed cases in Europe in 2010 (117) and a mortality of 1.8/100.000 (U.S., 2012 – 2016, data from the National Cancer Institute (78)). Histopathologically, DLBCL is characterised by a diffuse growth pattern and large B lymphoid cells with nuclei that are at least twice as large as common lymphocyte nuclei (112). Without treatment the disease is lethal, and even under treatment the 5-year overall survival rate is around 65 % (112). The average age of DLBCL patients is around 70 years with men being slightly more affected than women (112). Risk factors of DLBCL include immunodeficiency due to an autoimmune disease, a HCV infection, a family history of lymphoma or a high body-mass index in younger years (75).

1.1.1 Diagnosis and staging

The best method of diagnosis is an excisional biopsy followed by flow cytometry and/or immunocytochemical analysis of the expression of indicative markers such as CD20, CD79A, BCL6 (B-cell lymphoma 6), CD10, MYC (v-myc avian myelocytomatosis viral oncogene homolog), BCL2 (B-cell lymphoma 2), Ki67, IRF4 (interferon regulatory factor 4), Cyclin D1, CD5 and CD23 (117). Further transcriptome analyses can be applied to detect the cell of origin, which represents a considerable prognostic factor (117). Based on the resulting gene expression signature, DLBCL can be subdivided into three major subvariants, differing in pathogenesis, response to chemotherapy and prognosis (3). Depending on the cell of origin, germinal centre B-cell (GCB), activated B-cell (ABC) lymphomas and a type 3 (“primary mediastinal B-cell type”) lymphoma are distinguished (84,100), while 10 – 15 % of all DLBCL cases still cannot be classified (112).

Apart from the molecular subvariants (GCB, ABC), the WHO (World Health Organisation) classification uses morphological features (centroblastic, immunoblastic, anaplastic, other variants) and immunophenotypic characteristics to further characterize and subdivide DLBCL forms (112). Other large B-cell lymphomas, such as DLBCL associated with chronic inflammation or the primary mediastinal large B-cell lymphoma, represent yet a different, more specific category (112).

The GCB subtype is associated with better overall survival and longer event-free survival (70 – 80 % five-year progression free survival under R-CHOP chemotherapy |rituximab, cyclophosphamide, hydroxydaunorubicin, oncovin, prednisolone] (112)) (3), but still has about 20 % relapse probability (84). 25 % of these relapses represent so called double-hit DLBCLs or high-grade B-cell lymphomas, where due to a translocation in the respective genes MYC and BCL2/6 are overexpressed and prognosis is very poor (84). ABC lymphomas are a lot more difficult to treat and the five-year progression free survival rate under R-CHOP is 40 – 50 % (112). It is therefore highly recommended to perform a subtype analysis via gene expression or immucytochemistry directly at diagnosis in order to enable a subtype-specific therapy (112).

For staging, the enrichment of fluorodeoxyglucose (FDG) in tumour cells measured via FDG-PET/CT is the gold standard to detect DLBCL foci and allows tumour grading via the Ann Arbor Classification (117). This classification differentiates between the number of tumour containing lymph nodes or extranodal sites and their localisation relative to the diaphragm (102). Prognosis is individually calculated with the international prognostic index (IPI), comprising age, LDH levels (lactate dehydrogenase), tumour stage, extranodal lesions and performance status (117), or the age-adjusted IPI, allowing a prognosis independent of the patient's age (31). On top of that, the WHO states that a tumour size > 10cm, male sex, vitamin D deficiency, low body mass index, concordant bone marrow infiltration, low absolute lymphocyte count and other laboratory parameters are known to correlate with poor prognosis (112).

1.1.2 Clinical manifestation

Most patients become symptomatic with a fast growing tumour within one or more lymph nodes. However, 40 % of all cases show an extranodal manifestation right from the beginning, for example in bone marrow or the gastrointestinal tract. (102,112) Patients are mainly asymptomatic, however, they can show B symptoms (namely fever, night sweat and involuntary weight loss) or symptoms due to the expansion of the tumour and consequent compression of the neighbouring tissue (112). In case of bone marrow infiltration (10–25 % of all patients), other typical symptoms are anaemia, thrombocytopenia as well as lymphopenia (108,112).

1.1.3 Pathogenesis and genetic drivers

DLBCL is known for its large genetic and biological heterogeneity. Most DLBCLs originate de novo, but they can also arise from other less malignant lymphomas. (112) Since treatment and outcome are highly dependent on the presence of the individual subvariant (3), the ontogeny and characteristics of ABC and GCB DLBCL will be ascribed particular attention in the following paragraphs. Even though both subvariants may share common cancerogenic mutations, they also show distinct genetic mutations, characteristic of only one specific subvariant. More than 30

different mutations, translocations and copy number aberrations are described in literature with the most prominent ones discussed below. (112)

The *GCB lymphoma* arises from neoplastic B-cells within the germinal centre. As overviewed by Lenz et al., the germinal centre is a structure within lymphoid nodes, comprising lymphoblasts in an inner dark zone and mature lymphocytes in the outer light zone, surrounded by follicular dendritic cells and antigen-specific T-cells. In a germinal centre reaction mature B-lymphocytes in the light zone encounter antigen presenting follicular dendritic cells, recognize and process the antigen and then expose it to T-cells in close proximity. After this antigen contact they either turn into antibody producing plasmablasts, become memory B-cells or return to be lymphoblasts. In order to traverse those developments, different gene alterations need to take place, such as somatic hypermutation in heavy chain immunoglobulin genes for optimizing the antibody's affinity for antigens or class switch recombination in order to produce different immunoglobulins. Both reactions, mainly triggered by an enzyme called AID (activation-induced cytidine deaminase), are needed for a functional immune response. However, their occurrence can at the same time promote lymphoma development as DNA damage is taking place at high frequency and introduced double-strand breaks can result in, for example, *MYC-IgH* translocations. (66)
GCB lymphomas show an overexpression of genes characteristic of germinal centre B-cells, such as *BCL6*, a transcriptional repressor that, among other effects, inhibits differentiation into plasma cells and is also deregulated in ABC lymphomas (3,66). Somatic mutations in the variable heavy chain of immunoglobulins, which are an on-going phenomenon in germinal centres to produce more specific antibodies, are at a high rate present in GCB but not ABC lymphomas (68). Other distinct mutations often found in GCB lymphomas are *t(14;18)* translocations, resulting in an overexpression of the anti-apoptotic *BCL2* gene, *PTEN* (phosphatase and tensin homolog) deletions or *TP53* (tumour protein p53) mutations (66).

The *ABC Lymphoma* on the other hand occurs when B-cells degenerate after activation (66). The ABC signature is to some extent similar to the signature of activated B-cells in the peripheral blood (3). Genes included in this signature are, for example, *IRF4*, an oncogene triggering proliferation and responsible for conversion into plasma cells, and FLIP (FLICE-like inhibitory protein), an inhibitor of apoptosis. High expression of BCL2 due to upregulated gene expression and the amplification of its locus, too, is typical for ABC lymphomas. (3,66) Furthermore, high levels of AID, potentially resulting in an elevated mutation rate, are present in ABC cells (66). However, the main transformation found within those cells is a constitutively active NF-κB

pathway (nuclear factor 'kappa-light-chain-enhancer' of activated B-cells pathway), which will be discussed in more detail below (25).

1.1.4 NF-κB pathway and DLBCL

The NF-κB pathway comprises five different transcription factors of the family of nuclear factor kappaB. Induced by different signalling pathways, they regulate transcription of genes important for cell proliferation and apoptosis, immune, inflammatory and stress responses, immunoreceptors and acute phase proteins. Amongst others, their target proteins are cell-cycle regulatory proteins like C-MYC, anti-apoptotic proteins such as BCL2, interleukins and other inflammatory and immunoregulatory proteins, signalling molecules and drug efflux pumps. (41,63,88)

Building heterodimers, the NF-κB transcription factors p65 (= RelA), p105/p50 (NF-κB1), p100/p52 (NF-κB2), RelB and c-Rel are omnipresent in most cells. With a common conserved Rel homology domain, the transcription factors can dimerise, translocate into the nucleus and bind to specific genomic regions. In the cytoplasm, however, they are bound and thereby inactivated by different inhibitors of κB (IκBα, β and ε). Through activating signals, the inhibitor of κB kinases (IKK) complex phosphorylates IκBs at conserved serine residues, which then leads to ubiquitinylation and proteosomal degradation of the IκBs (Figure 1.1). The transcription factors previously bound by the IκBs are now free to translocate into the nucleus and to start transcription. (63)

Regarding activation of NF-κB regulated transcription, two main pathways are described: the canonical and the non-canonical pathway. In the canonical pathway, the IKK complex comprises three subunits: the catalytic IKKα and β, and the regulatory subunit IKKγ, also called NEMO (NF-kappa-B essential modulator), that acts as a scaffold for the IKK complex (Figure 1.1). (73) The IKK complex is activated via PAMPS (pathogen-associated molecular patterns), inflammatory cytokines and immune stimulatory signals binding to tumour necrosis factor receptors (TNFR), B- and T-cell receptors (BCR, TCR), toll-like receptors (TLR) or interleukin receptors (IL-1R), but also by chemicals or radiation (63). The transcription factors best explored within this pathway are p50 (processed from p105) and p65/RelA, both of which are bound by IκBα until activation and can form heterodimers such as p50/RelA or p50/c-Rel (86). In a self-regulating negative feedback loop, IκBα, which is resynthesized as a NF-κB target gene, can transfer into the nucleus, separate NF-κB transcription factors from the DNA and carry them back into the cytoplasm (73). As the activation of NF-κB itself enhances IκBα transcription, it thus regulates its own activity (86). IκBβ is similar to IκBα, but exhibits slower kinetics and has an additional regulatory function in the nucleus, where it targets NF-κB complexes that are already interacting with the DNA. Its degradation and synthesis are stronger regulated by stimuli, and IκBβ deletion does not

significantly influence the kinetics of the NF-κB pathway. (86) In general, the canonical pathway is responsible for a fast, but not long-lasting response (63).

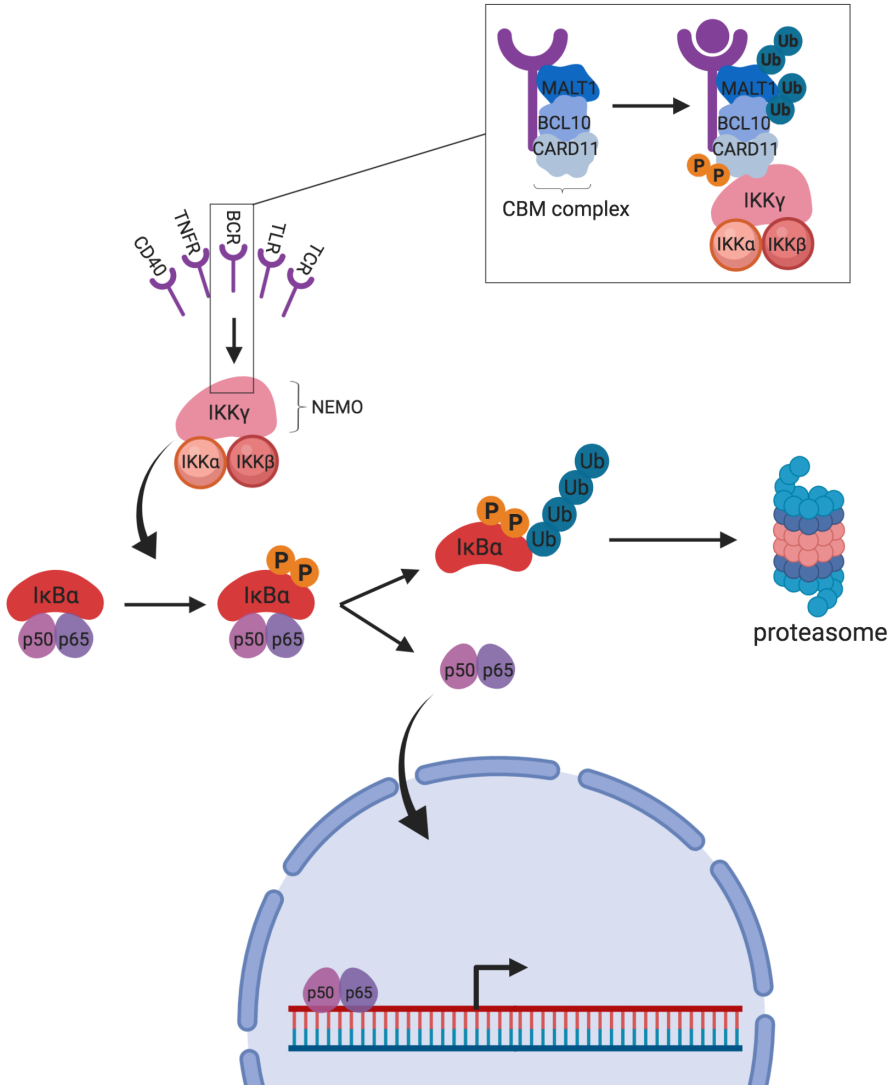

Figure 1.1: The canonical NF-κB signalling pathway

Upon binding of different stimuli to receptors such as the CD40-receptor, TNFR, TLR, BCR and TCR, the CBM complex, consisting of CARD11 (caspase recruitment domain family member 11), BCL10 and MALT1 (mucosa-associated lymphoid tissue lymphoma translocation protein 1) acts as a scaffold and transfers the activation signal to IKKγ. IKKα and β are activated and phosphorylate IκBα, which leads to its ubiquitinylation and subsequent proteosomal degradation. NFκB transcription factors such as p50 and p65 are released and translocate into the nucleus to enhance transcription. (Figure adapted from (88,119).)

In the non-canonical pathway, NF-κB inducing kinase (NIK) and IKKα form a complex (Figure 1.2). NIK in an unstimulated status is continuously degraded via the c-IAP1/2 (cellular inhibitor of apoptosis protein 1/2) ligases, which bind to NIK via TRAF2/TRAF3 (TNF receptor associated factor 2/3). This TRAF2/3-cIAP E3 ligase complex first needs to be degraded before allowing the

then stabilized NIK to activate IKKα through phosphorylation – a process induced after stimuli such as B-cell activating factor (BAFF), lymphotoxin β and CD40 ligands bind to their respective receptors. (63,73) IKKα can then process p100 to p52, which builds a transcriptionally active NF-κB dimer together with RelB (86). The non-canonical pathway is a lot slower and more preserving than the canonical pathway and is required for a number of homeostatic processes including B-cell survival (63,73).

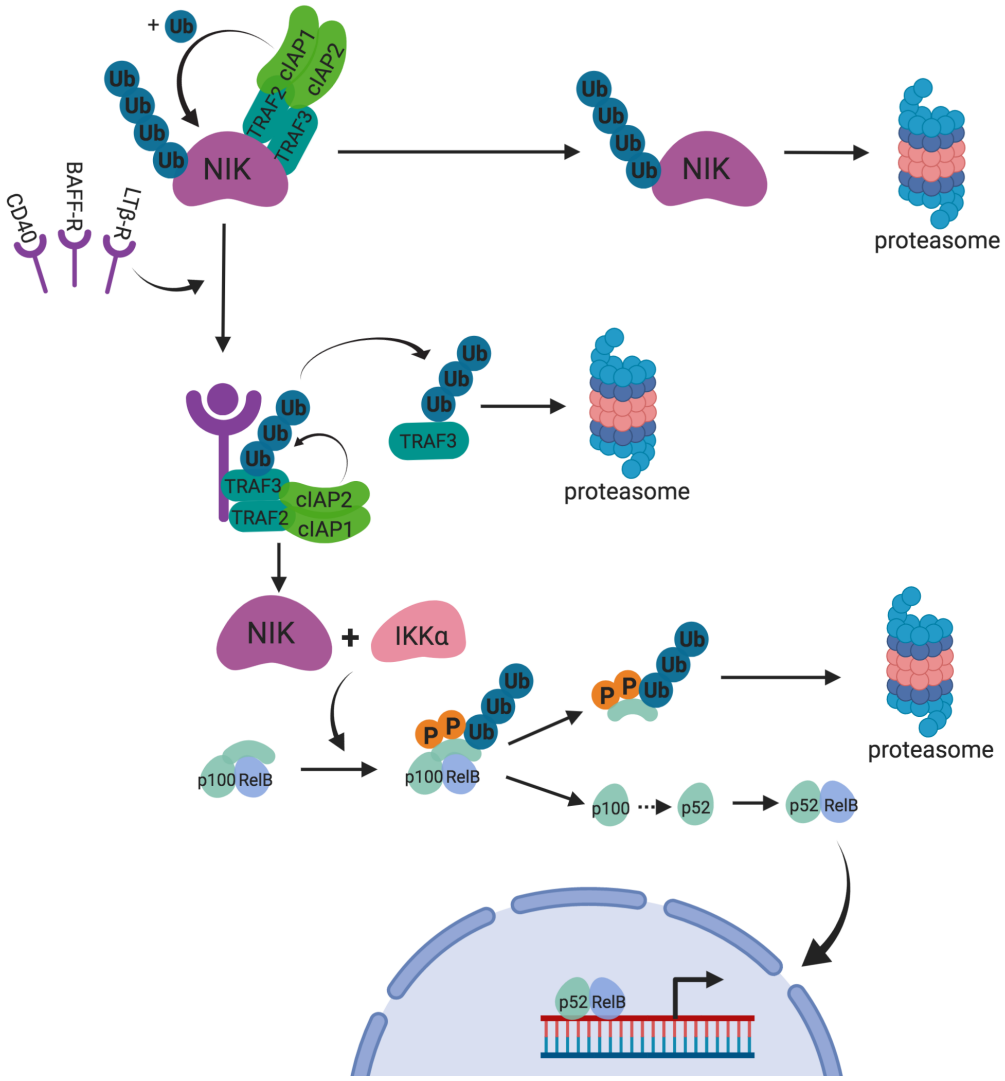

Figure 1.2: The non-canonical NF-κB signalling pathway

In the non-canonical NF-κB pathway, IKKα needs to be activated by NIK before processing p100 to p52 and thereby enabling p52-RelB dimerization. NIK, however, is bound by TRAF2/TRAF3, which act as adapters for c-IAP1/2 ligases. Those ligases ubiquitinylate NIK, which leads to its degradation. Only after BAFF, lymphotoxin β or CD40 stimuli the TRAF2/TRAF3 complex is degraded and IKKα can be activated by NIK. (Figure adapted from (2,88,109,110).)

1.1.4.1 κB-Ras as regulator of the NF-κB pathway

The NF-κB pathway is, amongst other mechanisms, regulated by a group of Ras-like proteins, namely κB-Ras1 and κB-Ras2. These members of the Ras family are encoded by *NKIRAS1* and *NKIRAS2* genes (NF-kappa-B inhibitor-interacting Ras-like protein), show a high similarity (85 %) and are present in many different cell types. (34,85,113) κB-Ras1 and κB-Ras2 differ from other Ras proteins in that they lack a carboxy-terminal sequence that is responsible for adhering the protein to the cell membrane. They carry mutations in codons 12 and 61, resulting in alanine or leucine/glycine and leucine/glutamine exchanges, respectively. (34) Mutations at these positions in the classical Ras GTPases are associated with different kinds of tumours as they activate the Ras protein by slowing down the GTP hydrolysis rate and thereby promoting the GTP-bound state (9,29,34,40,103). In line with this, Tago et al. reported that κB-Ras2 proteins mostly bind GTP, however also GDP-bound states can be found (113). They also postulated that the cellular localization of κB-Ras2 might depend on the different guanosinphosphates they bind, with GDP-bound κB-Ras2 being predominantly located in the cytoplasm (113). Chen et al. described that κB-Ras is found to build ternary complexes with IκBβ and NF-κB transcription factors. κB-Ras1 binds to different regions of IκBβ, as for example the signal response region, and thereby conceals the side where IκBβ is phosphorylated by the IKK complex. (18) Consequently, IκBβ in association with κB-Ras is more slowly degraded and the NF-κB transcription factor pathway is delayed (Figure 1.3) (34). The impediment of IκBβ phosphorylation seems to be independent of whether κB-Ras1 is binding GDP or GTP (18). Interestingly, this whole mechanism does not apply for IκBα (18) This could be an explanation as to why IκBβ, responsible for a long-lasting activation of NF-κB, is not degraded as fast as IκBα (34,116). The durable activation of NF-κB through IκBβ is important for reactions such as activation of T-cells (5). Tago et al. on the other hand claimed that the preservation of IκBβ alone is not strong enough to explain the observed inhibitory effect of κB-Ras. They proposed that especially the GDP bound state of κB-Ras prevents phosphorylation of the p65/RelA protein itself, thereby disrupting the interaction between the transcription factor and p300, a coactivator for transcription. (113)

So far κB-Ras has been suggested to play a role in few cancerogenic events, such as the development of human renal cell carcinomas (39,85).

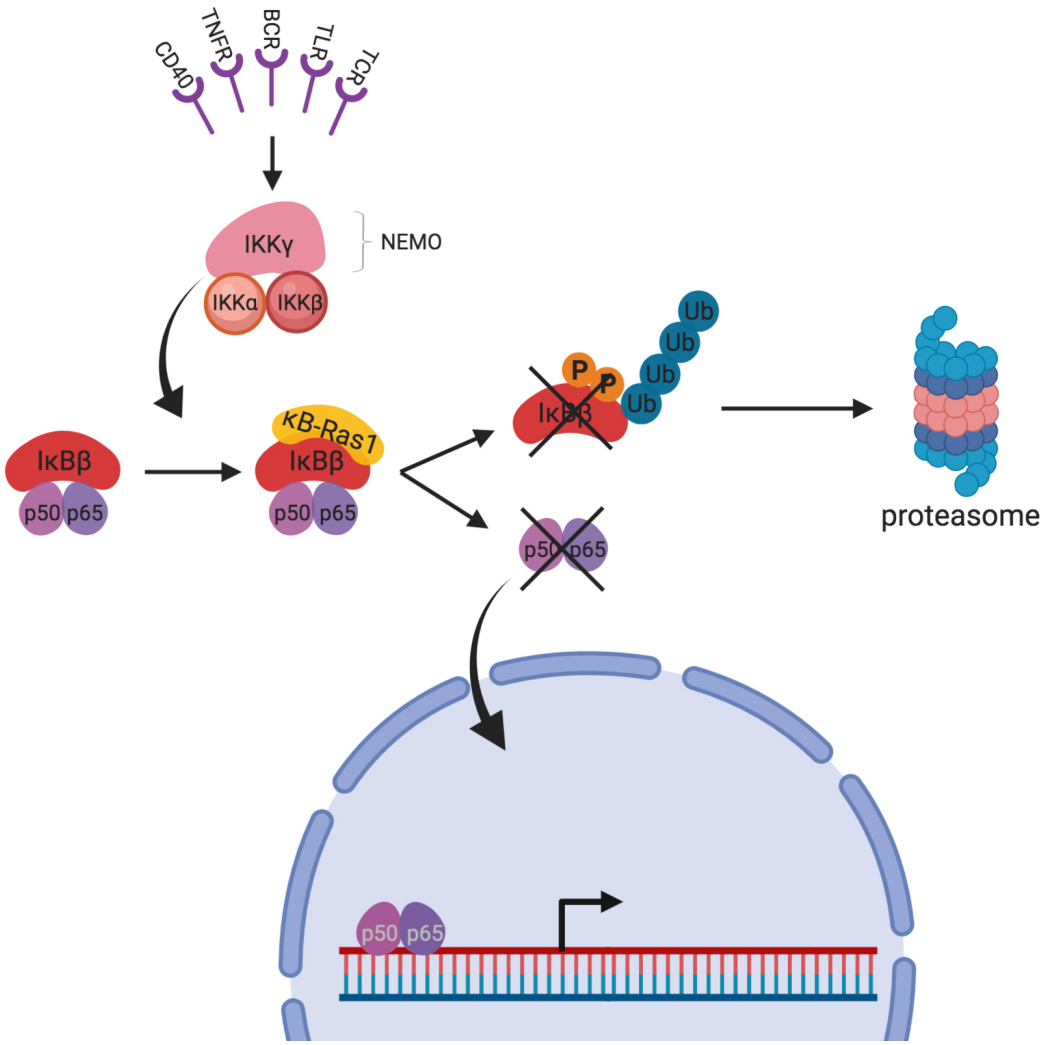

Figure 1.3: κB-Ras regulation of the NF-κB pathway

κB-Ras1 binds to IκBβ, thereby preventing its phosphorylation. IκBβ is therefore neither ubiquitinylated nor degraded, and NF-κB transcription factors p50 and p65, remaining bound to IκBβ, are unable to translocate into the nucleus. (Figure adapted from (88).)

1.1.4.2 Mutations in the NF-κB pathway in ABC DLBCL

The constitutive activation of the NF-κB pathway is essential for the survival of ABC lymphoma cells. When the NF-κB pathway is inhibited, the cells are arrested in G1-phase or die, underlining its importance for this type of lymphoma. (25) Using NF-κB inhibitors sets off the anti-apoptotic effect of NF-κB. Consequently, the additional use of those inhibitors with chemotherapy (e.g., daunorubicin) or radiation reinforces the intended cytotoxic reaction. (6) Conversely, this explains why ABC lymphoma cells with constitutive active NF-κB show a poor response to chemotherapeutic drugs (66).

In DLBCL, *REL* gene amplification as well as Rel truncation due to splicing variability have been described. Resulting high numbers of c-Rel that lack one C-terminal transactivation domain are

capable of transforming DLBCL cells with a GCB signature into ABC DLBCLs, supporting the notion that an increased expression of truncated c-Rel may play an important role in lymphomagenesis. (19,63) Krappmann et al. named another oncogenic mechanism for IκBζ that binds to p50 and p52, thereby promoting transcription of particular NF-κB genes (63). In ABC DLBCL, amplification of the IκBζ encoding gene locus *NFKBIZ* (NFKB inhibitor zeta) has been described to occur repeatedly (67). Furthermore, small numbers of lymphomas also show point mutations in the *NFKBIA/E* genes that result in an inactivation of IκBα/ε (63).

Concerning the *non-canonical pathway*, some DLBCLs show a *TRAF3* deletion, which results in a less functional TRAF2/3-cIAP E3 ligase complex and therefore a higher presence of NIK and thus enhancement of the NF-κB pathway. In DLBCL, BCL6 is often deregulated, leading to downregulated BLIMP1 (B-lymphocyte-induced maturation protein-1) and stalling of final B-cell differentiation. Especially in combination with this BCL6 overexpression, the *TRAF3* mutation is a key player for murine development of DLBCL. (63,90)

As for the *canonical pathway*, mutations within CD79A/B, an important participant for BCR association and signalling, can prevent an internalization of BCR after stimulation and keep the pathway active (26,38). Self-antigens that bind to the BCR and autostimulation are regarded as important factors for ensuring the survival of DLBCL cells (63). Further downstream, the CBM (CARD11/BCL10/MALT1) complex is responsible for transducing the BCR and TCR signals to the NF-κB pathway and IKK by drawing NEMO to the CBM complex once MALT1 and BCL10 are ubiquitinylated (63). In ABC DLBCL this complex is strongly stabilized and therefore constantly present due to CARD11 mutations (63). CARD11 is a scaffolding protein in the cytoplasm that is important for CBM assimilation and thus IKK activation upon antigen stimulation (97). Base pair substitutions within the gene are known to transform *CARD11* into an oncogene. Mutated CARD11 is found to aggregate with MALT1 and BCL10 independently of extracellular signals. Consequently, IKK and thus the NF-κB pathway are activated constitutively and regardless of BCR signalling. (63,65) Interestingly, MALT1 also displays paracaspase activity, and its continuous cleavage capability is important for ABC DLBCL (35). Amongst others, it cleaves the protein A20, a tumour suppressor that stops the NF-κB response and thus causes cell growth arrest and apoptosis (20,63). Independently of MALT1 mutations, A20 is inactivated or deleted in around 30 % of DLBCL patients (20).
Ligand binding to TLRs activates IRAK1 and IRAK4 (interleukin-1 receptor-associated kinase 1/4) via MYD88 (myeloid differentiation primary response 88) to initiate the IKK cascade (63). Mutations within MYD88 are described in 39 % of all ABC DLBCLs (82). 29 % of ABC DLBCL biopsies show a single nucleotide variant resulting in a gain of function within the

Toll/interleukin 1 receptor domain of MYD88, which allows IRAK4 to bind faster to the receptor and thus accelerates signalling (63,82). In mice this mutation alone can create ABC-like lymphomas (61).

1.1.5 Therapy

At first diagnosis a curative therapeutic approach should be aspired for all patients (102). First line therapy for DLBCL is, according to ESMO (European Society for Medical Oncology), a combination of chemotherapy (CHOP) and rituximab, an immunomodulator (117). The exact scheme and dosage vary between patient groups, depending on age and tumour stage (117). Optionally radiation can be performed, especially when the tumour bulk is bigger than 7.5 cm (31). In case of a relapse, which is seen in overall 30 % of patients, autologous hematopoietic stem cell transplantation in combination with high dose chemotherapy is advised (117).

At present, there are many clinical trials aiming at improved treatment and personalized therapy tailored specifically to the DLBCL subtype presented by individual patients. Especially the treatment of the more aggressive DLBCL forms such as ABC and double-hit lymphoma are at the centre of interest. Novel agents such as proteasome inhibitors to supress NF-κB (bortezomib), immunomodulatory drugs to reduce, among other activities, the activity of NF-κB signalling (lenalidomide) or kinase inhibitors to prevent constant activation of the B-cell receptor (ibrutinib) are tested in combination with the R-CHOP scheme. (84) Up to today, phase 3 studies for bortezomib showed no improved outcome for most of the patients (23). However, phase 2 and 3 trials for lenalidomide indicated high rates of progression-free survival for therapy with lenalidomide in addition to R-CHOP (16,115). In contrast, phase 3 studies with ibrutinib indicated that it confers a prolonged event- and progression-free as well as improved overall survival only for patients under 60 years of age (124).

Recently, NF-κB pathway inhibition is increasingly explored as therapeutic target. This includes IKKß inhibitors and inhibitors of heat shock protein 90 (HSP90) that prevent IKK activity as well as the stalling of ubiquitin ligase SCFßTRCP (Skp1-Cullin1-F-box sprotein ubiquitin ligase complex with beta-transducin repeat containing E3 ubiquitin protein ligase) to stop the transfer of IκBα to the proteasome. (66) Phase 1 studies with HSP90 inhibitor KW-2478 for example revealed a disease stabilisation for relapsed NHL and multiple myeloma patients in 96 % of cases (123).

BCL2 inhibitors, too, show promising results concerning some forms of DLBCLs: Venetoclax, for example, is currently in a phase 2 trial, as previous study results suggested a very high complete response rate for DLBCL patients with increased BCL2 levels (125).

In addition, MALT1 inhibitors such as mepazine and thioridazine (76) are thought to be promising drugs, and IRAK4 inhibitors such as CA-4948 are currently tested in phase 1 trials (22,63).
In summary, development of subvariant and pathway specific drugs has an important role in optimising DLBCL treatment and accomplishes to ameliorate patients‘ outcome.

1.2 Gene regulatory elements in tumourigenesis and their assessment

1.2.1 Regulatory elements and their identification

Gene regulatory elements, also known as non-coding elements, can be roughly divided into cis-regulatory elements and non-coding RNAs. Cis-regulatory elements are elements regulating DNA transcription of a gene located on the same DNA molecule and are again subclassified into promoters, enhancers, silencers, insulators and untranslated regions. (58) As the focus of this thesis lies upon silencers, they are going to be picked out as a central theme here.

Silencers are regulatory elements that have a negative effect upon transcription by providing binding sites for negative transcription factors, so-called repressors. They are described to work orientation-independent and irrespective of the distance between silencer and promoter. (70) However, some silencers also work in a position-dependent way (77). They can be contained in a promoter, an enhancer or be a regulatory element of their own. Silencers might be located kilobases away from their target (so called long-range silencers that can influence more than one promoter or enhancer) or less than 100 bp from their target gene (so called short-range silencer) and can even be part of the target gene’s intron or 3’-untranslated region. (70) Looping of the DNA strand allows an interaction between the transcription machinery close to the promoter and the repressive transcription factors bound to the silencer (70,118). The repressing mechanisms of silencers vary from case to case: They can inhibit the binding of an activator by standing in competition with it or occupying the respective site, they can recruit enzymes to modify histones and therefore change chromatin accessibility or they can even prevent the aggregation of a preinitiation complex, necessary to start transcription (70).

Identification of silencers

Many different approaches exist to predict functional silencers across the genome. A computational approach is applied to predict regulatory elements in vitro by using so called transcription factor binding motifs. One such motif consists of 6 – 10 bp and is bound by a specific transcription factor. It often contains degenerate bases, which means that the transcription factor binds to the motif even if at a specific position different nucleotides are present. (104) These transcription factor binding motifs can be identified by experimental

methods such as chromatin immunoprecipitation DNA sequencing (ChIP-Seq; see below) and computational approaches like, on the one hand, over-representation of the motif's sequence in regions that are likely to contain regulatory elements or, on the other hand, a conservation of the sequence between closely related species. Those calculations are introduced into different databases, which can then predict transcription factor binding motifs within an entered sequence. (104)

In vivo silencers are identified by examining the transcription factors themselves: After fixing the repressors with a chromatin immunoprecipitation to their respective transcription factor binding motifs within the silencer, the DNA is fragmented and the silencer region is extracted with specific transcription-factor binding antibodies and sequenced (ChIP-Seq) (55,104). However, not all regions predicted by ChIP-Seq that bind transcription factors have a regulatory function, as proteins might also bind only transiently to the DNA and are coincidently fixed in that position by chemical crosslinking (104).

Another way of predicting silencing elements is by using DNAse I hypersensitivity sites (58). DNAse I is an enzyme that hydrolyses DNA molecules. As it needs open chromatin regions in order to catalyse this reaction, silencers and other regulatory elements are preferentially cut and can then be sequenced. When proteins are bound to the DNA however, the DNAse I cannot cut in this precise region and creates a specific cleavage pattern (also called footprinting) that shows where within the open chromatin region transcription factors and other proteins bind. (43,58,104) A further method to identify open chromatin regions is the ATAC-Seq (assay for transposase-accessible chromatin with high-throughput sequencing), where a hyperactive transposase Tn5 cuts accessible chromatin regions and aligns adapter sequences to it (Figure 1.4 A, page 19). Subsequent sequencing allows conclusions about open chromatin regions. (12)

In addition, methylation patterns are used to identify putative silencer elements, as regulatory elements are frequently hypomethylated (111).

Furthermore, histone marks can give a hint concerning enhancer and silencer presence: Different post-translational acetylation and methylation patterns are associated with transcriptional activity as they influence the access of transcription factors to their binding motif. For example a trimethylation of lysine 4 on histone 3 (H3K4me3) is found at active promoters and repressed regions can amongst other marks be associated with trimethylation of lysine 27 on histone 3 (H3K27me3). (58,104)

To map a silencer to its respective target gene, the three-dimensional genome structure is evaluated by a method called chromosome conformation capture (3C), which biochemically fixes the 3D structure of the genome and retains elements located close to one another (27). With this method mainly interactions between promoters and their enhancers are assessed, but also other

regulatory elements such as silencers can be predicted (104,106). In 4C assays (circular chromosome conformation capture) the whole genome can be screened for DNA fragments that bind to one specific DNA region (e.g., a silencer), and in 5C assays (chromosome conformation capture carbon copy) interactions between many different DNA fragments and regions are examined, whereas in 3C only the communication between two definite DNA fragments is tested. For whole genome interactions a HiC method (high-throughput chromosome conformation capture) has been developed to test all DNA fragments against all potential binding partners in the genome. (58,106)

To then prove the predicted silencing activity, the silencer sequence can be inserted upstream of a promoter and reporter gene. This can be done either in an ectopic plasmid or through integration into the genome of embryonic cells, and even genome wide functional screens such as STARR-Seq (self-transcribing active regulatory region sequencing) are possible. (104)

1.2.2 The functional impact of mutations within regulatory elements

Mutations in protein-coding genes resulting in altered activity of the correspondent protein are long known to have an impact on cancerogenesis. However, protein-coding genes only make up around 2 % of the whole genome. The examination of mutations within the non-coding genome with regards to potential importance for tumourigenesis has more and more become a centre of interest. Indeed, it is known that disease-related genomic mutations (including cancer-associated mutations) are often located in regulatory elements. (58,122) In cancer genome screens, around 3 mutations per megabase have been found in promoters and enhancers alone (122). Mutations of interest can be single nucleotide variants (SNVs), but also large insertions or deletions many base pairs long, or fusion of different genes (58). Melton et al. discussed that mutations in regulatory elements are often located in elements close to known cancer driving genes. By altering the base pair sequence and thereby the transcription factor binding site, these mutations can stimulate oncogenes or impede tumour suppressors and thereby further cancerogenesis. (71)

Weinhold et al. and Khurana et al. reviewed many regulatory elements that harbour impactful mutations (58,122). The most popular example for the importance of mutations within regulatory elements is the promoter of the telomerase reverse transcriptase (*TERT1*) gene. *TERT1* encodes a catalytic subunit in telomerases, and its promoter shows point mutations in over 7 different types of cancer. These mutations form new transcription factor binding sites and thereby lead to upregulated gene transcription. (50,122) On the other hand, a mutation within the *SDHD* (succinate dehydrogenase) promoter impairs transcription factor binding sites,

leading to a decreased transcription of this gene and even shortens overall survival of melanoma patients presenting this mutation. *SDHD* encodes a subunit of the succinate dehydrogenase and is supposed to work as a tumour suppressor. (7,122)

Mutations within enhancers are also described to modify transcription factor binding capability and therefore correspondent gene expression. For example, in prostate cancer the *RFX6* gene (regulatory factor X6), which is important for cell growth, is overexpressed due to single nucleotide polymorphisms (SNPs) in an enhancer element. These SNPs change the enhancer's sequence in a way that HOXB13 (homeobox B13) can bind better to it. As a result the transcription of *RFX6* is increased and prostate cancer cells grow faster. (51,58) Moreover, Pomerantz et al. described how a SNP in an enhancer that interacted with the *MYC* proto-oncogene resulted in reinforced binding of the corresponding transcription factor in colorectal cancer cells and suggested that this altered binding behaviour might contribute to higher risks of developing cancer (92).

In addition, mutations within introns can either change splice sites or trigger an impairment of negative regulatory elements (58).

1.2.2.1 Computational methods to identify non-coding mutations

Predicting driving mutations in the non-coding genome causes some difficulties as non-coding regions have a more complex way of functioning than coding regions and are not as well understood. Plus there are a lot more mutations within those sites than within coding regions, thereby providing more passenger mutations that have to be discriminated against important functional mutations. (58) Nonetheless, different methods and prediction tools of forecasting non-coding driver mutations have been developed. For example, conservation between different species and humans is also for non-coding regions a strong indication that this element or respectively this mutated variant might harbour a relevant function. (58) Prediction tools may reveal a variants function (e.g., whether it presents transcription factor binding motifs or whether a mutation within a variant changes transcription factor binding sites) and use additional information concerning linkage disequilibrium between variants or recurrence of somatic mutations, as important driver mutations are suggested to undergo "positive selection" (58). Weinhold et al. described a hotspot analysis to find regions where recurrent mutations occur significantly more often than the normal rate of random mutations throughout the genome would suggest (122). However, this detection of "positive selection" has to factor in other mechanisms that can lead to heterogeneity throughout the genome (e.g., transcriptional activity) (58) and is improved when performing a second so called "regional recurrence approach" where detected mutation frequencies are additionally checked against mutation frequencies in nearby regions and in comparable regions elsewhere in the genome (122). On top of that, driving mutations in regulatory elements are searched by concentrating on transcription

factor binding sites for ETS (E26 transformation specific) transcription factors, as they are known to be involved in cancerogenesis of different cancer types (50). With these different variables some prediction tools even generate scores to estimate the probability of a given mutated variant having a relevant effect (58).

1.2.2.2 Experimental approaches to identify non-coding mutations

In order to confirm or negate the computational method's predicted functional impact of a mutation within a regulatory element, the variant of interest can be inserted into a cell line for further functional assays. This is achieved either by site-directed mutagenesis (see also 2.2.3.9, page 39) or by a CRISPR-Cas9 (clustered regularly interspaced short palindromic repeats-associated endonuclease 9) system (Figure 1.4 D, page 19). (58) Jinek et al. first described a CRISPR-Cas9 mediated genome editing in bacteria: Based on the capability of Cas9 endonucleases to cut DNA at a position directed by RNA molecules, double-strand breaks can be inserted at specific sites. crRNAs (CRISPR RNAs) contain base pair sequences complementary to the so-called protospacer on the DNA and are therefore able to bind to the region of interest. tracrRNAs (trans-activating crRNA) connect to the crRNAs and prompt Cas9 cleavage at the target region. A PAM (protospacer adjacent motif) region next to the protospacer is also required for Cas9 binding and cleaving. Jinek et al. furthermore showed that crRNA and tracrRNA can be combined in one RNA molecule, enabling genome editing with one single RNA guiding the Cas9. (54) Cong et al. demonstrated that CRISPR-Cas9 mediated genome editing can also be applied to human cells (21).

The functional impact of the inserted mutation is then assessed via high- or low-throughput techniques. A visible reporter assay such as a luciferase assay easily verifies whether the mutation has an impact on transcription or not; however, it is not suitable for high-throughput assays as transfection efficiency varies a lot between individual cells. (58) In this assay the variant is inserted into a luciferase plasmid and its effect upon transcription can be seen when measuring the amount of light emitted from a reaction that is catalysed by the luciferase enzyme (10). Consequently, an enhancing effect upon transcription results into the presence of more luciferase enzymes and thereby more produced light (Figure 1.4 C, page 19).

A high-throughput dimension, however, is achievable with CRE-Seq or STARR-Seq assays. In a CRE-Seq (cis-regulatory element analysis by sequencing) regulatory elements (primarily promoters) with and without mutation are cloned into a vector upstream of a reporter gene. Each regulatory element is coupled to a so-called barcode, which – after RNA sequencing – allows matching of the transcript to the regulatory element inserted. Measuring the number of cDNA copies (complementary DNA) from one specific promoter element makes it possible to reconstruct the mutation's impact. (58,64)

The STARR-Seq assay is also based on the principle of an inserted library of regulatory elements; however, only silencers and enhancers are examined as most of them are supposed to influence transcription position-independently and do not have to be placed upstream of the reporter gene. Being positioned behind the reporter gene, the regulatory element enhances or represses its own transcription (Figure 1.4 B, page 19). By sequencing the originated cDNA strands, each enhancer's or silencer's impact upon transcription is measured. (4,58)
In a second step, oncogenic features such as proliferation or invasion can be evaluated in vitro by testing cell lines or in vivo after having created a mouse model (58).

1.2.3 Prediction and selection of the silencing element described in this thesis

The silencing element examined in this thesis was not yet described, however, previous work in the laboratory had predicted many regulatory elements with potential functional impact upon DLBCL cancerogenesis.
First of all, Alexander Tönges from the group of Prof. Dr. Rosenbauer had performed an ATAC-Seq to cut out open chromatin regions from HBL-1 (human diffuse large B-cell lymphoma) and OCI-ly1 cells (Ontario Cancer Institute, cell line ly1) that contain putative regulatory elements. Cut DNA strands with 80 – 100 bp length, which were supposed to contain only DNA without any histones, were inserted as a library into a STARR-Seq vector, and after sequencing potential silencers and enhancers their regulatory effect and functional impact was predicted. The potential regulatory elements were then compared to whole-genome-sequencing data of 33 DLBCL patients published by Morin et al. in 2013 (74). 760 mutations that overlapped with the regulatory elements were found, suggesting that they might be functional mutations in cancerogenesis of DLBCL. As mutations, which play a relevant role in cancerogenesis, are supposed to occur repeatedly in different patients, for further investigation only recurrently mutated regulatory elements were selected. Within those an additionally focus was placed on regulatory elements located within genes that are known to be important for proliferation, apoptosis or major pathways in DLBCL. Following those criteria, the vast number of putative regulatory elements predicted by the STARR-Seq assay was narrowed down and the putative silencer element, chosen to be central for this thesis, was detected. This putative silencer element is positioned within the first intron of *NKIRAS1*, which encodes κB-Ras1, and is recurrently mutated in DLBCL patients.

1.3 Aim and design of this thesis

Previous experiments with ATAC-Seq and STARR-Seq assays (Figure 1.4 A and B, page 19) have shown that many putative regulatory elements in DLBCL cell lines overlap with mutations found in DLBCL patients. One such regulatory element with putative silencing activity is recurrently

mutated and positioned within the *NKIRAS1* gene. *NKIRAS1* encodes κB-Ras1, which prevents the degradation of IκBβ and therefore acts as an inhibitor of NF-κB (18,34,85). As the NF-κB pathway is known to play a major role in the pathogenesis of DLBCL subtypes (25), the main interest was to validate the silencing function of this regulatory element and to investigate its impact on κB-Ras1 expression.

The first aim of this thesis was thus to verify the silencer activity predicted by STARR-Seq assays with a luciferase assay. To that end, a luciferase plasmid containing the silencing element in different positions within the construct had to be cloned.

A second aim was to study the impact of the recurrent mutation found in patients with DLBCL within the putative silencer by modifying this silencer element using site-directed mutagenesis and subsequent analysis of the mutated element in luciferase assays (Figure 1.4 C).

A third aim to be addressed was to elucidate the influence of the putative silencer element on the expression of genes adjacent to its endogenous locus with a particular focus on κB-Ras1. To answer this question, a CRISPR-Cas9 knockout of the silencer element was to be conducted, followed by an assessment of phenotypic changes with respect to cell proliferation (Figure 1.4 D).

As final aim it was to be explored whether the *NKIRAS1* gene itself impacts proliferation of DLBCL cells, as up until now there is no data on the role of κB-Ras1 in DLBCL cell lines. This goal included a CRISPR-Cas9-based knockout of the whole *NKIRAS1* gene in order to prove or refute an effect of κB-Ras1 on DLBCL cell proliferation.

A: ATAC-Seq

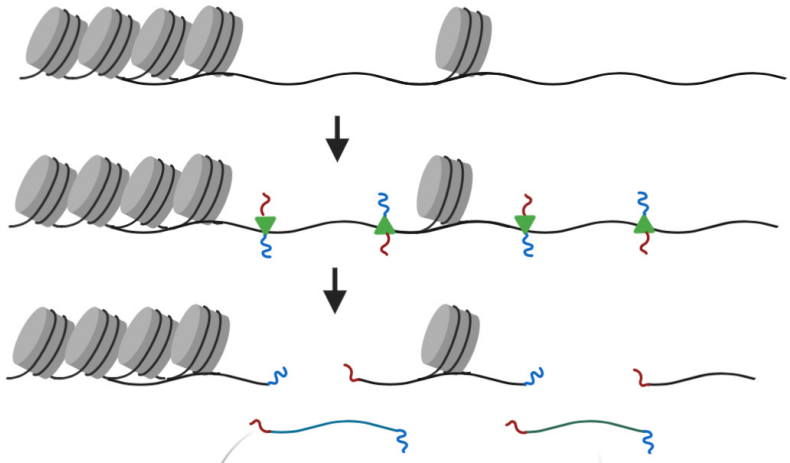

B: STARR-Seq

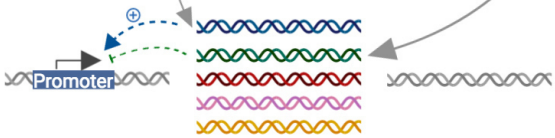

transcripts:

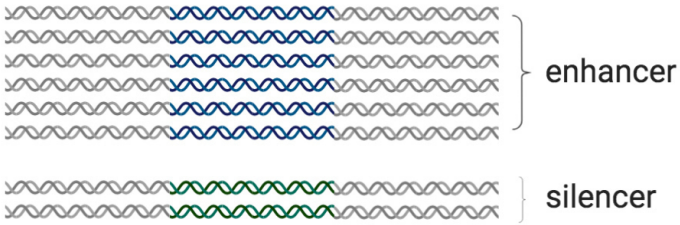

C: Luciferase assay

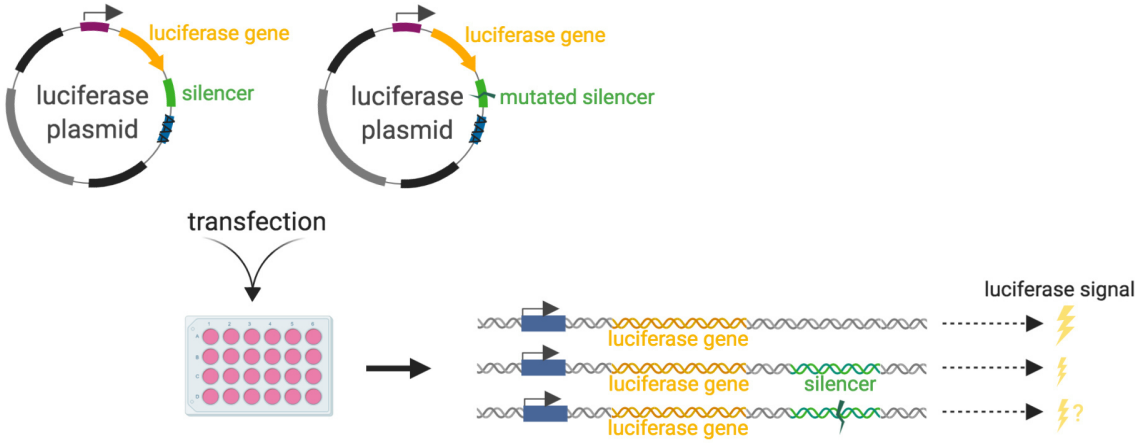

D: CRISPR-Cas9 based genome editing

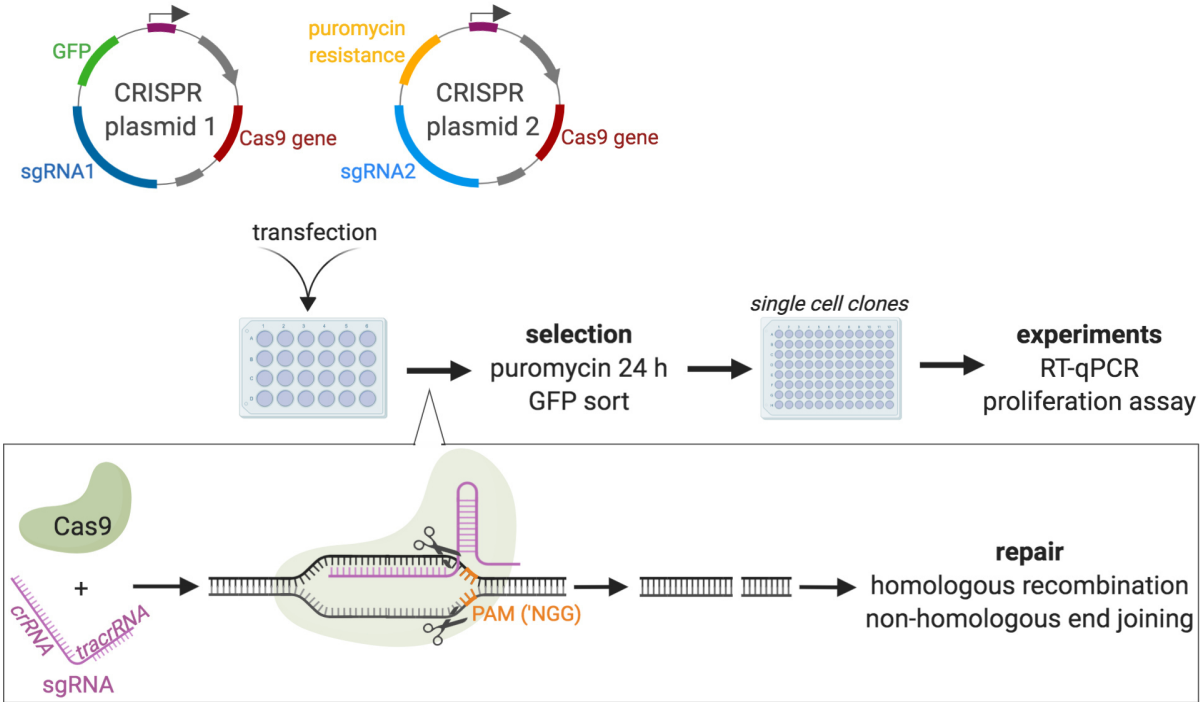

Figure 1.4: Key technologies used to predict and validate the putative silencer element in this thesis

(A) In ATAC-Seq open chromatin regions are cut out with Tn5, ligated to adapters and then introduced into a STARR-Seq vector. **(B)** In the STARR-Seq vector the potential regulatory elements are positioned downstream of the promoter, where they regulate their own transcription. Insertion of enhancers and silencer elements results in increased and decreased transcript levels, respectively. After sequencing, the transcripts can be assigned to the inserted regulatory element. **(C)** In a next step, a luciferase assay can verify the high-throughput results, and a mutation of interest can be examined via site-directed mutagenesis. Mutated and wild-type silencers are inserted in the luciferase plasmid, transfected into the cell, and luciferase activity is measured and compared to the empty vector's luciferase activity. A silencer will produce less luciferase signal than the empty vector and the mutation's effect can be evaluated. **(D)** In a final step, the silencer is knocked out in a cell line using CRISPR-Cas9 targeting. To that end, plasmids containing the *Cas9* gene as well as sgRNAs (single-guide RNAs) and a reporter gene are transfected into the cell. The sgRNAs, consisting of crRNA and tracrRNA, guide the Cas9 to the DNA-region of interest, which presents a PAM sequence as recognition site for the Cas9. The Cas9 can then carry out a double-strand break, which is repaired by the cell via homologous recombination or non-homologous end joining. Positively transfected cells are selected with puromycin and GFP (green fluorescent protein) FACS (fluorescence-activated cell sorting), as the reporter genes on the plasmids represent a puromycin resistance and a *GFP* gene. Selected cells are single cell sorted, expanded over several weeks and then subjected to downstream experiments.

(Figures adapted from (1,4,12,58).)

2 Materials and methods

2.1 Materials

2.1.1 Equipment

Table 2.1: Equipment

Device	Description	Producer	Head office
Autoclave	Vakulab PL 666 - 1H R Dampfsterilisator	MMM Group	Planegg/München
Bunsen burner	Bunsen burner	Campingaz	St Genis Laval
Calculator	Sharp EL-243S calculator	SHARP	Sakai
Centrifuge	Heraeus Multifuge 3SR	ThermoFisher scientific	Waltham
Centrifuge 96-well plates	Laboratory Centrifuge lmc-3000	BioSan	Riga
Cell culture centrifuge	Heraeus Multifuge X3	ThermoFisher scientific	Waltham
Electrophoresis device	Electrophoresis Power Supply Ev231	Consort	Turnhout
Electroporation device	Gene Pulser Xcell	BioRad	Hercules
FACSorter	BD FACSAria III Sorter	BD Biosciences	Berkshire
Fluorescence microscope	Inversmicroscope CKX41 + CoolLed P6 Excitation System	Olympus, CoolLed	Tokio, Andover
Freezer – 80 °C	Ultra low temperature freezer	New Brunswick Scientific	New Jersey
Freezer -160 °C	LS-6000	Taylor Wharton	Minnetonka
Freezer -20 °C	Premium NoFrost, laboratory freezer	Liebherr, Ewald Innovationstechnik GmbH	Bulle, Rodenberg
Freezing box	"Mr. Frosty" Nalgene Cryo 1°C Freezing Container	ThermoFisher scientific	Waltham
Gel electrophoresis set (comb, tray, chamber)	Horizontal Electrophoresis System kuroGEL Midi 13 700-0056	VWR	Radnor
Gel imager	Gel Doc XR System Universal Hood2	BioRad	Hercules
Ice machine	Chip ice maschine	Ziegra EisMaschinen GmbH	Isernhagen
Incubator cell culture	CO2-incubator	Binder	Tuttlingen
Incubator for bacterial cultures (static)	Universal oven UN30	Memmert	Schwabach

Incubator for bacterial cultures (shaker)	Incubator shaker series Innova 44	New Brunswick Scientific	New Jersey
Laminar airflow hood	BioHazard	BDK Luft und Raumtechnik	Sonnenbühl
Magnet rack	Magna GrIP™ Rack (8 well)	Sigma-Aldrich	St. Louis
Magnet spinner	IKA RCT classic	IKA	Staufen im Breisgau
Microplate reader	TriStar LB 941	Berthold Technologies	Bad Wildbad
Microscope (cell culture)	Primovert Inverted Microscope	Zeiss	Oberkochen
Microwave oven	Microwave 700	Severin	Sundern
MultiChannel pipette	100 µl, 300 µl	Eppendorf	Hamburg
N2 tank	XL180	Taylor Wharton	Minnetonka
Neubauer chamber	Counting chamber, Imp Neubauer (40442702)	VWR	Radnor (Pennsylvania)
pH-Meter	Basic pH MeterPB-11	Sartorius	Göttingen
Pipet boy	Pipetboy2, Biohit Midi Plus Pipetting Controller	Integra LifeSciences, Sartorius	Plainsboro NJ, Göttingen
Pipettes	10 µl, 20 µl, 200 µl, 1000 µl	Eppendorf	Hamburg
Printer	MITSUBISHI P 95	Mitsubishi	Tokyo
Real time thermocycler	Applied Biosystems StepOnePlus Real-Time PCR Systems	ThermoFisher scientific	Waltham
Repeating pipette	Multipette plus	Eppendorf	Hamburg
Refrigerator 4 °C	Comfort NoFrost	Liebherr	Bulle
Rotation shaker	Unimax 1010	Heidolph	Tehran
Scale	Analysis Scale Adventurer	Ohaus	Parsippany, New Jersey
Scale	BP 610	Sartorius	Göttingen
Spectrophotometer	Nanodrop 1000 spectrophotometer	peqlab Biotechnologie GmbH	Erlangen
Table centrifuge	Centrifuge 5424	Eppendorf	Hamburg
Table centrifuge with cooling system	Centrifuge 5424R	Eppendorf	Hamburg
Thermocycler	Mastercycler Pro Vapo Protect	Eppendorf	Hamburg
Thermomixer	Thermomixer Comfort	Eppendorf	Hamburg
UV transilluminator	UV Star 365 nm biometra	Biometra GmbH	Göttingen
Vacuum pump	Vacuum System BVC 21 NT	Vaccubrand GmbH	Wertheim
Vortex mixer	VortexGenie 2 G560E	Scientific Industries Inc	Bohemia (New York)
Water bath	Water bath TW20 / TW2, water bath 1003 (14 liters)	Julabo, GFL	Seelbach, Burgwedel

Water sterilisator	Arium 611VF	Sartorius	Göttingen

2.1.2 Plastic and glassware, general lab ware

Table 2.2: Expendable materials

Material	Description	Reference number	Producer	Head office
8-strip PCR tubes	PCR stripes	781327	BRAND GmbH + CO AG	Wertheim
96-well PCR plate	MicroAmp fast 96-well reaction plate (0.1ml)	4346907	ThermoFisher Scientific	Waltham
96-well PCR plate white	Microplates, 96 well	23300	Berthold TechnologiesGmbH & Co. AG	Bad Wildbad
Adhesive PCR sealing foil	MicroAmp optical adhesive film	4311971	ThermoFisher Scientific	Waltham
Alu foil	Laboratory alu foil	60100	Korff Isolmatic	Dietzenbach
Bunsen burner gas	Gas cartridge C206 GLS Super	515987	Diagonal GmbH	Münster
Cell culture flasks (T25, T75, T175)	Cellstar cell culture flask 175 cm^2/ 75 cm^2/ 25 cm^2	661175, 658175, 690175	Greiner BioOne	Kremsmünster
Cell spreader glass	Drigalski-Spatel	41049010	Diagonal GmbH	Münster
Culture tubes	Culture and sample tubes, disposable	211-0133	VWR	Radnor (Pennsylvania)
Cover glas	Haemacyto-meter cover glass, 20 mm×26 mm× 0.4 mm	350000	Paul Marienfeld GmbH & Co. AG	Lauda-Königshofen
Electropo-ration cuvettes	Cuvettes 4 mm, 800 µl, sterile yellow cap	7321137	VWR	Radnor (Pennsylvania)
FACS tubes	Falcon 5 ml round bottom polystyrene test tube	352054	Corning	New York
Falcon tubes (15 ml, 50 ml)	50 /15 ml CELLSTAR polypropylen tube	227261, 188271	Greiner Bio-One	Kremsmünster
Freezing tubes	CryoPure tube 1.8 ml white	72.379	Sarstedt	Nümbrecht
Glass bottles and	1000 ml		Duran Schott AG	Mainz

Erlenmeyer flasks	500 ml 50 ml		Kavalier - SIMAX Technische Glaswerke Ilmenau GmbH	Sázava Illmenau
Gloves	XS nitrile-powder free Abena classic	881701	Abena	Aabenraa
Manual cell counter	Handstück-zähler	EE53.1	Carl Roth GmbH + Co. KG	Karlsruhe
Microcentri-fuge tubes	Eppendorf safe-lock tubes, 2.0 ml / 1.5 ml	30-120-094, -086	Eppendorf	Hamburg
Microcentri-fuge tubes safelock	Micro tube, 2.0 ml / 1.5 ml	72690001, 72691	Sarstedt	Nümbrecht
Needle	Hypodermic Needle-Pro G20x1 1/2'' / 0,90x38 mm	4658311	B. Braun	Melsungen
Non sterile pipette tips	Pipette tips reload system 1-10 µl	613-1068P	VWR	Radnor (Pennsylvania)
	Pipette tips 200 µl	70.760.002	Sarstedt	Nümbrecht
	Pipette tip 100-1000 µl, blue	686290	Greiner BioOne	Kremsmünster
Parafilm	Parafilm M-labor film	#PM996	Bemis	Oshkosh
Pasteur pipettes	Pasteur pipette glas 2 ml, 145 mm	747715	BRAND GmbH + CO AG	Wertheim
Petri dishes	Falcon 100 x 20 mm TC-treated cell culture dish	353003	Corning	New York
Pipette dropper	Pasteurpipetten-Sauger 1 ml	3101010	Diagonal GmbH	Münster
Plastic pipette (5 ml, 10 ml, 25 ml)	Costar stripette 5 ml, 10 ml, 25 ml	4487, 4488, 4489	Corning	New York
Plastic syringe	10 ml syringe BD Discardit II	300296	BD Biosciences	Berkshire
	Omnifix solo luer lock 50 ml	4613554F	B. Braun	Melsungen
Repeating pipette tips	Combitips advanced 5 ml, 10 ml	00300894-56, 003006-9242	Eppendorf	Hamburg
	Combitips plus 2.5 ml	5620660/1	Eppendorf	Hamburg
Scalpel	Feather disposable scalpels No 22	200130022	Feather	Osaka
Sterile filter (bottle)	Filtermax filter top 500 ml	99505	TPP	Trasadingen
Sterile filter (syringe)	Minisart syringe filter 0.20 µm	16534K	Sartorius	Göttingen
Sterile pipette	SafeSeal tips	691000	Biozyme Scientific	Hessisch

tips (10er, 100er, 1000er)	premium 1000 µl sterile		GmbH	Oldendorf
	Biosphere fil. tip 200 µl neutral	70.760.211	Sarstedt	Nümbrecht
	SafeSeal tips professional 10 µl, steril	770005	Biozyme Scientific GmbH	Hessisch Oldendorf
Surgical mask	Surgical mask	428901	Barrier	Göteborg
Tissue wipes	Precision wipes	5511	Kimberly-Clark Corporation	Dallas
Well plate 96-well U-bottom	Tissue culture test plate 96-well U-version	92097	TPP	Trasadingen
Well plates (6,12,24,48,96)	Non-tissue well plates flat bottom Cellstar 6-/12-/24-/48-/96-well	657185, 665102, 351147, 351178, 650185	Greiner BioOne, Corning	Kremsmünster, New York

2.1.3 Chemicals

Table 2.3: Chemicals

Name	Producer	Head office
2-Propanol	Roth	Dautphetal
Acetic acid 100%	Carl Roth GmbH + Co. KG	Karlsruhe
Adenosine 5`-triphosphate, sodium salt	Carl Roth GmbH + Co. KG	Karlsruhe
Calcium chloride	Carl Roth GmbH + Co. KG	Karlsruhe
Di-potassium hydrogen phosphate	Carl Roth GmbH + Co. KG	Karlsruhe
Dimethyl sulfoxide	Carl Roth GmbH + Co. KG	Karlsruhe
DPBS	PanBiotech	Aidenbach
EGTA	Carl Roth GmbH + Co. KG	Karlsruhe
Ethanol 70% denatured	Liquid Production GmbH	Flintsbach am Inn
Ethidium bromide 10mg/ml	Carl Roth GmbH + Co. KG	Karlsruhe
Ethylenediaminetetra-acetic acid	Carl Roth GmbH + Co. KG	Karlsruhe
HEPES	Carl Roth GmbH + Co. KG	Karlsruhe
L-Glutathione reduced	Carl Roth GmbH + Co. KG	Karlsruhe
Magnesium chloride hexahydrate	Carl Roth GmbH + Co. KG	Karlsruhe
NP-40	Sigma-Aldrich	St. Louis
Potassium chloride	Carl Roth GmbH + Co. KG	Karlsruhe
Potassium dihydrogen phosphate	Merck KGaA	Darmstadt
Rnase Away, molecular BioProduct	Thermo Fisher Scientific	Waltham
Sodium chlorid	Carl Roth GmbH + Co. KG	Karlsruhe
TRIS pufferan 5 kg	Carl Roth GmbH + Co. KG	Karlsruhe
Tween 20	Sigma-Aldrich	St. Louis

2.1.4 Molecular biology

Table 2.4: Kits

Name	Producer	Catalogue number	Head office
DNeasy Blood & Tissue Kit	Qiagen	69504	Venlo
Invisorb Spin DNA Extraction Kit	Stratec	1020110300	Birkenfeld
Invisorb Spin Plasmid Mini Two	Stratec	1010140300	Birkenfeld
NucleoSpin Gel and PCR Clean-up	Macherey-Nagel	740609.5	Düren
Promega Dual-Luciferase Assay Kit	Promega	E1910	Madison, Wisconsin
PureLink HiPure Plasmid Maxiprep Kit	ThermoFisher Scientific	K210007	Waltham
PureLink HiPure Plasmid Midiprep Kit	ThermoFisher Scientific	K210005	Waltham
Q5® Site-Directed Mutagenesis Kit	New England BioLabs	E0554S	Ipswich
QIAshredder	Quiagen	79654	Venlo
RevertAid First Strand cDNA Synthesis Kit	ThermoFisher Scientific	K1622	Waltham
RNase-Free DNase Set	Qiagen	79254	Venlo
RNeasy Mini Kit	Qiagen	74104	Venlo

Table 2.5: Agarose gel reagents

Name	Producer	Head office
Agarose NEEO Ultra-Qualität	Carl Roth GmbH + Co. KG	Karlsruhe
GeneRuler 100 bp DNA-Ladder	Thermo Fisher Scientific	Waltham
GeneRuler 1 kb Plus DNA-Ladder	Thermo Fisher Scientific	Waltham
6x DNA Loading	Thermo Fisher Scientific	Waltham

Table 2.6: General reagents

Name	Producer	Head office
AMPure XP beads	Beckman Coulter	Brea
CellTiter-Glo Luminescent Cell Viability Assay	Promega	Madison

Table 2.7: Enzymes

Reaction	Name	Producer	Head office
CRISPR-Cas9	Antarctic Phosphatase	New England BioLabs	Ipswich
	BbsI (BpiI)	ThermoFisher Scientific	Waltham
	Proteinase K Solution	ThermoFisher Scientific	Waltham
	T4 Polynucleotide Kinase	ThermoFisher Scientific	Waltham
PCR	2x KAPA HiFi HotStart Ready Mix, 6.25 ml	Roche	Basel

	GoTaq G2 Hot Start Green Master Mix (1000x), 25 ml	Promega	Madison
RT-qPCR	Luna® Universal qPCR Master Mix	New England BioLabs	Ipswich
	Power SYBR Green Master Mix	ThermoFisher Scientific	Waltham
	RevertAid Reverse Transcriptase	ThermoFisher Scientific	Waltham
	Ribolock	ThermoFisher Scientific	Waltham
vector digestion	BglI	New England BioLabs	Ipswich
	BglII	New England BioLabs	Ipswich
	FseI	New England BioLabs	Ipswich
	HindIII	New England BioLabs	Ipswich
	KLD Enzyme Mix (10X)	New England BioLabs	Ipswich
	NheI	New England BioLabs	Ipswich
	PshAI	New England BioLabs	Ipswich
	XbaI	New England BioLabs	Ipswich
vector fusion	In-Fusion HD Cloning Kit, 50 rxns	Clontech Laboratories, Takara Bio USA	Mountain View
	T4 DNA Ligase	New England BioLabs	Ipswich

Table 2.8: Plasmids

Name	Number	Producer
pGL4-gateway-SCP1 vector	#71510	Addgene
pRL-TK	E2241	Promega
px458	#48138	Addgene
px459	#62988	Addgene

Table 2.9: Oligonucleotides

Reaction	Description	Name	Sequence
silencer PCR	5' postition	f#JB_sil13_cloning	ACATTTCTCTGGCCTGCAATCCACCCACTCCATGA
		r#JB_sil13_cloning	TACCCTAGGGAGATCCGAGAGGTGAGAGAGTTGGC
	3’ z fwd position	f#JB_sil13_cloning_oh	GTGTAATAATTCTAGAGCAATCCACCCACTCCATGA
		r#JB_sil13_cloning_oh	GCTCGAAGCGGCCGGCCCGAGAGGTGAGAGAGTTGGC
	3’ z rev position	f#JB_sil13_clon_oh_z_rev	GCTCGAAGCGGCCGGCCGCAATCCACCCACTCCATGA
		r#JB_sil13_clon_oh_z_rev	GTGTAATAATTCTAGACGAGAGGTGAGAGAGTTGGC
	3’ h fwd position	f#JB_sil13_clon_oh_h_fwd	CGCGGGGCATGACTAGCAATCCACCCACTCCATGA
		r#JB_sil13_clon_oh_h_fwd	TAAGTGCGGCGACGACGAGAGGTGAGAGAGTTGGC
	3’ h rev position	f#JB_sil13_clon_oh_h_rev	TAAGTGCGGCGACGAGCAATCCACCCACTCCATGA

		r#JB_sil13_clon_oh_h_rev	CGCGGGGCATGACTACGAGAGGTGAGAGAGTTGGC
	3’ v fwd position	f#JB_sil13_clon_oh_v_fwd	TACGGACCGGGCTAGCGCAATCCACCCACTCCATGA
		r#JB_sil13_clon_oh_v_fwd	CCGGATTGCCAAGCTTCGAGAGGTGAGAGAGTTGGC
	3’ v rev position	f#JB_sil13_clon_oh_v_rev	TACGGACCGGGCTAGCCGAGAGGTGAGAGAGTTGGC
		r#JB_sil13_clon_oh_v_rev	CCGGATTGCCAAGCTTGCAATCCACCCACTCCATGA
suicide gene replacement		f#JB_SEG	GGTAACCGTATCCATCCG
		r#JB_SEG	GATCCGGATGGATACGGTTACCGTT
site directed mutagenesis		f#JB_sil13.1_mut	AGGGACAGCGTAGCGCGGAGA
		r#JB_sil13.1_mut	CTCTGGCCACCGCACGAC
colony PCR		primer RV3 (primer fwd)	CTAGCAAAATAGGCTGTCCC
		R#pGL4_SCP1_ColPCR (primer rev)	TCGCGACTGAGGACGAAC
silencer knockout	sgRNA cloning	mut_gRNA1_fwd	CACCGGGAGACGCAGAGACTCCGCA
		mut_gRNA1_rev	AAACTGCGGAGTCTCTGCGTCTCCC
		mut_gRNA2_fwd	CACCGCCTCTCTGGCCACCGCACGA
		mut_gRNA2_rev	AAACTCGTGCGGTGGCCAGAGAGGC
		mut_gRNA3_fwd	CACCGCCGTCGTGCGGTGGCCAGAG
		mut_gRNA3_rev	AAACCTCTGGCCACCGCACGACGGC
		mut_gRNA4_fwd	CACCGAGACGCAGAGACTCCGCAGG
		mut_gRNA4_rev	AAACCCTGCGGAGTCTCTGCGTCTC
	Bulk screen PCR	mut_PCR-Primer_fwd	CCGTATGCAGAAAAAGCGCC
		mut_PCR-Primer_rev	ACAGGTTTGTTTCACGCACC
	Clones screen qPCR	primer1_mut_region_fwd	GCGCAGCGCGGAGAC
		primer1_mut_region_rev	CGAGAGGTGAGAGAGTTGGC
		primer2_mut_region_fwd	TAGGACAAAATCCCTGGGCG
		primer2_mut_region_rev	CTGCGCTGTCCCTCTCTG
	RT-qPCR κB-Ras1	hkB1_RT_F	ACAGACCGAGGAGTAAAAGAACA
		hkB1_RT_R	TCTCTGCTCAGAAAGGTCGAT
		GAPDH fwd	ACGGGAAGCTTGTCATCAAT
		GAPDH rev	TGGACTCCACGACGTACTCA
	RT-qPCR RPL15	RPL15_Ex_Ex_2_fwd	AAGGGTGCAACTTACGGCAA
		RPL15_Ex_Ex_2_rev	CTCCTCTGCAACGGACTGAA

NKIRAS1 knockout	sgRNA cloning	gDNA kB1Ex2+81 F	CACCGGTTGATGGTACATAAAGGGG
		gDNA kB1Ex2+81 R	AAACCCCCTTTATGTACCATCAACC
		gDNA kB1Ex2-195 F	CACCGAATGCTTATTGCTCTAAGGG
		gDNA kB1Ex2-195 R	AAACCCCTTAGAGCAATAAGCATTC
	Bulk screen PCR	kB1_Ex2_Screen_2F	TGCCCACTGGAAAGTTATGT
		kB1_Ex2_Screen_2R	TGTGCCTGGCCTGTATTCTT

2.1.4.1 Buffers

Table 2.10: Purchased buffers

Name	Producer	Head office
2X KLD reaction buffer	New England BioLabs	Ipswich
Antarctic phosphatase reaction buffer	ThermoFisher Scientific	Waltham
Cutsmart buffer	New England BioLabs	Ipswich
NEB buffer 3.1	New England BioLabs	Ipswich
Q5 Hot Start High-Fidelity 2X Master Mix	New England BioLabs	Ipswich
T4 DNA ligase buffer (10X)	New England BioLabs	Ipswich

Table 2.11: 50x TAE buffer

Reagent	Quantity
Tris pH 7.5 - 8	2 M
acetic acid 100 %	1 M
EDTA pH 8	50 mM
water	to 1 l
adjust to pH 8.3	
before using dilute 1:49 with distilled water	

Table 2.12: Tris buffer 10 mM

Reagent	Quantity
Tris pufferan	1,2114 g
water	1 l
adjust to pH 7.5 - 8	

Table 2.13: Tail lysis buffer

Reagent	Quantity
Tris pH=8	50 mM
KCl	50 mM
EDTA	2.5 mM
NP-40	0.45 %

Table 2.14: Annealing buffer

Reagent	Quantity
Tris pH 7.5 - 8	10 mM
NaCl	50 mM
EDTA	1 mM

2.1.4.2 Bacterial reagents

Table 2.15: Reagents for bacterial medium

Name	Producer	Head office
Ampicillin sodium salt, 10 g	Carl Roth GmbH + Co. KG	Karlsruhe
SOC Outgrowth Medium	New England BioLabs	Ipswich
LB-Medium (Lennox)	Carl Roth GmbH + Co. KG	Karlsruhe
Agar-Agar, Kobe I	Carl Roth GmbH + Co. KG	Karlsruhe

Table 2.16: LB agar

Reagent	Quantity
Agar-Agar	6 g
LB Lennox	8 g
water	400 ml
heat in the autoclave, shake and cool down	

Table 2.17: LB medium

Reagent	Quantity
LB-Medium (Lennox)	20 g
water	1 l
autoclave for 20 min at 121 °C and close the lid straight afterwards	

Table 2.18: Bacteria

Name	Catalogue number	Producer/Reference
E.coli ChemiComp GT115	gt115-11	ThermoFisher Scientific
NEB® 5-alpha Competent E. coli	C2987	New England BioLabs
pGL4-gateway-SCP1 vector containing bacteria	DR2064	sent in bacteria as agar stab, cloned into DH5alpha
Subcloning effieciency DH5a competent cells	18265-017	ThermoFisher Scientific

2.1.5 Cell culture

Table 2.19: Cell culture reagents

Name	Producer	Head office
Amphotericin B 250 µg/ml	Biochrom GmbH	Berlin
Ciprofloxacin 5g	Sigma-Aldrich	St. Louis
DPBS	Gibco - ThermoFisher Scientific	Waltham
FBS Superior	Biochrom GmbH	Berlin
Gentamicinsolution 10 mg/ml	Sigma-Aldrich	St. Louis
IMDM 500 ml	Gibco - ThermoFisher Scientific	Waltham
L-Glutamine 200mM (100X)	Gibco - ThermoFisher Scientific	Waltham
Pen Strep Penicillin Streptomycin	Gibco - ThermoFisher Scientific	Waltham
Puromycin 10 mg/ml	Gibco - ThermoFisher Scientific	Waltham
Trypan Blue Solution	Sigma-Aldrich	St. Louis

Table 2.20: Cell culture media

Name	Composition
Conditioned medium	IMDM 500ml 1 % Pen/Strep 10 % FBS 20 % OCI-Ly1 supernatant
Hunger medium	IMDM 500ml 1 % Pen/Strep
IMDM 10%	IMDM 500ml 1 % Pen/Strep 10 % FBS
IMDM 20%	IMDM 500ml 1 % Pen/Strep 20 % FBS

Table 2.21: Cytomix (120)

Reagent	Quantity
K2HPO4- KH2PO4	10 mM
KCl	120 mM
CaCl2	0,15 mM
HEPES	25 mM
EGTA	2 mM
MgCl2	5 mM
water	to 200 ml
ATP powder	2 mM
Glutathione	5 mM
adjust to pH 7.6	
sterile-filtered, stored at - 20°C	

Table 2.22: Cell lines

Name	RRID	Provided by
HBL-1	CVCL_4213	AG Lenz
OCI-ly1	CVCL_1879	AG Lenz
OCI-ly3	CVCL_8800	AG Lenz

2.1.6 Software

Table 2.23: Software

Purpose	Name	Producer	Head office
Primer design	Basic Local Alignment Search	National Center for Biotechnology	Bethesda

	Tool (BLAST)	Information	
	Integrative Genomics Viewer	Broad Institute	Cambridge, USA
	NEB Tm Calculator	New England BioLabs	Ipswich
	SnapGene Viewer	GSL Biotech LLC	Chicago
CRISPR sgRNA design	GPP Web Portal	Broad Institute	Cambridge, USA
Ligation calculation	NEBio Calculator	New England BioLabs	Ipswich
Luciferase measurements	MikroWin 2000	Labsis Laborsysteme GmbH	Neunkirchen-Seelscheid
Spectrophotometer measurements	NanoDrop 1000 Spectrophotometer V3.3.0	NanoDrop Technologies	Wilmington
Gel documentation	Quantity One 1-D Analysis Software	BioRad	Hercules
RT-qPCR analyses	StepOne Software V2.3	ThermoFisher Scientific	Waltham
Statistical analyses	GraphPad Prism 6.0	GraphPad Software	San Diego
	Microsoft Office 2011 Excel	Microsoft Corporation	Redmond
Writing and citations	Microsoft Office 2011 Word	Microsoft Corporation	Redmond
	RefWorks	Ex Libris - ProQuest Company	Ann Arbor
Figure design	BioRender	Aoki, S.; Shteyn, K.;Marien, R.	Toronto
	MicrosoftOffice 2011 Powerpoint	Microsoft Corporation	Redmond

2.2 Methods

2.2.1 Cell culture

Cell culture work is done sterile. The working bench was treated with UV-light every morning and disinfected with 70 % ethanol before and after working there. Every item taken to the working bench was disinfected as well; hands were washed and sanitised.

OCI-ly1 and OCI-ly3 (Ontario Cancer Institute, Cell Line ly3) cells were cultured at a density of approximately 200.000 cells/ml in T25, T75 or T175 cell culture flasks. OCI-ly1 cells were maintained in IMDM 10 %; OCI-ly3 cells in IMDM 20 %. For splitting, cells were diluted at a ratio of 1/6 (e.g., 8.5 ml cell-containing medium from the old flask and 51.5 ml new medium) or 1/8 every two or three days. When cells needed to be centrifuged for example for counting or resuspension in a new medium, this was always done for 5 minutes at 20 °C and 314 g.

2.2.1.1 Cell count

Cells were centrifuged, and the pellet was resuspended in 0.1 to 10 ml cell culture medium. 10 µl of this suspension were again diluted with 90 µl trypan blue, which is a dye that helps to

distinguish between living and dead cells, as living cells do not take up the dye whereas dead cells are no longer able to prevent it from infiltrating and turn blue. A Neubauer chamber and a correspondent cover glass were cleaned with 70 % ethanol, placed over one another, and the cleft in between was filled with the trypan blue stained aliquot. Cells were counted using an inverted microscope. All four squares were counted, and the mean value was used for final cell count determination considering the respective dilution factors (e.g., multiplied with 10 for the trypan blue dilution and, if necessary, multiplied with 10 when the cell pellet was taken up in 10 ml medium) and chamber volumes (multiplied with 10.000).

2.2.1.2 Freezing and defreezing cells

To freeze cells 5 – 10 million cells were pelleted by centrifugation. The pellet was resuspended in medium containing 10 % DMSO (dimethyl sulfoxide), and the suspension was transferred to labelled freezing tubes. In a freezing container, which provides a constant cooling rate of 1 °C per minute, the tubes were left in a -20 °C freezer for one night and the next day placed in a -80 °C freezer for 24 hours. Cells were then left in the -80 °C freezer or transferred into a N2 tank for long-term storage.

In order to defreeze cells, medium was preheated, frozen cells were thawed in a 37 °C water bath and transferred into falcon tubes containing 10 – 20 ml warm medium. They were spun down and the cell pellet was resuspended in normal medium, plated at a density of 200.000 cells/ml and incubated at 37 °C.

2.2.2 Molecular biology

2.2.2.1 Agarose gel and gel electrophoresis

Gel electrophoresis is a method to separate DNA strands relating to their size. Probes are placed into an agarose gel and when applying an electric current to the gel, they migrate through the electric field. DNA is negatively charged, which makes it migrate towards the positive electrode. As smaller DNA strands encounter less resistance from the gel, they migrate faster than the bigger strands and therefore cover a larger distance. This method is used to check for the correct size of DNA strands or to furthermore purify the relevant DNA probe.

To produce an agarose gel, 200 ml TAE (TRIS-acetate-EDTA) buffer were mixed in a glass flask with the respective amount of agarose powder (e.g., 2 g for a 1 % gel) and then boiled in the microwave. After cooling down, 17.5 µl ethidium bromide were added. Ethidium bromide binds to the DNA strands and enables the visualization of DNA under UV-light. The fluid gel was then poured into a gel tray and a comb that creates small pouches for the probes was placed. Any produced air bubbles were removed and the gel was then left to harden. After approximately 20 minutes it was transferred into a gel box (full with TAE buffer) and the comb was removed before loading the gel with the probes. The latter were mixed with 10 µl 6x loading buffer,

colouring and weighting the probes to simplify the loading of the pouches. One or two pouches were loaded with molecular weight ladders (1 kb and/or 100 bp), which contain standardized DNA sizes and make it possible to read off the exact size of a migrated DNA probe.
The gel was run for approximately 30 minutes at 130 V, 300 mAmp and 300 W or 1 hour and 100 V, 300 mAmp and 300 W, and then placed into a gel imager, where UV-light was applied and probe sizes were checked and cut out with a scalpel as needed. As the probes were still covered in gel, they were purified, using a gel purification kit.

2.2.2.2 Nanodrop

A nanodrop spectrophotometer is based on the principle of measuring the absorbance of molecules at different wavelength (e.g., 260 nm for DNA). 1 µl sample was applied to the machine and the given result was surveyed concerning purity and therefore usability. Purity was determined by the absorbance curve's peaks and with the aid of the 260/280 and 260/230 ratios. (114)

2.2.3 Silencer cloning and luciferase assay

2.2.3.1 Preparation of the receiving vector 5'

Frozen bacteria, containing the pGL4-gateway-SCP1 vector, were thawed on ice and few µl were transferred into 250 ml LB-ampicillin (100 µg/ml) to grow at 37 °C and 180 rpm for 24 hours. The plasmids were purified with a Maxiprep kit**,** following the manufacturers instructions. 5 µg from the purified vector were digested in a 50 µl reaction with BglI and BglII (Table 2.24) and then separated on a 0.8 % agarose gel, run at 100 mV for 1 hour, cut out and purified with a gel purification kit.

Table 2.24: Vector digestion 5'

Reagent	Quantity
pGL4-gateway-SCP1 vector	5 µg
BglI	1 µl
BglII	1 µl
NEB buffer 3.1	5 µl
water	to 50 µl
2 hours at 37 °C	

2.2.3.2 Silencer PCR 5'

To obtain the silencer DNA strands of interest, primers flanking the DNA sequence of interest were designed via PrimerBlast and ordered from Eurofins Genomics. They were diluted with 10 mM Tris-buffer to a 10 µM working solution. The silencer sequence was then amplified from

genomic HBL-1 DNA (obtained with the DNeasy Blood & Tissue Kit) via a polymerase chain reaction (PCR) (Table 2.25, Table 2.26, see also manufacturer's instcructions), run on a 1 % agarose gel (130 mV, 45 min) and purified with the gel purification kit as well as AMPure XP beads if the simple gel purification was not sufficient**.** For the purification with DNA-binding beads water was added to the sample to obtain 50 µl reaction volume. 40 µl AMPure XP paramagnetic beads were added (0.8x ratio), and the mixture was incubated at room temperature for 5 minutes to let the beads bind to the DNA. The tube was placed on a magnet for 2 minutes before carefully aspirating the liquid. To wash the beads, 200 µl 80 % ethanol were added and removed after 30 seconds. This step was done twice and the beads were then left to air-dry for 5 minutes. The tube was removed from the magnet and the beads were resuspended in 20 µl elution buffer (10 mM Tris, pH 7.4). After 5 minutes incubation at room temperature, the tube was placed on the magnet again for 2 minutes, then the DNA containing liquid was transferred into a new tube.

Table 2.25: Silencer PCR reagents

Reagents	Quantity
gDNA	100 ng
primer fwd	1.5 µl
primer rev	1.5 µl
2x KAPA HiFi HotStart Ready Mix (including the polymerase)	25 µl
water	to 50 µl

Table 2.26: Silencer PCR 35 cycles

Phase	Temperature, Time
Initialization	95 °C, 3 minutes
Denaturation	98 °C; 20 seconds
Annealing	primer specific annealing temperature (calculated with NEB Tm Calculator), 30 seconds
Elongation	72 °C, 15 seconds
Final elongation	72 °C, 1 minute
Final hold	4 °C

2.2.3.3 Silencer cloning and bacterial transformation 5'

Digested vector and silencer inserts were fused in a 5 µl FusionHD ligation reaction (Table 2.27). LB agar plates were prepared before starting the transformation. Previously prepared LB agar (Table 2.16) was melted in the microwave, cooled down to a temperature around 35 °C and ampicillin was added at a ratio of 1/1000 (to 100 µg/ml). The fluid agar was then poured into sterile petri dishes (100 mm x 15 mm) and allowed to cool down and harden. As bacterial work is done as sterile as possible, all the steps were performed in close proximity to a burning Bunsen burner.

For the bacterial transformation 50 µl *Escherichia coli* GT115 were thawed on ice, then mixed with 2.5 µl cloning reaction and incubated on ice for 30 minutes. To make the bacterial cell wall permeable for the plasmids, the bacteria were heatshocked in a water bath at 42 °C for 30 seconds. After having incubated the mixture on ice again for 2 minutes, it was shaken in 950 µl SOC medium at 300 rpm and 37 °C for 1 hour to allow the bacteria to recover. 150 µl bacteria solution were plated on a LB-ampicillin agar plate with a sterile glass cell spreader and grown overnight at 37 °C.

Table 2.27: FusionHD ligation reaction

Reagent	Quantity
cut vector	25 ng
silencer insert	x µl
(5:1 molar excess over vector,	
calculated with NEBio Calculator)	
FusionHD (5x Master Mix)	1 µl
water	to 5 µl
50 °C for 15 minutes	

2.2.3.4 Colony PCR

The next day 6 clones per insert were picked with a sterile tip. Each clone was first tapped into the PCR mix (Table 2.28) and then shaken off into a 96-well plate well with 100 µl LB-ampicillin (100 µg/ml). PCR was run (Table 2.29) and the 96-well plate was incubated at 37 °C. On a 2 % agarose gel (120 V, 45 min) the product size was checked, positive colonies were transferred into 8 – 10 ml LB-ampicillin (two tubes per colony) and left to grow overnight (180 – 200 rpm, 37 °C). The following day plasmids were purified with a Midiprep kit and plasmid-containing bacteria were frozen with 1:10 DMSO.

Table 2.28: Colony PCR reagents

Reagent	Quantity
bacteria	1 tip
primer fwd	1 µl
primer rev	1 µl
Taq-polymerase (GoTaq G2 Hot Start Green Master Mix)	10 µl
water	8 µl

Table 2.29: Silencer PCR 30 cycles

Phase	Temperature, Time
Initialization	95 °C, 2 minutes
Denaturation	95 °C, 30 seconds
Annealing	58 °C, 30 seconds
Elongation	72 °C, 30 seconds
Final elongation	72 °C, 1 minute
Final hold	4 °C

2.2.3.5 Sequencing

After Midiprep purification, plasmids were prepared following the instructions of Eurofins Genomics and sent there for sequencing.

2.2.3.6 Transfection to B-cells

Transfection was done in groups of 6 replicates per approach. For each replicate 1 million cells were harvested and spun down, resuspended in 300 µl Cytomix (Table 2.21), mixed with 1 µg plasmid DNA (Firefly) and 200 ng *pRL-TK* (HSV-thymidine kinase promoter) (for OCI-ly3 cells) / 300 ng *pRL-TK* (for OCI-ly1 cells). The mix was electroporated in electroporation cuvettes with the Gene Pulser Xcell (275 V – 20 ms – 1 SW for OCI-ly1 cells**,** 250 V – 10 ms – 1 SW for OCI-ly3 cells), diluted with 200 µl prewarmed medium and transferred to 700 µl medium.

2.2.3.7 Luciferase assay

A luciferase assay was performed to measure the activity of the inserted regulatory element: The pGL4-gateway-SCP1 vector contains a luciferase gene, and according to the potency of the inserted silencer, more or less luciferase enzyme is transcribed. The amount of emitted light, which is proportional to the number of transcribed and translated luciferase enzymes, is measured after adding luciferase substrate (LARII). As the amount of luciferase enzyme corresponds to the activity of the inserted silencer, its potency is hereby predicted. To minimize pipetting mistakes and global silencer-independent effects, Renilla-TK, a control plasmid with its own luciferase enzyme and substrate (Stop-and-Glo) is used. (10)

For the luciferase assay, a Promega Dual-Luciferase Assay Kit was applied according to the manufacturer's instructions. Briefly: cells were harvested 24 hours after transfection, spun down, resuspended in 500 µl PBS (phosphate-buffered saline), spun down again and resuspended in 25 µl passive-lysis-buffer (diluted 1:5). The solution was then slowly shaken at room temperature to accelerate cell lysis. After 15 minutes 20 µl of the lysate were transferred to a white 96-well PCR plate and luciferase activity was measured using a microplate reader with a specific program for luciferase assays (Table 2.30).

Table 2.30: Luciferase program, MicroWin 2000

Phase	Description
Dispense	injection LARII, 100 µl volume, middle speed
Shake	duration 3 seconds, fast speed, diameter 3.0, orbital type
Delay	duration 2 seconds
Firefly	counting time 10 seconds
Dispense	injection Stop-and-Glo-buffer, 100 µl volume, middle speed
Shake	duration 3 seconds, fast speed, diameter 3.0, orbital type
Delay	duration 2 seconds
Renilla	counting time 10 seconds

2.2.3.8 Silencer cloning and luciferase assay at 3' position

To test out the position dependency of the silencer element, different positions within the plasmid were tried out. The 3' positions refer to a location downstream of the promoter, and for every position a new silencer cloning was performed. 5' from the promoter the plasmid normally contains a suicide gene, which was cut out when annealing the silencer in the 5' position mentioned above. In order to obtain a plasmid where inserts can be placed at a 3' position, this suicide gene was cut out and replaced by non-functional oligonucleotides before starting the silencer cloning. The pGL4-gateway-SCP1 vector was digested with BglI and BglII as when prepared for the 5' position silencer cloning (see chapter 2.2.3.1). The excised suicide gene was replaced by annealed oligonucleotides (Table 2.31) in a 10 µl ligation reaction (Table 2.32). The new plasmid was transformed into *E coli* GT115 as described in chapter 2.2.3.3 and the next day checked for positive colonies with the colony PCR (see chapter 2.2.3.4). Positive colonies were grown overnight, frozen and purified with a Maxiprep kit. The new plasmid without suicide gene was then called vector-SG.

Table 2.31: Annealing oligonucleotides

Reagent	Quantity
oligos fwd	1 µl
oligos rev	1 µl
annealing buffer (Table 2.14)	48 µl
5 minutes at 95 °C	

Table 2.32: Ligation reaction

Reagent	Quantity
annealed Oligos (diluted 1:10)	1 µl
cut vector	50 – 100 ng
T4 ligase	1 µl
T4 buffer	1 µl
water	to 10 µl
1 hour at room temperature	

Silencer PCRs were performed as described above (chapter 2.2.3.2) with new primers with different overhangs (see Table 2.9). The new receiving vector (vector-SG) was cut with different enzymes, depending on where the silencer was to be inserted. The following positions were created:

- **3'_h_fwd_position**: silencer downstream of the polyadenylation (poly-A-) signal, forward orientation
- **3'_h_rev_position**: silencer downstream of the poly-A-signal, reverse orientation
- **3'_z_fwd_position**: silencer between luciferase gene and poly-A-signal, forward orientation
- **3'_z_rev_position**: silencer between luciferase gene and poly-A-signal, reverse orientation
- **3'_v_fwd_position**: silencer between promoter and luciferase gene, forward orientation
- **3'_v_rev_position**: silencer between promoter and luciferase gene, reverse orientation

The vector for the 3'_h_fwd/rev position was cut with PshAI (Table 2.33) and fused with the new inserts with a FusionHD ligation reaction as described above (Table 2.27).

Table 2.33: Vector digest 3'_h_fwd/rev

Reagent	Quantity
vector-SG	5 µg
PshAI	1 µl
Cutsmart buffer	5 µl
water	to 50 µl
2 hours at 37 °C	

For the 3'_z_fwd/rev_position the vector was cut with FseI and XbaI (Table 2.34) and ligated with the new inserts in a T4 ligation reaction (Table 2.35).

Table 2.34: Vector digest 3'_z_fwd/rev

Reagent	Quantity
vector-SG	5 µg
FseI	1 µl
XbaI	1 µl
Cutsmart buffer	5 µl
water	to 50 µl
2 hours at 37 °C	

Table 2.35: T4 ligation reaction

Reagent	Quantity
silencer insert (5:1 molar excess over vector, calculated with NEBio Calculator)	x µl
cut vector	50 ng
T4 ligase (1:5 diluted)	1 µl
T4 buffer (stock 10x)	2 µl
water	to 20 µl
1 hour at room temperature	

HindIII and NheI were used to cut the vector for 3'_v_fwd/rev position (Table 2.36), the inserts were ligated with help of FusionHD (Table 2.27).

Table 2.36: Vector digest 3'_v_fwd

Reagent	Quantity
vector-SG	5 µg
HindIII	1 µl
NheI	1 µl
Cutsmart buffer	5 µl
water	to 50 µl
2 hours at 37 °C	

Bacterial transformation, colony PCR, sequencing and luciferase assay were conducted as described in the silencer cloning 5' protocols (chapters 2.2.3.3 - 2.2.3.7).

2.2.3.9 Site directed mutagenesis

Site directed mutagenesis is a principle where specific mutations are inserted into a plasmid. Special primers that comprise the silencer region with the mutation contain the modified bases, providing a template for the mutation that is to be recreated. In an inverse PCR reaction these primers create a linear plasmid copy with the mutation within (Figure 2.1). A kinase phosphorylates both ends of the copy, enabling the ligase to ligate the linear construct to a circle, and the enzyme DpnI removes all original templates (81). The mutated plasmid is then transformed into NEB® 5-alpha competent *E coli.*

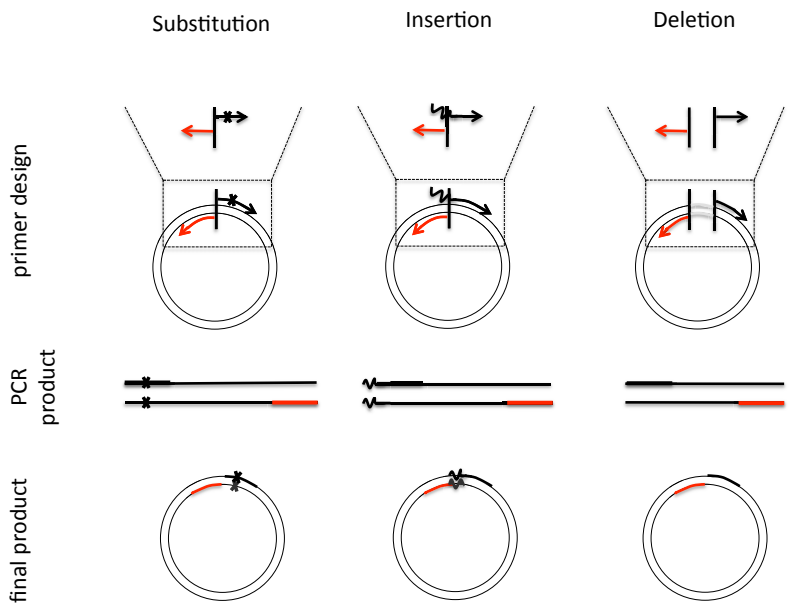

Figure 2.1: Generation of different mutation types with site-directed mutagenesis With an inverse PCR, different types of mutations can be created: For a base pair substitution, primers containing the new base are used. For an insertion the base pairs to be inserted are added to one end of the primer. To introduce a deletion, the PCR primers are created to leave out the region to be deleted. After the inverse PCR, the replicated DNA with the mutation of interest represents a linear construct and can then be transformed into a plasmid. (Figure adapted from (81).)

A Q5® Site-Directed Mutagenesis Kit was used according to the manufacturer's instructions: After the mutagenesis PCR (Table 2.37, Table 2.38), the KLD-reaction (kinase, ligation, DpnI) was performed with 1 µl PCR product (Table 2.39); then 5 µl KLD-reaction mix were transformed into ice cold NEB® 5-alpha competent *E coli* bacteria (see chapter 2.2.3.3, similar to the manufacturer's instructions).

Table 2.37: Mutagenesis PCR reagents

Reagent	Quantity
template DNA	1 ng
primer fwd	1.25 µl
primer rev	1.25 µl
Q5 Mastermix	12.5 µl
water	25 µl

Table 2.38: Mutagenesis PCR, 25 cycles

Phase	Temperature, Time
Initialization	98 °C, 30 seconds
Denaturation	98 °C, 10 seconds
Annealing	primer specific annealing temperature, 30 seconds
Elongation	72 °C, 30 seconds per kb
Final elongation	72 °C, 2 minutes
Final hold	4 °C

Table 2.39: KLD reaction

Reagent	Quantity
PCR product	1 µl
KLD reaction buffer	5 µl
KLD enzyme mix	1 µl
water	3 µl
5 minutes at room temperature	

After colony PCR, midiprep and plasmid purification (as in chapter 2.2.3.4) the now mutated silencer insert (verified via sequencing) was cut out and annealed into a new pGL4-gateway-SCP1 vector to ensure there were no newly created mutations within the luciferase gene. The mutated silencer insert for the 3'_z_fwd/rev_position and the undigested vector were cut in the vector digestion reaction with XbaI and FseI (Table 2.40). Mutated insert and cut vector were fused in the T4 ligation reaction (Table 2.35). Hereafter the plasmid was again sequenced to confirm that there is only the intended mutation within the silencer insert.

Table 2.40: 2° vector digest 3'_z_fwd/rev

Reagent	Quantity
vector	10 µg
FseI	1 µl
XbaI	1 µl
Cutsmart buffer	2 µl
water	to 50 µl
2 hours at 37 °C	

The verified mutated plasmid was then transfected to OCI-ly1 and OCI-ly3 cells for luciferase assays (see chapters 2.2.3.6 – 2.2.3.7).

2.2.4 CRISPR-Cas9 silencer knockout

2.2.4.1 Puromycin killing curve

As cells with successful transfection were selected on the basis of their newly acquired puromycin resistance, a general puromycin killing curve for OCI-ly1 cells was generated beforehand. Cells were seeded at 400.000 cells in 2 ml and puromycin concentrations from 0.2 – 1.2 µg/ml were added. After two days living and dead cells were counted and the minimal concentration of puromycin that can kill over 95 % of cells was determined (0.4 µg/ml).

2.2.4.2 SgRNA cloning and plasmid preparation (according to (96))

For the CRISPR-Cas9 silencer knockout a dual vector system was used. Each vector contained a Cas9 gene to encode the enzyme. Vector px458 additionally comprised a *GFP* (green fluorescent protein) ORF (open reading frame) and vector px459 a puromycin N-acetyl-transferase gene (puromycin resistance). Two different single-guide RNAs (sgRNA), that direct the Cas9 to the region of interest, were used to cut out the silencer region. One sgRNA was inserted into the px458 vector, one into the px459 vector. Two different sgRNA pairs were tested (for exact sgRNA sequences see Table 2.9), from which one was selected based on performance for downstream studies (mut_gRNA3/4).

5 µg of the px458/459 vectors were digested with BbsI (Table 2.41), run on a gel, cut out and purified, dephosphorylated with Antarctic phosphatase (Table 2.42) and cleaned by running it on a gel, cutting it out and purifying it again. SgRNA oligonucleotids were annealed in a 10 µl reaction with T4 polynucleotide kinase (Table 2.43) and then ligated into the dephosphorylated and digested vector using T4 ligase (Table 2.44). Vector px458 was ligated with one time mut_gRNA1 and one time mut_gRNA3 and vector px459 with mut_gRNA2 and mut_gRNA4. A control without the annealed oligonucleotides was done at the same time. The following bacterial transformation of 10 µl plasmid to *DH5alpha*, the colony PCR, the midiprep and the sequencing were done as described before (see chapters 2.2.3.3 – 2.2.3.5).

Table 2.41: Vector px458/459 digestions

Reagent	Quantity
vector	5 µg
BbsI	1 µl
Cutsmart buffer	2 µl
water	to 20 µl
37 °C, o/n	

Table 2.42: Vector px458/459 dephosphorylation

Reagent	Quantity
digested vector	20 µl
Antarctic phosphatase	1 µl
Antarctic phosphatase reaction buffer	3 µl
water	to 30 µl
80 °C, 2 minutes	

Table 2.43: SgRNA annealing

Reagent	Quantity
sgRNA fwd	1 µl
sgRNA rev	1 µl
T4 polynucleotide kinase	1 µl
T4 ligation buffer 10x	1 µl
water	to 10 µl
37 °C, 30 minutes 95 °C, 5 minutes to 25 °C at 5 °C/minute	

Table 2.44: SgRNA ligation

Reagent	Quantity
digested vector	1 µl
annealed sgRNA (diluted 1:200)	6 µl
T4 ligase	1 µl
T4 ligation buffer	2 µl
water	to 20 µl
> 2 hours at 16 °C	

2.2.4.3 Transfection of OCI-ly1 cells

After counting, 10 million cells were spun down and resuspended in 500 µl Cytomix. 20 µg vector were added: 10 µg px458 with mut_gRNA1 and 10 µg px459 with mut_gRNA2; 10 µg px458 with mut_gRNA3 and 10 µg px459 with mut_gRNA4; control group with 20 µg GFP vector. Cells were electroporated (275 V – 20 ms – 1 SW) and transferred into 9 ml medium.

2.2.4.4 Selection for transfected cells

The *GFP* gene on vector px458 and the puromycin resistance gene on vector px459 made it possible to select cells with successful transfection. After selection only cells that contained both vectors and therefore both sgRNAs remained.

24 hours after transfection, 0.4 µg/ml puromycin were added for one day. GFP positive cells were then single cell sorted with a BD FACSAria III sorter into 100 µl IMDM containing 20 % FBS, 1 % penicillin/streptomycin and 20 % conditioned medium. Conditioned medium was made by extracting the supernatant of regular OCI-ly1 cell cultures and then filtering the liquid with a 0.2 µm filter. In addition to the single cell sort, a GFP positive bulk of cells was created to allow early screening. Gentamicin, ciprofloxacin and amphotericin B were added to a

concentration of 10 µg/ml, 10 µg/ml and 0,25 µg/ml respectively to prevent contamination. The cells were then left to grow for several days.

2.2.4.5 Bulk screen

A bulk screen was performed to find out whether the knockout in general had worked or not. Genomic DNA (gDNA) was extracted from the bulk with a DNeasy Blood & Tissue Kit and the region of interest was amplified with a bulk screen PCR (Table 2.45, Table 2.46) and separated on a gel. Positive knockout cells showed a 46 bp shorter band. Bands were cut out, purified with a gel extraction kit and then sent for sequencing. Positive bulks were frozen in growth medium containing 10 % DMSO.

Table 2.45: Bulk screen PCR reagents

Reagent	Quantity
gDNA	1 µl
mut_PCR_primer_rev	1.25 µl
mut_PCR_primer_fwd	1.25 µl
GoTaq G2 HotStart Polymerase	6.25 µl
water	12.5 µl

Table 2.46: Bulk screen PCR, 35 cycles

Phase	Temperature, Time
Initialization	95 °C, 3 minutes
Denaturation	95 °C, 30 seconds
Annealing	58 °C, 30 seconds
Elongation	72 °C, 1.2 minutes
Final elongation	72 °C, 5 minutes
Final hold	4 °C

2.2.4.6 Clone screening

Single cell clones were expanded for some weeks and subsequently transferred into 48/24/12/6 well plates. As soon as a sufficient number of cells had grown, they were screened for effective deletion of the genomic region of interest. Cells were spun down and resuspended in tail lysis buffer (Table 2.13) and proteinase K to extract gDNA (Table 2.47). The gDNA was amplified with the bulk screen PCR (Table 2.45, Table 2.46) and examined on an agarose gel.
Knockout clones from the end-point PCR were further screened to ensure that the knockout had occurred at the correct place and to see if the silencer really had been completely knocked out. For this a quantitative PCR (qPCR) was performed with gDNA from the DNeasy Blood & Tissue Kit and primers that would bind within the knockout region (primer1/2_mut_region) (Table 2.48, Table 2.49). Knockout clones were supposed to show no signal (see also figure 3.8 A, page 59).

Table 2.47: Clone screen gDNA extraction

Reagent	Quantity
Tail lysis buffer	50 µl
Proteinase K	1.5 µl
55 °C, 2.5 hours	
95 °C, 10 minutes	

Table 2.48: Clone screen qPCR

Reagent	Quantity
gDNA	1 µl
primer fwd	1 µl
primer rev	1 µl
PSG MM (SYBR Green)	12.5 µl
water	9.5 µl

Table 2.49: Clone screen qPCR program

Phase	Temperature, Time
Initiation	95 °C, 10 minutes
40 Cycles	95 °C, 15 seconds
	60 °C, 1 minute
Step & hold	95 °C, 15 seconds
	60 °C, 1 minutes
	95 °C, 15 minutes

2.2.4.7 RT-qPCR for κB-RAS1 and RPL15 (as described in RevertAid First Strand cDNA Synthesis Kit)

The expression of κB-Ras1 was assessed in knockout clones with a reverse transcriptase qPCR (RT-qPCR). In a first step approximately one million cells were spun down, and the pellet was used to extract RNA with a Qiagen RNeasy Mini Kit and the Qiashredder following the manufacturer's instructions and including the optional on column DNAse digest.

Reverse transcriptase is an enzyme that transcribes RNA into cDNA, which is then used for a qPCR. The cDNA synthesis was done with the Revert Aid First Strand cDNA Synthesis Kit, first using a random hexamer primer to anneal to the RNA (Table 2.50) and then performing the cDNA synthesis (Table 2.51).

Table 2.50: RNA primer annealing

Reagent	Quantity
RNA	60 ng
random hexamer primer	1 µl
DEPC water	to 12 µl
65 °C, 5 minutes	
on ice	

Table 2.51: cDNA synthesis

Reagent	Quantity
reaction buffer	4 µl
Ribolock	1 µl
dNTPs	2 µl
RevertAid RT / water	1 µl
RNA mix (primer annealed)	12 µl
25 °C, 5 minutes	
42 °C, 60 minutes	
70 °C, 5 minutes	

For the κB-Ras1 cDNA detection a qPCR was performed with the primer pair hkB1_RT_F/R as well as primers for a house keeping gene (*GAPDH* (glyceraldehyde-3-phosphate dehydrogenase)) (Table 2.52, Table 2.53). With this house keeping gene measurement samples can be normalized and pipetting mistakes, different amounts of background DNA levels or intracellular reverse transcriptases do no longer influence the results (62). Every sample was tested in duplicates and with both κB-Ras1 primers and GAPDH primers. A negative control with water instead of cDNA was also tested. Expression of RPL15 was measured following the same protocol, using different primers (RPL15_Ex_ex_2).

Table 2.52: κB-Ras1 qPCR

Reagent	Quantity
cDNA	1 µl
primer fwd	1 µl
primer rev	1 µl
Luna SYBR	5 µl
water	to 10 µl

Table 2.53: κB-Ras1 qPCR program

Phase	Temperature, Time
Initiation	95 °C, 10 minutes
40 Cycles	95 °C, 15 seconds
	60 °C, 1 minute
Step & hold	95 °C, 15 seconds
	60 °C, 1 minutes
	95 °C, 15 minutes

2.2.4.8 CTG assay (following the promega CTG-cell-viability-assay protocol (94))

A CTG (CellTiter-Glo) assay was used to evaluate the growth behaviour of the different clones based on the following luciferase triggered reaction:

$$\text{D-Luciferin} + O_2 + \text{ATP} \xrightarrow{+\text{ Luciferase, } + Mg^{2+}} \text{Oxyluciferin} + \text{PPi} + \text{AMP} + CO_2 + \text{light (94)}$$

As D-Luciferin and luciferase are added in a constant ratio, only the amount of ATP (adenosine triphosphate) is proportional to the emitted light. ATP is an indicator of metabolically active cells and is not produced by dead cells, which makes it a marker to look for living cells and to calculate cell growth rates (46).

Clones were measured in 24 – 48 hour intervals and each time the number of living cells was evaluated. In a pretest the optimal number of cells to start with per well had been determined to be 500 cells in 100 µl. On day 0 cells were counted, diluted to 500 cells/100 µl and transferred into white 96-well microplate reader plates. The wells at the border of the plate were filled with PBS, as they are more prone to dry up. 3 – 4 positive clones were compared to 3 – 4 unmodified OCI-ly1 samples. All wells for the following days were prepared on day 0. Cells were measured in triplicates every day by adding 25 µl CTG reagent per well and quantifying the amount of emitted light with help of the microplate reader (Table 2.54).

Table 2.54: MicroWin 2000, CTG program

Phase	Time
Shake	120 seconds
Delay	720 seconds
Shake	10 seconds
Measurement	1 second counting time

2.2.5 CRISPR-Cas9 *NKIRAS1* knockout

2.2.5.1 Plasmid preparation, transfection and selection for transfected cells

The plasmid preparation with *NKIRAS1* knockout sgRNAs was similar to the silencer knockout plasmid preparation (chapter 2.2.4.2). The plasmids px458_Ex2+81 and px459_Ex2-195 had already been created following the protocol by Ann Ran (96) and kindly provided by the working group of Dr. Andrea Oeckinghaus.

Transfection to OCI-ly1 cells, selection for transfected cells and bulk screen were the same as in the silencer knockout protocol (chapters 2.2.4.3 – 2.2.4.5). However different screening primers were used (kB1_Ex2_Screen_2, Table 2.9).

2.2.5.2 Clone screen

The clone screen was based on a similar principle as the clone screen for the silencer knockout: A bulk screen PCR was performed with gDNA extracted with proteinase K and tail lysis buffer (chapter 2.2.4.6). Afterwards however, clones with a complete knockout were determined via RT-qPCR. Cells with a successful knockout (-/-) had no intact *NKIRAS1* gene left and could therefore not produce any κB-Ras1 RNA and consequently no correspondent cDNA. There was no signal to be seen in RT-qPCR. The RT-qPCR was done as described earlier (chapter 2.2.4.7).

2.2.5.3 CTG assay

A CTG assay was performed after screening for -/- knockout clones (as in chapter 2.2.4.8). 3 – 4 of those -/- clones were compared to 3 – 4 +/+ knockout clones and OCI-ly1 samples.

2.2.6 Statistics

For statistical analyses the software GraphPad Prism 6.0 for Mac OS X, GraphPad Software, San Diego, California, USA (www.graphpad.com) and Microsoft Excel (2011), Microsoft Corporation, Redmond, were used. Experiments were repeated several times; the exact number of biological and technical replicates is stated in the graph legends. Bar graphs represent the mean and error bars indicate the standard deviation (SD). For the comparison of two independent groups (i.e., site-directed mutagenesis experiments and RT-qPCR experiments) the *P* value was calculated with the non-parametric Mann-Whitney-U test. When comparing multiple independent groups with one another (i.e., experiments regarding position dependency) the non-parametric correlate of the ANOVA (analysis of variance) – a Kruskal-Wallis test – was performed and a Dunn's test was furthermore used to allow statements about the individual difference between the separate groups. Non-parametric tests were chosen due to small numbers of cases ($n < 10$ in at least one of the groups compared).

3 Results

3.1 In silico analyses predict a silencer element in the first intron of *NKIRAS1*

The putative silencer element studied in this thesis was identified via STARR-Seq analysis and selected based on its potential impact on κB-Ras1 transcription levels and the location of mutations in DLBCL patients. It is located on chromosome 3 (position 23916632 – 23916765) in the first intron of the *NKIRAS1* gene (Figure 3.1). At position 23916720 a base substitution from cytosine to thymine is recurrently found in DLBCL patients: Data from Morin et al. show that 3 out of 33 DLBCL patients present this base substitution (74). However, an elevated base substitution rate at this position is also found in healthy individuals: A global study from TOPMed (Trans-Omics for Precision Medicine Program) shows that 47 % of the normal population feature a cytosine at position 23916720, while 53 % present a thymine (80). It is, therefore, more likely that the base pair substitution presents a single nucleotide polymorphism (SNP) than a mutation. SNPs describe genomic positions where one base is frequently (more than 1 %) alternated by a second base. SNPs occur very often in the human genome and do most of the time not lead to a functional difference, even though they can also result in a functional impact. (107) The putative silencer element therefore comprises a SNP in healthy people and DLBCL patients.

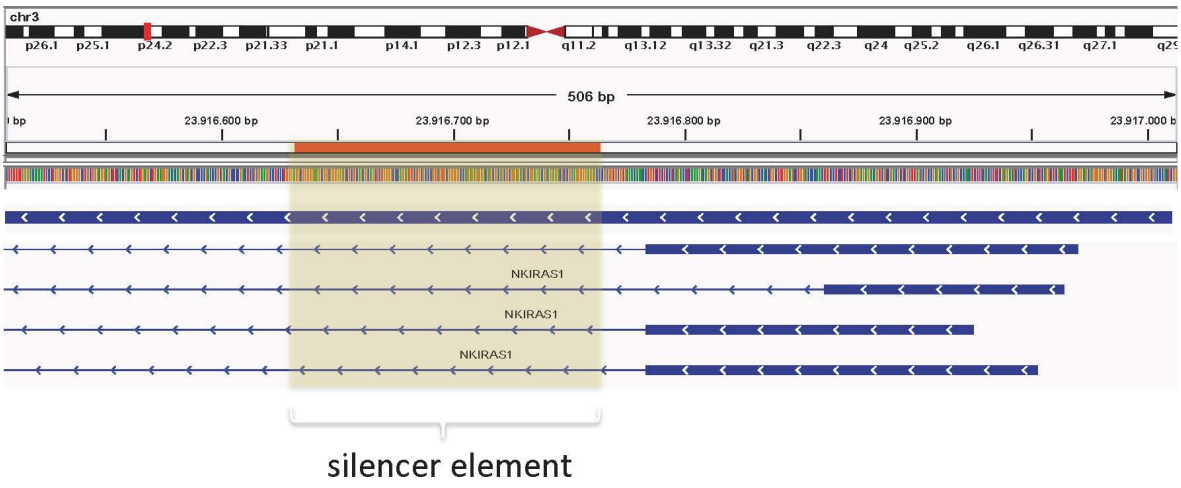

Figure 3.1: Position of the putative silencer in the genome

The 133 bp long regulatory element (in red) is positioned in the first intron of the *NKIRAS1* gene on chromosome 3. Data shown here is taken from the IGV viewer with the set of data for the Hg38 reference genome (99).

3.1.1 Histone modifications and ATAC-Seq data suggest an open chromatin region involved in active transcription processes

In cooperation with Alexander Tönges computational approaches with data from the ENCODE project have been applied to the regulatory element of interest in order to predict its characteristics and functions. To that end, human histone modification databases of the ABC cell line OCI-Ly3 generated by the Bradley Bernstein lab (Broad Institute) as part of the ENCODE project were used (ENCSR581LZU, ENCSR857GMX, ENCSR996GHD, ENCSR548PZS; available via https://www.encodeproject.org/). These analyses revealed H3K4me3 (3rd histone, 4th lysin, tri-metylation) and H3K9ac (3rd histone, 9th lysin, acetylation) marks at the putative silencer's position and very low signal concerning H3K27ac (3rd histone, 27th lysin, acetylation) and H3K4me1 (24,32). The acetylation of H3K27 as well as the mono-methylation of H3K4 are known to be associated with active enhancer elements (48,49,95) and especially the co-occurrence of both marks is thought to be an important characteristic of active enhancers (60). Given that both marks show little positivity at the position of the regulatory element, it seems unlikely that the element acts as an enhancer. On the other hand, the positive signals for H3K4me3 and H3K9ac are both found in the context of active transcription processes: Guenther et al. found H3K4me3 marks usually in close proximity to transcriptional start sites and describe them as a marker of promoter regions of active and repressed protein-coding genes (the more the gene is transcribed, the higher the levels of H3K4me3) (44). H3K4me3 is linked to transcription initiation (37,44) and favours H3K9 acetylation, which is proposed to enhance transcription initiation (36) by recruiting the super elongation complex and supporting polymerase II pause release in order to start elongation (37). On the other hand, Pekowska et al. also described H3K4me3 to be correlated with active enhancers (91). All things considered the positive marks for H3K4me3 and H3K9ac suggest that the regulatory element might be, to some extent, involved in transcriptional regulation – a presumption supported by the ATAC-Seq data produced by Alexander Tönges that show an open chromatin region at the predicted regulatory element (Figure 3.2). However, the missing H3K27ac and H3K4me1 signatures would argue against an enhancer element at this position. Thus, further validation is required to clarify whether this sequence could present another regulatory element, such as a silencer.

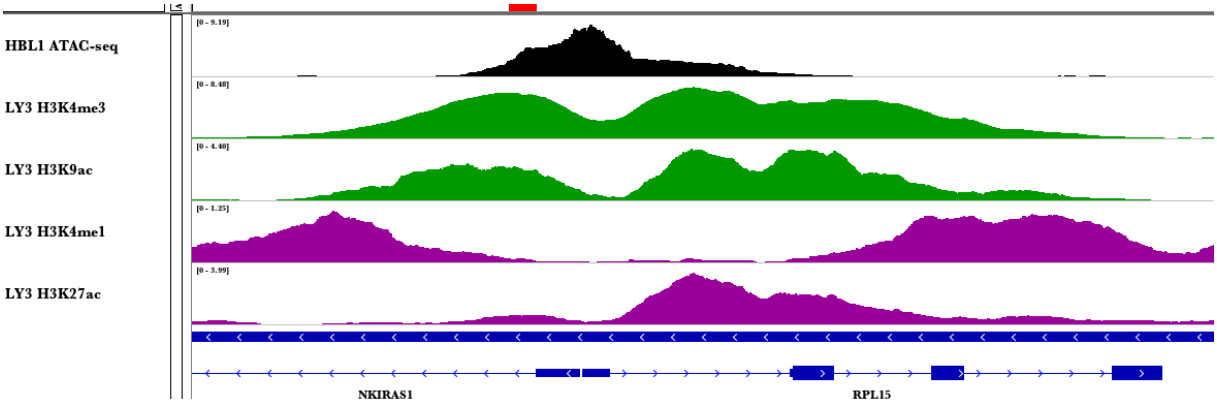

Figure 3.2: Histone modifications and ATAC-Seq data of the putative silencer element

The putative regulatory element (depicted in red) shows positive signals for H3K4me3 and H3K9ac and very few deflection concerning H3K4me1 and H3K27ac (24,32,99). In addition, unpublished ATAC-Seq data from Alexander Tönges (represented in black) show an open chromatin region at this element (Tönges, unpublished data).

3.1.2 Transcription factor binding analyses suggest binding of PAX5 to the silencer element

Different prediction tools (PROMO, JASPAR) were used to identify many potential transcription factor binding motifs for the putative silencer site and particularly promising matches have been found for the transcription factor PAX5 (paired box 5) (Figure 3.3 A) (33,56,72). PAX5 is a transcription factor essential for B-lymphopoiesis by repressing the transcription of lineage incongruous genes and activating gene expression important for B-cell development. It is also known to be deregulated in some B-cell lymphomas. (13,15) Publicly available ChIP-seq data, produced by the Richard Myers lab (HudsonAlpha Institute for Biotechnology) as part of the ENCODE project (again available via https://www.encodeproject.org, the data set with the accession number ENCSR000BHD was used) tend to support the prediction tools' notion and indicate that PAX5 could actually bind to the regulatory element in the lymphoblastoid cell line GM12878 (Figure 3.3 B) (24,32). Taken together, these published data are in line with the hypothesis that PAX5 might bind to the putative silencer element.

A

B

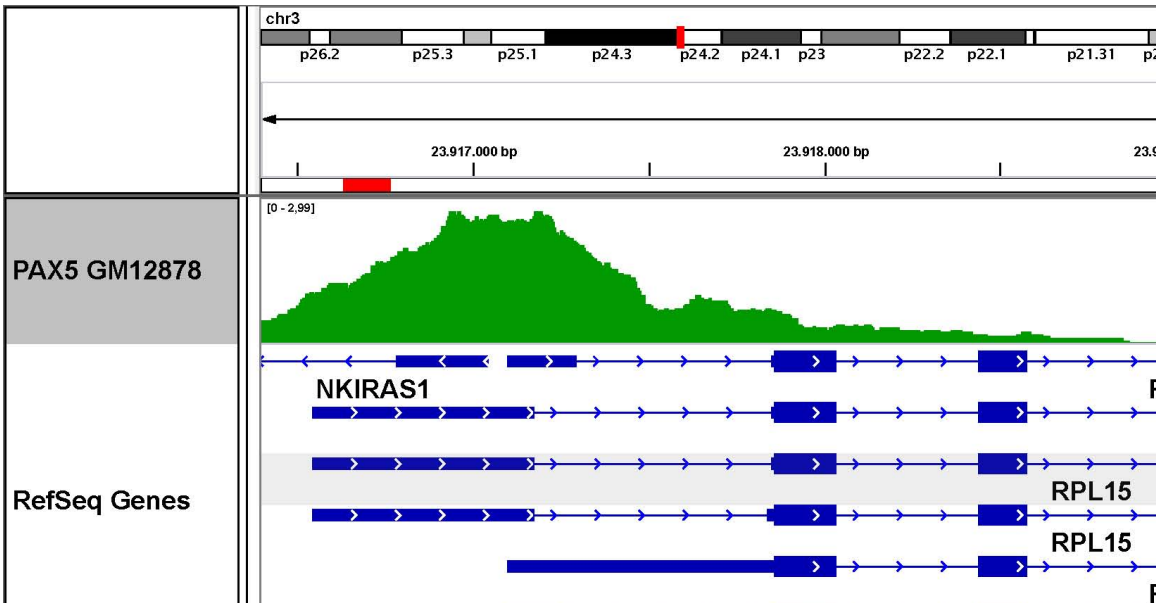

Figure 3.3: Evidence for PAX5 binding to the putative silencer element

(A) According to the publicly available prediction tool JASPAR the here presented transcription factor binding motif for PAX5 is present within the regulatory element. In the binding motif sequence redundant base pairs still allow transcription factor binding. In this illustration (taken from the open-access database JASPAR), preferential bases are featured taller than less frequent bases (52,56). **(B)** ChIP-Seq data, publicly available from the ENCODE project, show that PAX5 binds to the silencer element (depicted in red) in the cell line GM12878 (24,32,99).

3.2 Biological validation of the putative silencer element

To verify the suggestions resulting from these in silico analyses and also the predictions from previous high-throughput STARR-Seq experiments, the putative silencing function of the regulatory element was investigated in a luciferase assay in ABC (OCI-ly3) and GCB (OCI-ly1) cell lines.

3.2.1 Silencing activity is position-dependent

Attempting to reproduce the STARR-Seq assay's results, which had shown silencing activity from the regulatory element described here, the putative silencer was first inserted in a luciferase plasmid between luciferase gene and poly-A signal. In addition, the potential silencer element was tested in different positions (5' of the promoter, 3' right next to the promoter and downstream of the poly-A signal) and orientations (forward and reverse) within the plasmid (Figure 3.4 A). Interestingly, the silencing effect turned out to be not only dependent on the position and orientation, but also on the cell line in which the plasmid was transfected. In OCI-ly1 cells the silencer element shows silencing activity in all tested positions and orientations except the 5' position right upstream of the promoter (Figure 3.4 B). Concerning the strength of luciferase signal and thus the silencing activity, there was a significant difference between the tested positions (P<.0001), and the by far strongest silencing effect could be seen directly downstream of the promoter, whereas lower silencing activity was observed downstream of the poly-A signal. No significant orientation dependency could be observed.

A significant position dependency was also found in OCI-ly3 cells (P<.0001). However, silencing activity was only detected upon insertion directly downstream of the promoter or between luciferase gene and poly-A signal. In comparison to OCI-ly1 cells, the position 3' of the poly-A signal did not show a silencing effect (Figure 3.4 C).

Taken together, these data show that the putative silencer element negatively influences transcription levels depending on its position in the luciferase plasmid and the cell line used.

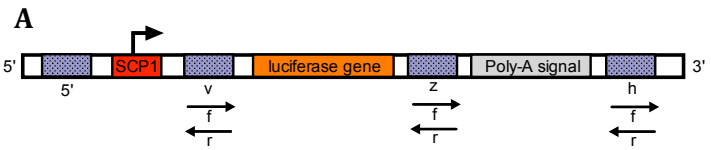
A
5'
SCP1
luciferase gene
Poly-A signal
3'
5'
v
z
h
f
r

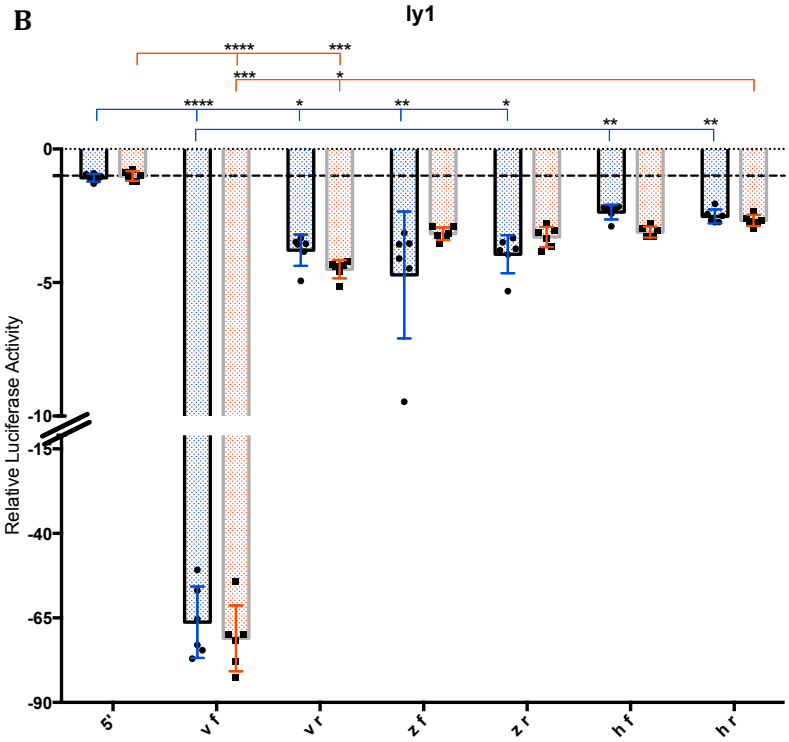
B
ly1
Relative Luciferase Activity
0
-5
-10
-15
-40
-65
-90
5'
v f
v r
z f
z r
h f
h r

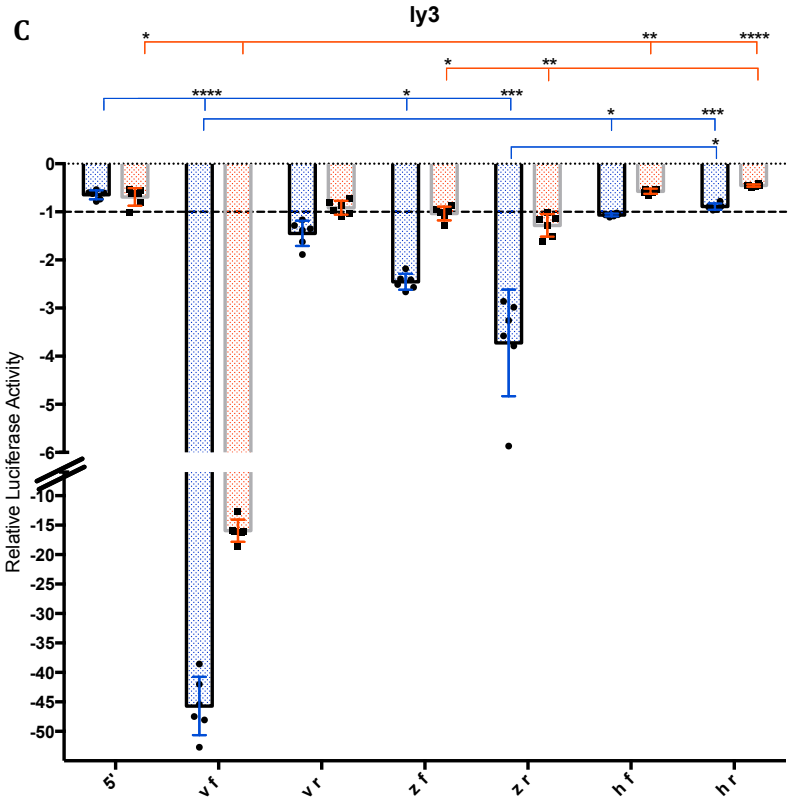
C
ly3
Relative Luciferase Activity
0
-1
-2
-3
-4
-5
-6
-10
-15
-20
-25
-30
-35
-40
-45
-50
5'
v f
v r
z f
z r
h f
h r

Figure 3.4: Assessment of a position-dependent silencing effect using luciferase assays

(A) The silencer element has been inserted in the plasmid upstream of the SCP1 promoter (5'), downstream of the promoter (v), in between luciferase gene and poly-A signal (z) and downstream of the poly-A signal (h) in forward (f) and reverse (r) orientation.

(B-C) Samples were measured in six replicates and each luciferase activity signal was related to the mean of the respective empty vector's signals. The reciprocal was used to better present silencing values, which are between zero and one. A value of -1 then represents the empty vector's activity, and values below -1 suggest a silencing activity. Shown are values from two biological replicates depicted in blue and red. Dunn's multiple comparison test was used to evaluate the significance between the different positions. *: $P<.05$, **: $P<.01$, ***: $P<.001$, ****: $P<.0001$. Data is depicted as mean, error bars show standard deviation (SD).

(B) In OCI-ly1 cells all positions and orientations except the 5' positions show silencing activity. A Kruskal-Wallis-Test was used to compare the different groups, for both experiments $P<.0001$. Therefore, the null hypothesis can be rejected and a significant difference between the different groups can be assumed. A third experiment with biological replicates showed comparable results (data not shown).

(C) In OCI-ly3 cells the silencer only influences transcription when being inserted in the v or z position. Again a Kruskal-Wallis-Test showed $P<.0001$ for both experiments, meaning there is a non randomly observed difference between the groups.

3.2.2 Site-directed mutagenesis does not impair silencing activity

Site-directed mutagenesis was chosen as a tool to insert the C > T SNP found in patients with ABC and GCB DLBCL as well as healthy individuals. Again, luciferase assays were used to study the impact of this SNP on silencer activity. The mutated silencer element was tested in the position between luciferase gene and poly-A signal and as this base pair substitution was described in both GCB DLBCL and ABC DLBCL patients, its effect upon silencer activity was investigated in OCI-ly1 and OCI-ly3 cells. However, neither in OCI-ly1 nor in OCI-ly3 cells a significant reduction in silencing activity could be observed reproducibly (Figure 3.5).

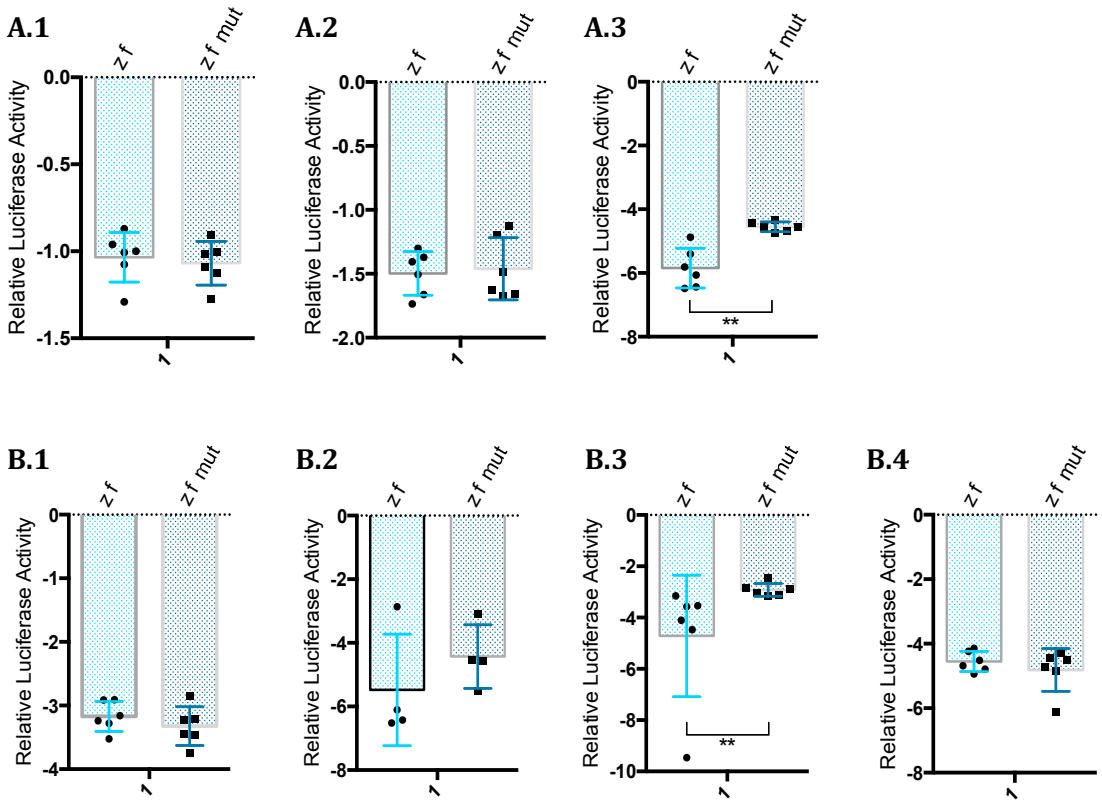

Figure 3.5: Effect of C > T substitution in the silencer element on luciferase activity

(A.1 – A.3) The graphs show biological replicates of the mutated silencer element (*z f mut*) compared to the silencer without SNP (*z f*) in the position between luciferase gene and the poly-A signal in OCI-ly3 cells (for position see also figure 3.4 A). The mean of the empty vector's values was taken to norm the measurements. Values are presented in the reciprocal. No reproducible effect of the base pair substitution can be seen in OCI-ly3 cells (Mann-Whitney-Test: **: *P*<.01, bars indicate mean, error bars show SD, n=6; A.1: *P*=.4740; A.2: *P*=.7879; A.3: *P*=.0022).

(B.1 – B.4) In OCI-ly1 cells the mutated silencer element doesn't show a reproducible effect when inserted between luciferase gene and poly-A signal (*z f mut*). B.1 – B.4 show biological replicates (Mann-Whitney-Test: **: *P*<.01, bars represent mean, error bars show SD; B.1: *P*=.5714, n=6; B.2: *P*=.3429, n=4; B.3: *P*=.0022, n=6; B.4: *P*=.6753, n=6).

3.3 CRISPR-Cas9 mediated knockout of the putative silencer element

To further assess the silencing activity of the silencer element and its potential impact on the expression of *NKIRAS1* and neighbouring genes in the context of its indigenous genomic location, CRISPR-Cas9-based genome editing was employed to knockout the putative silencer in a DLBCL cell line carrying the C > T SNP. In a dual plasmid approach with two different sgRNAs, 46 bp, including the SNP described above, were eliminated from the silencing element (Figure 3.6).

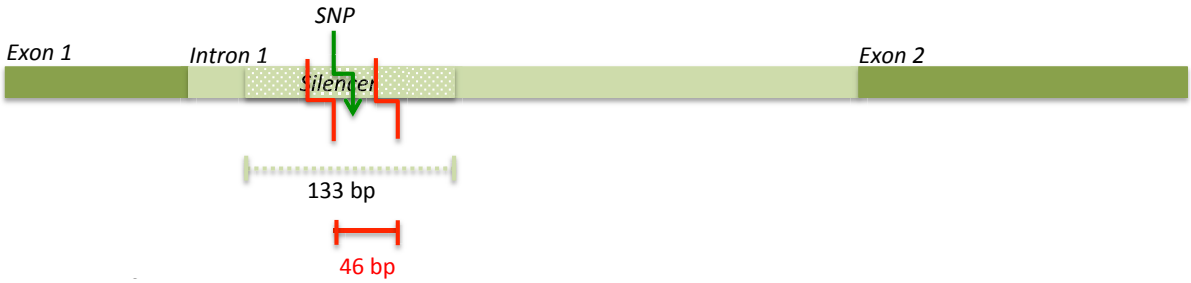

Figure 3.6: Targeting strategy for the CRISPR-Cas9 mediated silencer knockout
46 bp within the 133 bp silencer were excised via CRISPR-Cas9 targeting.

3.3.1 PCR validation reveals homozygous knockout clones

After transfecting OCI-ly1 cells with CRISPR-plasmids, targeting the silencer region and encoding *GFP* and puromycin resistance genes, knockout cells were isolated by puromycin selection and subsequent FACSorting for GFP. Retrieved single cell clones were left to grow for some weeks and then screened with a diagnostic end-point PCR with primers encompassing the knockout region (Figure 3.7). From 136 clones, 44 were found to exhibit a homozygous knockout (-/-). In addition, a total of 29 heterozygous clones (+/-) were observed. Thus, PCR analysis revealed efficient targeting of the silencer region.

A

B

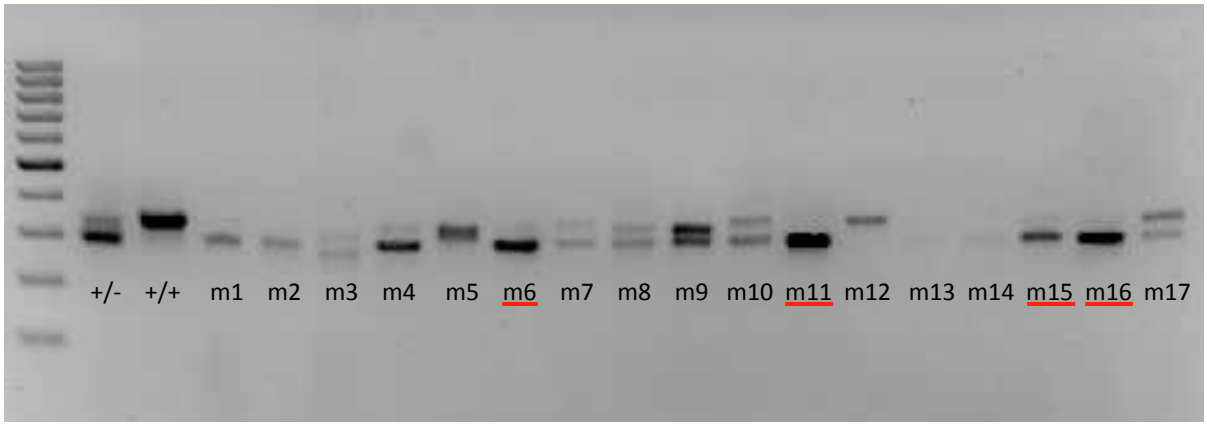

Figure 3.7: End point PCR used for screening CRISPR-Cas9-edited DLBCL cells

(A) Schematic drawing showing the location of the diagnostic primers used to screen for knockout clones. Untreated cells and +/+ clones with an unsuccessful knockout are supposed to show a band at 331 base pairs, whereas -/- knockout clones should generate a 285 bp amplicon. **(B)** Shown are representative PCR results depicting 17 clones (m1 – m17) in comparison to +/- and +/+ controls. Clones m6, m11, m15 and m16 revealed a clear amplicon at 285 bp and were chosen for further examination.

A total of 44 putative knockout clones selected on the basis of the end-point PCR were subjected to a gDNA qPCR for further validation (Figure 3.8 A). Surprisingly, these clones still revealed residual amplification of silencer DNA. Still, 43 of the 44 clones showed a gDNA reduction > 50 % compared to untreated cells (data not shown). For further experiments only clones with < 4 % residual silencer DNA levels and reliable melting curves in the qPCR were used, resulting in 11 confirmed -/- knockout clones (Figure 3.8 B).

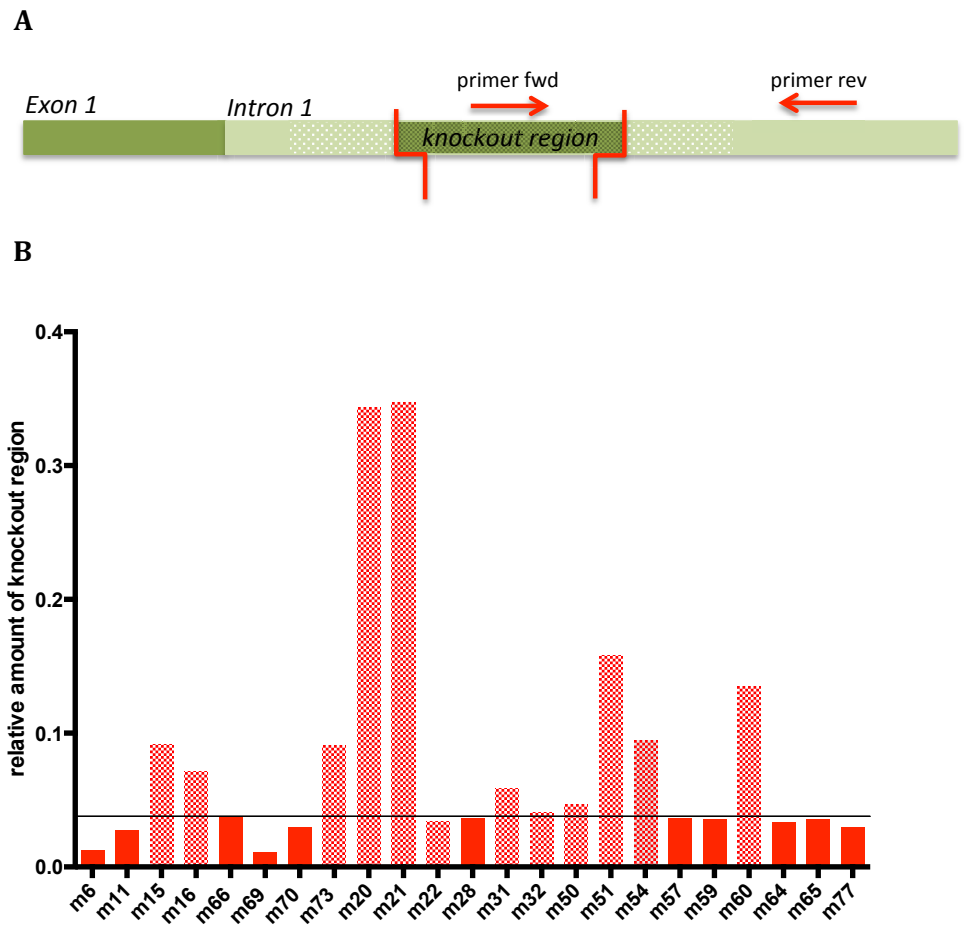

Figure 3.8: Silencer knockout clone validation via qPCR

(A) Schematic illustration showing the location of the primer pair used to screen for knockout clones in a qPCR. As one primer binds within the knockout region and one outside of it, -/- knockout clones are supposed to reveal no qPCR signal**. (B)** Shown are representative data of qPCR analysis. Out of 44 knockout clones 12 clones revealed silencer gDNA levels < 4 % as compared to non-edited +/+ OCI-ly1 cells (set to 1), 11 of these 12 clones displayed reliable melting curves and were therefore used for further studies (illustrated in full red). Additional clones, screened in a second attempt, were found to present over 4 % residual signal for silencer DNA and were therefore excluded (data not shown). Data were assessed in two technical replicates, and results were set off against *GAPDH* signals before normalizing them to the OCI-ly1 value. The scale shows the relative amount of silencer gDNA levels with OCI-ly1 values being 1.0 (≙ 100%).

3.3.2 Confirmation of single cell origin

Considering that the residual amplification of the silencer knockout sequence might be due to the cells not being single cell clones after all and to exclude mosaic clones, a second round of clonal selection was performed. To that end, clones m6 and m69 of OCI-ly1 silencer knockout cells were single-cell spotted via FACS, and from the emerging clones 8 each were subjected to

qPCR. All 16 newly generated single cell clones showed less than 3 % silencer DNA (Figure 3.9), making it therefore unlikely that the two mother clones presented heterozygous mosaic clones.

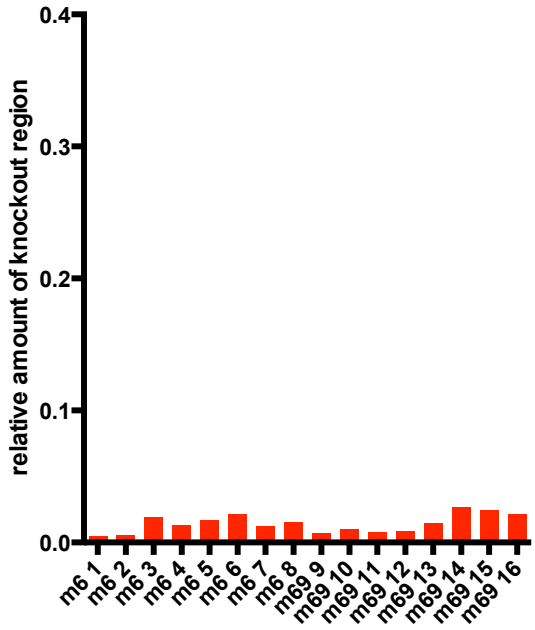

Figure 3.9: Exclusion of mosaic clones via subcloning

In a second round of single cell clone generation, clones m6 and m69 only produced clones with less than 3 % residual silencer DNA amplification in the qPCR (as compared to untreated OCI-ly1 cells, set to 1 (≙ 100 %)). Again the scale shows the relative amount of silencer gDNA levels with OCI-ly1 values set to 1.

3.3.3 Impact on κB-Ras1 expression

As the silencing element is located within the first intron of the *NKIRAS1* gene, the effect of its knockout on κB-Ras1 transcription was examined. A RT-qPCR was conducted to determine κB-Ras1 RNA levels in OCI-ly1 silencer knockout clones compared to OCI-ly1 wildtype cells. Even though in a first experiment all clones showed an increase of RNA levels when compared to a wild-type OCI-ly1 sample, these results could not be reproduced in two following experiments with two technical replicates for each clone compared to the mean expression level of OCI-ly1 wildtype cells generated from 3 biological replicates. No significant differences between RNA levels in OCI-ly1 cells and silencer knockout cells could be detected (Figure 3.10). Therefore, no effect from the silencer on *NKIRAS1* transcription can be deducted from this RT-qPCR screen.

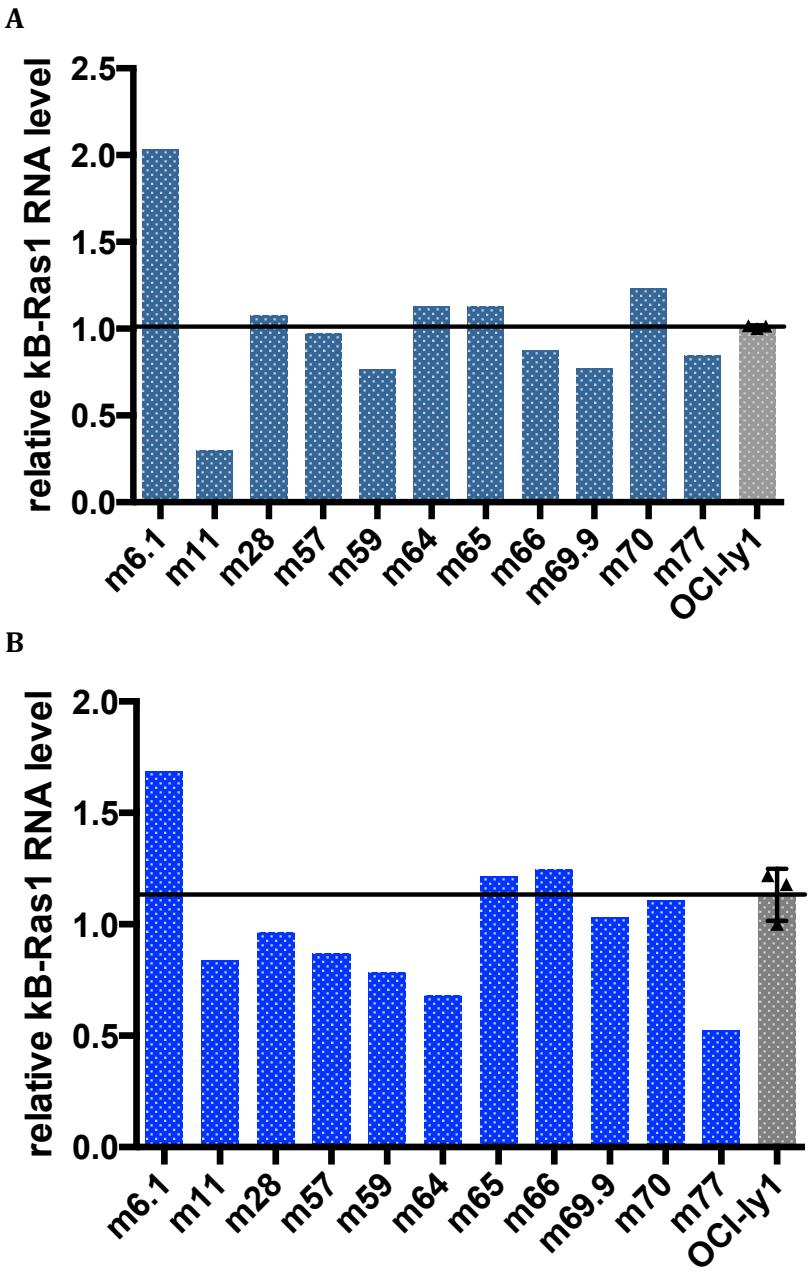

Figure 3.10: RT-qPCR analysis of κB-Ras1 expression in OCI-ly1 silencer knockout clones

(A – B) κB-Ras1 RNA levels from silencer knockout and untreated OCI-ly1 cells were measured in a RT-qPCR. One OCI-ly1 RNA value was set to 1 and the knockout samples as well as the remaining OCI-ly1 samples were normed to that control group. In a second step, the mean of all OCI-ly1 RNA values was calculated (represented by the black line) and the knockout samples were related to that value.

The two experiments **(A** and **B)** represent two biological replicates (taken from the same batch on two following days). 11 knockout clones (m6.1 – m77) were compared to three control lines. There is no significant difference between κB-Ras1 RNA levels from knockout clones and RNA levels in OCI-ly1 cells (Mann-Whitney-Test used, OCI-ly1 bar and error bars show mean and SD, knockout clones n=11, control n=3; A: *P*=.8846, B: *P*=.3681).

3.3.4 No effect on transcription of the adjacent *RPL15* gene

As the silencer element is located directly upstream of the *RPL15* gene (ribosomal protein L15), the influence of the silencer knockout on RNA levels of this gene was analysed. *RPL15* encodes a ribosomal protein known to be upregulated in gastric and oesophageal cancer tissue (79,121). The RT-qPCR data revealed no significant difference in *RPL15* RNA expression levels between knockout and wild-types cells (Figure 3.11).

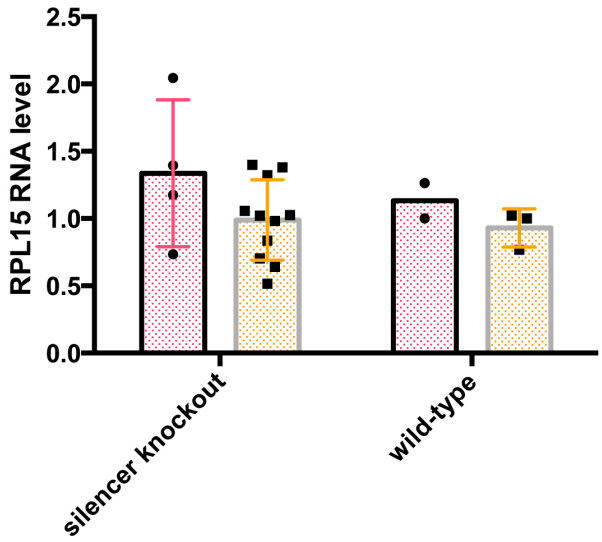

Figure 3.11: RT-qPCR analysis of *RPL15* expression in OCI-ly1 silencer knockout clones

RT-qPCR was conducted to investigate *RPL15* expression in -/- silencer knockout cells in comparison to untreated +/+ OCI-ly1 cells. One +/+ OCI-ly1 sample was set to 1 and the other samples were normed to it. Shown are two independent experiments (in red and yellow) with n=4/n=11 for the knockout cells and n=2/n=3 for the untreated OCI-ly1 control cells. In both analyses no differing amounts of *RPL15* RNA between -/- silencer knockout cells and +/+ OCI-ly1 cells could be observed (Mann-Whitney-Test used, data depicted as mean, error bars show SD for n ≥ 3; 1st experiment in red: *P*=.2667, knockout clones n=4, control n=2; 2nd experiment in yellow: *P*=.5769, knockout clones n=11, control n=3).

3.3.5 Analysis of cell proliferation shows no uniform growth alterations

Even though the silencer element did not show an effect on gene expression in the experiments testing the two adjacent genes, a strong regulatory effect on transcription in luciferase assays could be observed. Figuring that the silencer might influence another gene apart from *NKIRAS1* and *RPL15* that could still be important for cancerogenesis or cell growth, a further aim was to investigate whether a knockout of the silencer element resulted in altered proliferation dynamics. To address this question, CTG proliferation assays were performed and the growth behaviour of silencer knockout OCI-ly1 cells in comparison to wild type OCI-ly1 cells was evaluated. Even though some silencer knockout clones showed a tendency towards slightly

enhanced proliferation, no consistent alteration of the growth curves could be observed (Figure 3.12). This suggests that the silencer does not have a decisive impact on cell proliferation.

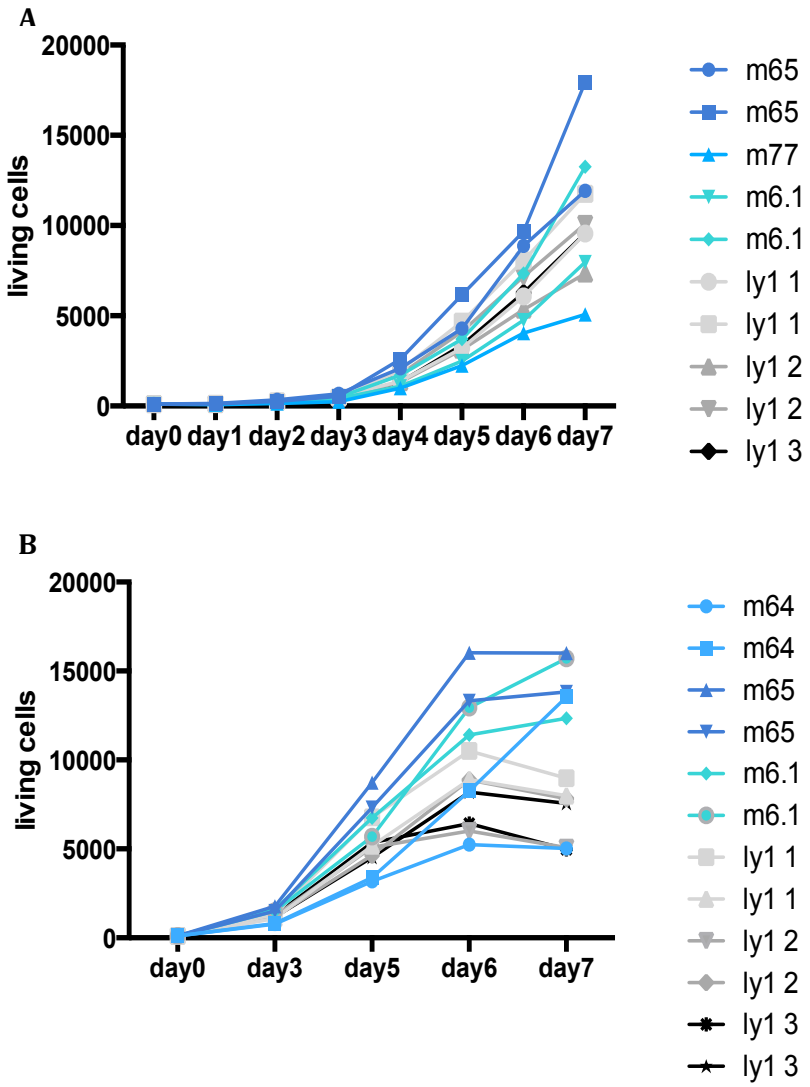

Figure 3.12: CTG proliferation assay of silencer knockout and OCI-ly1 control cells

In each illustration two biological separate experiments performed in technical triplicates are shown. Cell numbers on day 0 were set to 100 and the measurements on the following 7 days were referred to this day 0.

(A) In a first experiment clones were counted and seeded to the same density two days prior to day 0. In 7 days of measuring cell numbers no consistent alteration of growth curves could be determined for OCI-ly1 silencer knockout clones. **(B)** In a second experiment clones were starved for 12 hours before re-seeding and counting them on day 0. Measuring cell numbers on day 3, 5, 6 and 7, no uniform growth patterns and no clear difference between the proliferation curves of silencer knockout and untreated OCI-ly1 cells could be observed.

3.4 CRISPR-Cas9 knockout of *NKIRAS1*

Independently of whether or not the silencer influenced the expression of the *NKIRAS1* gene, further experiments were carried out in order to define more precisely the function of *NKIRAS1* in DLBCL cells, as there is no data published concerning the role of this important regulator of the NF-κB pathway in lymphoma cell lines, despite the fact that this pathway is considered highly relevant for the development of some DLBCL subvariants (25). To investigate this question, another CRISPR-Cas9 mediated knockout was conducted to create *NKIRAS1*-deficient OCI-ly1 cells. For this purpose sgRNAs that cut out the second exon of *NKIRAS1*, which contains the ATG codon, were used.

3.4.1 Confirmation of homozygous *NKIRAS1* knockout clones via PCR

Similar to the investigation of the silencer knockout OCI-ly1 cells, *NKIRAS1* knockout clones were screened with an end-point PCR. In a total of 70 screened clones 13 -/- *NKIRAS1* and 7 +/- *NKIRAS1* clones were identified (Figure 3.13).

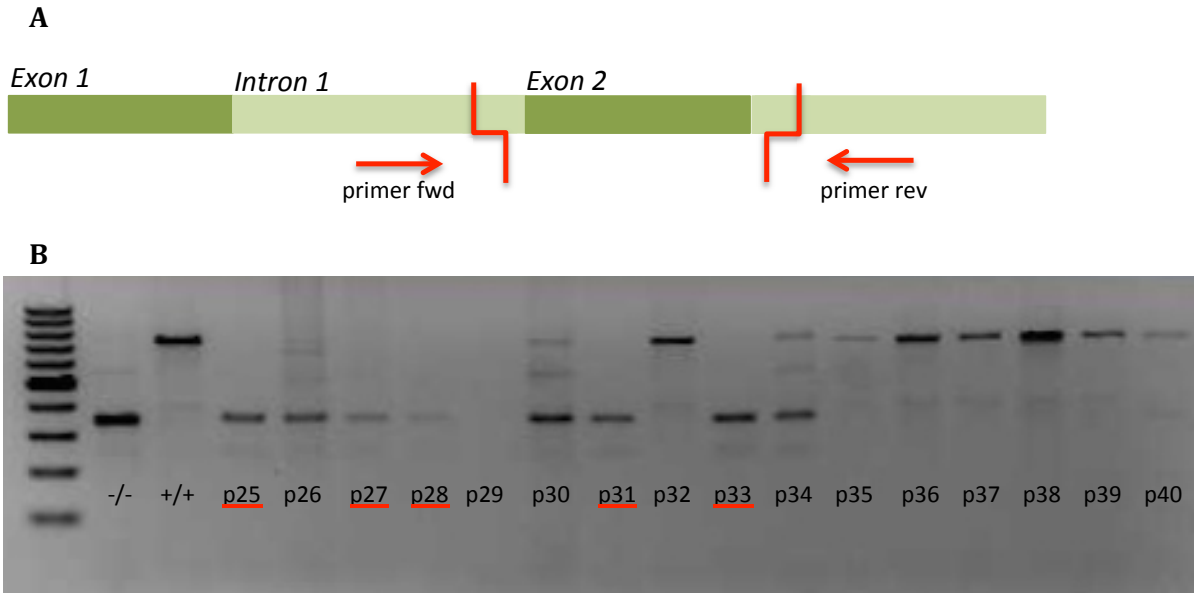

Figure 3.13: End point PCR screening for *NKIRAS1* knockout clones

(A) Schematic illustration depicting the knockout strategy and position of the diagnostic primers.

(B) Untreated cells and +/+ clones show an amplimer at 737 base pairs, -/- clones present an amplimer at 320 bp. In this exemplary PCR screen clones p25 – p40 were screened; 5 -/- *NKIRAS1* clones (underlined in red) could be observed. -/- and +/+ controls were used as comparison.

In a second step, a RT-qPCR for *NKIRAS1* RNA was performed to further validate the *NKIRAS1* knockout at RNA levels. Out of 13 clones identified as presumptive knockout clones in the screening PCR, 5 showed *NKIRAS1* levels < 0.002 when compared to untreated OCI-ly1 cells set to 1 (Figure 3.14).

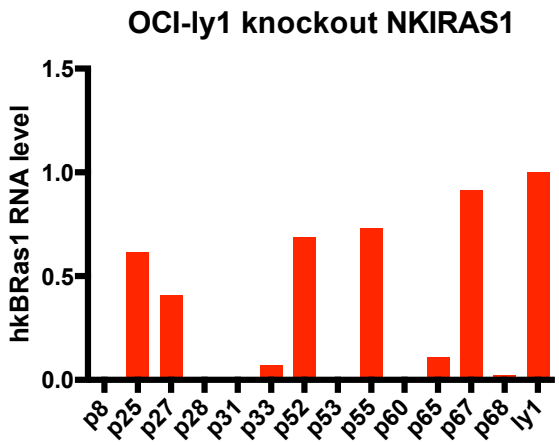

Figure 3.14: κB-Ras1 RNA levels in putative *NKIRAS1* knockout clones

Illustrated is a RT-qPCR analysis of κB-Ras1 expression in *NKIRAS1* knockout and untreated OCI-ly1 cell lines. OCI-ly1 cells were used as control group and set to 100 % (≙ 1.0). Knockout cells were set off against the control group. Clones p8, p28, p31, p53 and p60 showed a complete knockout with less than 0.2 % residual signal for κB-Ras1 RNA compared to wildtype cells.

3.4.2 Growth curve analysis of *NKIRAS1*-deficient clones reveals no consistent changes

Identified knockout clones were used to assess a potential impact of a *NKIRAS1* knockout on the proliferation of OCI-ly1 cells using a CTG assay. Across a window of seven days, no consistent differences in growth rates were detected between *NKIRAS1* knockout and untreated OCI-ly1 cells (Figure 3.15).

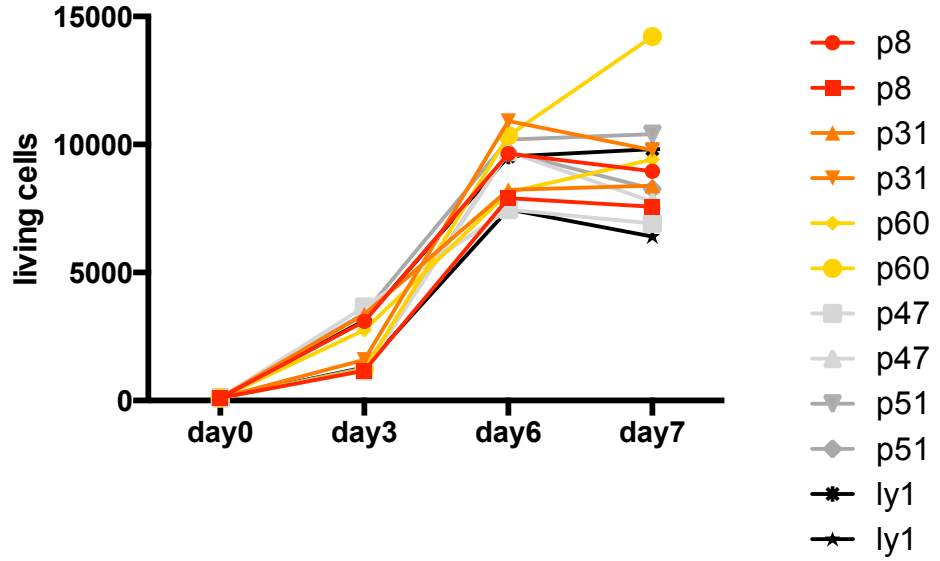

Figure 3.15: Growth curve analysis of *NKIRAS1* knockout and wildtype OCI-ly1 cells using CTG assays

Shown are two experiments with different biological replicates, each carried out with 3 technical replicates. Cell numbers were counted for 7 days and referred to day 0, where measured values were set

to 100. Two days before measuring clones were seeded to the same density. The -/- *NKIRAS1* knockout clones (p8, p31, p60) were compared to +/+ clones that underwent the same CRISPR-Cas9 procedure, but did not have a successful knockout (p47, p51) and parental OCI-ly1 cells. No uniform growth differences could be seen between the different groups. Analyses with two further biological replicates showed the same tendency (data not shown).

4 Discussion

Even though diagnostic possibilities and therapeutic approaches have already become much better and many studies with promising new drugs are currently ongoing to further improve the patient's outcome, DLBCL still remains a very aggressive type of tumour where around 35 % of all patients do not survive longer than 5 years after diagnosis (112). It is therefore of high importance to better understand this type of disease and to develop more specific and efficient drugs. For cancer in general and more specifically DLBCL many different genes have been discovered to play a crucial role in cancerogenesis and due to mutations be causative for pathway deregulation and cancer development itself (63). Identifying and investigating regulatory elements controlling these genes represents an essential part not only for understanding the pathomechanism leading to lymphomagenesis but also opens up new possibilities for treatment as transcription factors contributing to unwanted gene regulation can directly be targeted (47).

The aim of this thesis was to verify the silencing function of a predicted putative silencer element, suggested to be involved in the pathogenesis of DLBCL, and to investigate its functional impact as well as the importance of a SNP located within the silencer. The data generated in this thesis project show that the regulatory element indeed functions as a position- and cell line-dependent silencer and that the SNP does not have an influence on silencer function. The silencer's impact on adjacent gene expression and proliferation as well as the function of *NKIRAS1* itself were further examined in assays including CRISPR-Cas9 genome editing and CTG proliferation assays.

4.1 The role of silencers in cancerogenesis and therapy

It is long known that alterations in silencing elements and processes can play a major role in triggering or promoting cancerogenesis. For example in 2000 Kikuchi et al. identified two negative regulatory elements within the *BCL6* gene and suggested that these elements are vital for regulating *BCL6* transcription and that deletion of or mutations in these elements might play an important part in lymphomagenesis (59). Lossos et al. further examined the relationship between one of those silencer elements and *BCL6* gene expression and found that mutations in the negative regulatory element in the first intron of the *BCL6* gene result in increased *BCL6* mRNA levels (messenger RNA). However, not all mutations within regulatory elements in the first intron lead to increased *BCL6* mRNA levels, and even if they do, this might lead to an altered or even aggravated pathogenesis and transformation into a more aggressive tumour, but not necessarily be sufficient for malignant conversion. (69) Capello et al. investigated

immunodeficiency-related non-Hodgkin lymphomas and described an increased methylation dependent silencing of the *PTPN6/SHP1* gene (tyrosine-protein phosphatase non-receptor type 6/Src homology region 2 domain-containing phosphatase-1) in those cells, which is important for inhibiting the JAK/STAT3 signalling pathway (januskinase/signal transducers and activators of transcription) (14,105). Decreased levels or complete lack of *SHP1*, for example due to silencing of its promoter, are depicted in many aggressive lymphomas such as natural killer/T-cell lymphomas, Hodgkin's disease and DLBCL, and a link between *SHP1* downregulation and the malignancy of lymphomas is suggested (87). Capello et al. could furthermore confirm that after methylation of the *SHP1* gene, the fraction of phosphorylated *STAT3*, one of its target genes, is increased (14,105). Elevated *STAT3* levels and the consequent upregulation of the JAK/STAT3 pathway additional to the in ABC DLBCL frequently activated NF-κB pathway is described to play an important role in ABC DLBCL lymphomagenesis (30). These findings strongly suggest that the epigenetic silencing of an inhibitor of the JAK/STAT3 pathway through increased methylation can serve as a trigger for cancer development.

Not only are findings about regulatory silencer elements important for understanding molecular cancerogenesis, but they might also open new perspectives for cancer treatment. Jiang et al. described a negative regulatory element within the *NKX3.1* gene, known to be a tumour suppressor gene particularly relevant for prostate cancer cells (8). They created double-stranded oligodeoxynucleotides (ODN) that target and consequently impede the transcription factor normally binding to the negative regulator of *NKX3.1*. As a consequence, the negative regulator displayed reduced silencing activity. Not only were mRNA and protein levels of *NKX3.1* increased after transfecting the ODNs to the cell, but also the prostate tumour cell proliferation was decreased. (53) Until today transcription factor decoy (TFD) ODNs represent promising approaches to target undesirable overexpression or downregulation of genes. Clinical trials were and are in progress with TFD ODNs interacting primarily with NF-κB and STAT3 pathways in patients with diseases such as atopic dermatitis, coronary stenosis, discogenic back pain and sub-acute inflammation related to rheumathoid arthritis, asthma or osteoarthritis. (47) But also different types of cancer could be treated with this innovative therapy: A clinical trial in phase 1 was performed for patients with head and neck squamous cell carcinoma with TFD ODNs against the CREB-transcription factor (cyclic AMP response element-binding protein). The decoy of CREB impairs the cells' protective mechanisms against γ-radiation and might thus reinforce the effect of radiotherapy on cancer cells. (47,89) These studies emphasize how crucial the understanding of gene regulation and the identification of positive and negative regulatory elements is for the improving treatment of neoplastic diseases.

These noteworthy discoveries and the knowledge that silencers themselves as well as their deregulation can be fundamental for cancerogenesis were major motivations for the presented study of a predicted silencer displaying a recurrent SNP within *NKIRAS1*, a gene that encodes a known regulator of the NF-κB pathway, which is commonly deregulated in DLBCL (25,34,113).

4.2 Verification of a silencing function of a predicted regulatory element within the *NKIRAS1* gene

Luciferase assays were chosen to investigate the functional impact of a computationally and by a STARR-Seq assay predicted regulatory element within the first intron of *NKIRAS1*. Having cloned the putative silencer in 7 different positions and orientations into a luciferase vector, subsequent experiments with two different cell lines confirmed that the predicted regulatory element acts as a silencer in OCI-ly1 cells (GCB cell line) in every position besides 5' upstream of the promoter. In OCI-ly3, which is an ABC cell line and originates from a different cell of origin, the silencer only showed striking silencing activity in the v' position with forward orientation directly downstream of the promoter and in the z' position with reverse orientation between luciferase gene and poly-A signal. Even though silencers often function irrespective of their relative position to the promoter, it is known that they can also function as a silencer only in a specific position. The necessity of one precise position with regards to the promoter or enhancer results in a high specificity of the silencer to its target gene. (77) As OCI-ly1 and OCI-ly3 are DLBCL cell lines derived from different cells of origin and therefore represent two different subvariants, it would be plausible that they both show differential responses to the same regulatory element. Given the fact that the experiments were conducted with two (OCI-ly3) or three (OCl-ly1) biological replicates, higher n-numbers, especially for OCI-ly3 experiments, would be desirable to consolidate the observations concerning position-specific effects of the silencer element in ABC cells.

From a methodological point of view, the data support the conception that luciferase assays are a very fast and efficient tool to predict the actual impact of silencers upon transcription in an episomal construct as well as the position dependency of regulatory elements.

4.3 No functional impact of a SNP within the verified silencer element

In a second step site-directed mutagenesis was performed to insert a SNP, frequently found within the silencer in DLBCL patients as well as in healthy individuals (74,80), into the silencer in order to investigate whether this base pair substitution had any influence on the silencer's function. This tool was found to be very precise and fast to use and its high suitability to create a base pair substitution within a plasmid with little effort can be confirmed. The data revealed that

the insertion of the base pair substitution has no significant effect when introduced at the z' position between the luciferase gene and the poly-A signal.
As the silencer element shows position-dependent silencing activity, it would be interesting to furthermore test the site-directed mutagenesis' effect upon the silencer in the v' position directly downstream of the promoter, as this position showed the biggest silencing effect for both OCI-ly1 and OCI-ly3 cells. However, it is not entirely clear whether or not this position is representative of the silencer's functional principle in the cell line and whether the results are relatable to in vivo silencer functioning at this position. The strong silencing effect observed upon positioning the silencer directly downstream of the promoter could also represent an artefact, as this very close proximity might sterically interfere with the promoter and the transcription machinery, thereby impeding the initiation of transcription, which could explain the very strong effect. However, the reverse orientation of the silencer within the same position did not result in such an extreme silencing activity, therefore questioning this theory.

4.4 CRISPR-Cas9 mediated silencer knockout shows no effect on mRNA levels of adjacent genes

In order to evaluate the silencer's function and impact in its indigenous context in the OCI-ly1 cell line, 46 bp from the 133 bp long silencer were knocked out in OCI-ly1 cells. Using CRISPR-Cas9-based genome editing, more than 100 silencer knockout clones were generated and screened, yielding a wide range of homozygous -/- knockout, homozygous +/+ wild type and heterozygous +/- clones. 11 clones were found to show less than 4 % remaining silencer knockout gDNA signal and their single cell origin could be confirmed. These data illustrate that CRISPR-Cas9 targeting is – from a methodical point of view – a very suitable tool to knockout a specific region from the genome. The question remains why homozygous -/- knockout clones did not show a complete knockout with 0 % of remaining gDNA. One explanation might be that the clones were grown in a medium containing 20 % conditioned medium from the supernatant of regular OCI-ly1 cells. Although this conditioned medium was filtered, contamination with gDNA from wild type OCI-ly1 cells, which could explain those small positive signals in the qPCR, cannot be excluded.

As the silencer element lies within the *NKIRAS1* gene and is also located in very close proximity to the adjacent *RPL15* gene, the transcription levels of those two genes presented a major field of interest. Performing RT-qPCR screens of knockout and wild type cells, no differences concerning *RPL15* RNA levels could be seen. Also, κB-Ras1 mRNA expression levels did not significantly differ between knockout and wild type clones. In the context of these studies, a striking variability between different experimental runs was observed. In a first experiment all knockout

clones showed higher κB-Ras1 cDNA levels than the wild type (data not shown), but this effect was not reproducible in two following repetitions of the same experiment, done at consecutive days. Only one clone showed increased κB-Ras1 RNA levels in all three experiments. Interestingly, *GAPDH* RNA levels, which were used as internal control, did not differ between the OCI-ly1 control cells from the different experiments. This variability could be due to a change in growth conditions such as varying cell densities. Also, between the first and the second run of the experiment the cells had gone through a number of passages and had been frozen and thawed. It is conceivable that this additional amount of stress or increased passaging itself could have influenced the cells' silencer knockout-associated cellular phenotype. It would therefore be interesting to redo the experiments with a smaller number of passages in between to ultimately clarify the impact of the silencer knockout on κB-Ras1 expression. However, as the results stand at the moment, it cannot be concluded that a knockout of the silencer element has a reproducible effect on κB-Ras1 mRNA expression. RNA-Seq experiments could help to shed light on the question as to which potential other genes might be targeted by the silencer. By comparing cDNA levels from silencer knockout and wild type OCI-ly1 cells, a difference in expression patterns could give a hint as to which gene is influenced by the silencer.

Another important point concerning the interpretation of the results is that silencer knockout clones were only compared to the parental OCI-ly1 wild type line. It might be more representative to furthermore compare the -/- knockout clones to +/+ clones that have unsuccessfully undergone the gene editing procedure, including puromycin selection and clonal expansion. While these procedures are necessary for the establishment of knockout clones, they represent at the same time a considerable stress factor for the cells, which might itself provoke for example epigenetic changes resulting in altered gene expression. While an impact of FACSorting on stress-associated alterations such as gene expression modification is controversial in literature (83,98), Guo et al. performed RNA-Seq experiments, detecting mRNA alterations due to puromycin selection, and Ryu et al. even observed a high amount of up- or downregulated genes (amongst others also transcription factor encoding genes important for cell cycle and growth) after using standard concentrations of antibiotics to avoid contamination in cell culture (45,101).

The silencer knockout experiment described here was conducted in OCI-ly1 cells, which are GCB DLBCL cells. Luciferase assays showed that the silencer does not function in the exact same manner in ABC (OCI-ly3) and GCB (OCI-ly1) cell lines. It would therefore be very interesting to see whether κB-Ras1 expression might be influenced by the silencer in ABC cell lines, where furthermore a deregulation of the NF-κB pathway is known to play an important role in

lymphomagenesis (25). A second knockout of the silencer in OCI-ly3 could shed light on this idea and answer the question.

Another potential issue is the disruption of the intron sequence by a 46 bp deletion, which might have a more general effect on gene expression levels, independently of the knockout's sequence and resulting from silencer- and position-independent effects such as frame shifts. To exclude this possibility, another knockout region with as well around 50 bp length around 300 bp downstream of the silencer knockout region was created as control region (data not shown). SgRNAs targeting DNA regions known to be non-essential are frequently recommended as negative control (17,42). However, comparison with publicly available databases for genomic homologies revealed that the knockout region chosen for this control is a highly conserved region and might thus be important for gene regulation itself. The control region was therefore abandoned in subsequent experiments. Yet, such a generic knockout control could be helpful in future studies to validate the results.

4.5 Neither silencer knockout cells nor *NKIRAS1* knockout cells show an altered growth behaviour

Even though no definite target gene could be determined in RT-qPCR screens, a closer look was taken on the proliferation of the silencer knockout cells. Even if it is not yet known which gene is targeted by the silencer, its influence on a so far unknown gene could still have a potential impact on processes such as cell growth. In CTG proliferation assays the majority of silencer knockout clones tended to grow faster than OCI-ly1 wild type cells, but there were also some clones that did not confirm this notion. It would be interesting to test a larger number of clones and compare them not only to parental OCI-ly1, but also to +/+ clones that have unsuccessfully undergone the genome editing procedure. Furthermore, the CTG assays performed here only measure viability differences over 7 days. It would be worth investigating proliferation over a longer period of time. When screening single cell clones for homozygous knockout cells, it struck that a relative large number of clones that grew faster and were therefore picked and screened first, showed less than 4 % remaining gDNA levels. Interestingly, none of the slower growing clones screened in a second attempt showed such an efficient knockout, and none of them had less than 4 % remaining gDNA (data not shown). This could suggest that clones with a complete silencer knockout might grow faster compared to incomplete knockout cells. While the CTG assays do not entirely confirm this theory, the possibility remains that maybe a 7-day-long CTG assay is just not sufficiently informative to detect subtle differences in proliferation. And even though no silencer knockout effects on proliferation could be seen, this does not imply that the

silencer element does not have any impact on cancerogenic events in the cell cycle as increased proliferation is only one of many characteristics of cancer cells.
In a second step, the role of *NKIRAS1* itself on OCI-ly1 cell growth was explored. *NKIRAS1* is known to be an important regulator of the NF-κB pathway (18,34). However, no data is yet published about its function in lymphoma cell lines. In order to better understand the role of *NKIRAS1,* a second CRISPR-Cas9 mediated editing was performed and the *NKIRAS1* gene was knocked out. Subsequent experiments should help to clarify whether *NKIRAS1* influences proliferation and whether cell growth differences were to be expected if the putative silencer element regulated κB-Ras1. Surprisingly, no growth effect could be seen in the knockout cells, which could be due to the fact that *NKIRAS1* might not impact cell growth after all. Provided that the silencer element influences *NKIRAS1*, assessment of the expression of other NF-κB target genes would be a more precise method to explore the cellular effect of the silencer's knockout.

Not only are there no publicly available data providing insight into the function of *NKIRAS1* in lymphomas, but also the role of this gene seems to be highly cell-type specific: *NKIRAS1* is described to be highly downregulated and to act as a tumour suppressor gene in renal cell carcinoma (39). In lung tumours, on the other hand, the *NKIRAS1* gene is suggested to display oncogenic features, as mRNA levels are a lot higher in tumour cells compared to healthy lung tissue. It has also been described that elevated NKIRAS1 mRNA levels in lung tumours are associated with demethylated *NKIRAS1* promoter regions and methylation of genes from *NKIRAS1* repressing miRNAs (microRNA), which causes their downregulation. (11) These two very differing papers demonstrate that the function of *NKIRAS1* is highly tissue specific and far from being entirely understood. It remains, therefore, important to not only examine the role of *NKIRAS1* in OCI-ly1 DLBCL cells, but also to investigate whether different DLBCL cell lines present differential effects of *NKIRAS1*. Even though no impact of *NKIRAS1* knockout on GCB cell proliferation could be shown, it would be an interesting experiment to knockout the *NKIRAS1* gene in OCI-ly3 cells and to see whether κB-Ras1 plays a more important role in ABC DLBCL cells, as the NF-κB pathway plays a major role in ABC pathogenesis (25). Furthermore, a fundamental exploration of the knockout's effect on different NF-κB target genes and an investigation of cancerogenic events apart from proliferation would be desired to obtain a more comprehensive picture of the impact of κB-Ras1 on DLBCL.

4.6 Predicted transcription factor - silencer interactions

Data from publicly available transcription factor binding prediction tools indicated that the transcription factor PAX5 binds to the putative silencer element, which is an interesting discovery that would be worth having a closer look at. PAX5 plays a major role in B-cell

development; more than 100 different genes have been reported to be enhanced or repressed by PAX5. Most of them are B-cell lineage specific and important for receptor and intracellular signalling, adhesion or transcription. (93) As PAX5 is consistently expressed in B-cells and present in all Hodgkin- and non-Hodgkin-lymphomas, it was proposed as a central marker for immunohistochemical identification of B-cell lymphomas (57). Since the binding of PAX5 to the silencer was only computationally predicted, it would be interesting to confirm binding of the transcription factor in vitro in a ChiP-Seq assay.

4.7 Future perspectives

As the function of gene regulatory elements is strongly influenced by their 3-dimensional context, future studies on the putative silencer element might be extended to tools such as 3C, which enables to visualize 3-dimensional interactions between DNA sequences (27). Silencers can be located up to multiple kilobases away from their respective promoter and only interact with it via looping of the DNA (70). Investigations concerning the silencer's sterical position within the chromatin landscape could, therefore, help to shed light on the question which gene is targeted by the putative silencer element. With 4C one could even screen for all DNA fragments that bind to the silencer element and should thereby be able to identify which enhancer or promoter is mainly influenced by the silencer (58).

To further narrow down the enormous number of possible target genes, topologically associated domains (TADs) should be closer examined. TADs are a few hundred up to two megabases long regions on the DNA that help to create a superordinate chromatin structure and control gene expression by allowing enhancer or silencer looping only within one TAD. This way, regulatory elements within one TAD are kept away from promoters in neighbouring TADs. Consequently, elements within the same TAD are more likely to interact with each other. TADs do not notably vary between different tissue types, and cell-type specificity has only been detected within internal looping pattern of TADs or even higher-level, so-called compartments that are made up by different TADs. (28) How exactly the isolation between TADs is organized still remains to be elaborated. However, the two proteins CTCF (11-zinc finger protein) and cohesin are thought to play a major role, for example by creating chromatin loops between different CTCF binding regions. (28) It is, however, obvious that insight into the TAD structure helps to predict which target genes are to be considered for a selected regulatory element. As the target gene of the silencer element described within the *NKIRAS1* gene could not be identified, a closer look at the TAD region could be beneficial for predicting potential targets other than *NKIRAS1* or *RPL15*.

5 References

(1) Addgene (n.d.) CRISPR guide, https://www.addgene.org/crispr/guide/, downloaded 11.03.2020

(2) Ahmed AU, Williams BR, Hannigan GE (2015) Transcriptional activation of inflammatory genes: Mechanistic insight into selectivity and diversity. Biomolecules 5: 3087-3111. doi: 10.3390/biom5043087

(3) Alizadeh AA, Eisen MB, Davis RE, Ma C, Lossos IS, Rosenwald A, Boldrick JC, Sabet H, Tran T, Yu X, Powell JI, Yang L, Marti GE, Moore T, Hudson J,Jr, Lu L, Lewis DB, Tibshirani R, Sherlock G, Chan WC, et al. (2000) Distinct types of diffuse large B-cell lymphoma identified by gene expression profiling. Nature 403: 503-511. doi: 10.1038/35000501

(4) Arnold CD, Gerlach D, Stelzer C, Boryń ŁM, Rath M, Stark A (2013) Genome-wide quantitative enhancer activity maps identified by STARR-seq. Science 339: 1074-1077. doi: 10.1126/science.1232542

(5) Attar RM, Macdonald-Bravo H, Raventos-Suarez C, Durham SK, Bravo R (1998) Expression of constitutively active IkappaB beta in T cells of transgenic mice: Persistent NF-kappaB activity is required for T-cell immune responses. Mol Cell Biol 18: 477-487. doi: 10.1128/mcb.18.1.477

(6) Baldwin AS (2001) Control of oncogenesis and cancer therapy resistance by the transcription factor NF-kappaB. J Clin Invest 107: 241-246. doi: 10.1172/JCI11991

(7) Baysal BE, Ferrell RE, Willett-Brozick J, Lawrence EC, Myssiorek D, Bosch A, Mey Avd, Taschner PEM, Rubinstein WS, Myers EN, Richard CW, Cornelisse CJ, Devilee P, Devlin B (2000) Mutations in *SDHD*, a mitochondrial complex II gene, in hereditary paraganglioma. Science 287: 848-851. doi: 10.1126/science.287.5454.848

(8) Bhatia-Gaur R, Donjacour AA, Sciavolino PJ, Kim M, Desai N, Young P, Norton CR, Gridley T, Cardiff RD, Cunha GR, Abate-Shen C, Shen MM (1999) Roles for Nkx3.1 in prostate development and cancer. Genes Dev 13: 966-977. doi: 10.1101/gad.13.8.966

(9) Bos JL (1988) The ras gene family and human carcinogenesis. Mutat Res 195: 255-271. doi: 10.1016/0165-1110(88)90004-8

(10) BPS Bioscience (n.d.) Dual luciferase (firefly-renilla) assay system, http://bpsbioscience.com/dual-luciferase-firefly-renilla-luciferase-assay-system-60683, downloaded 24.03.2020

(11) Braga EA, Loginov VI, Pronina IV, Khodyrev DS, Rykov SV, Burdennyy AM, Friedman MV, Kazubskaya TP, Kubatiev AA, Kushlinskii NE (2015) Upregulation of RHOA and NKIRAS1 genes in lung tumors is associated with loss of their methylation as well as with methylation of regulatory miRNA genes. Biochemistry (Mosc) 80: 483-494. doi: 10.1134/S0006297915040124

(12) Buenrostro JD, Wu B, Chang HY, Greenleaf WJ (2015) ATAC-seq: A method for assaying chromatin accessibility genome-wide. Curr Protoc Mol Biol 109: 21.29.1-21.29.9. doi: 10.1002/0471142727.mb2129s109

(13) Busslinger M, Klix N, Pfeffer P, Graninger PG, Kozmik Z (1996) Deregulation of PAX-5 by translocation of the emu enhancer of the IgH locus adjacent to two alternative PAX-5 promoters in a diffuse large-cell lymphoma. Proc Natl Acad Sci USA 93: 6129-6134. doi: 10.1073/pnas.93.12.6129

(14) Capello D, Gloghini A, Baldanzi G, Martini M, Deambrogi C, Lucioni M, Piranda D, Fama R, Graziani A, Spina M, Tirelli U, Paulli M, Larocca LM, Gaidano G, Carbone A, Sinigaglia F (2013) Alterations of negative regulators of cytokine signalling in immunodeficiency-related non-hodgkin lymphoma. Hematol Oncol 31: 22-28. doi: 10.1002/hon.2010

(15) Carotta S, Holmes M, Pridans C, Nutt SL (2006) Pax5 maintains cellular identity by repressing gene expression throughout B cell differentiation. Cell Cycle 5: 2452-2456. doi: 10.4161/cc.5.21.3396

(16) Castellino A, Chiappella A, LaPlant BR, Pederson LD, Gaidano G, Macon WR, Inghirami G, Reeder CB, Tucci A, King RL, Congiu A, Foran JM, Pavone V, Rivera CE, Spina M, Ansell SM, Cavallo F, Molinari AL, Ciccone G, Habermann TM, et al. (2018) Lenalidomide plus R-CHOP21 in newly diagnosed diffuse large B-cell lymphoma (DLBCL): Long-term follow-up results from a combined analysis from two phase 2 trials. Blood Cancer J 8: 108. doi: 10.1038/s41408-018-0145-9

(17) Chen CH, Xiao T, Xu H, Jiang P, Meyer CA, Li W, Brown M, Liu XS (2018) Improved design and analysis of CRISPR knockout screens. Bioinformatics 34: 4095-4101. doi: 10.1093/bioinformatics/bty450

(18) Chen Y, Vallee S, Wu J, Vu D, Sondek J, Ghosh G (2004) Inhibition of NF-kappaB activity by IkappaBbeta in association with kappaB-ras. Mol Cell Biol 24: 3048-3056. doi: 10.1128/mcb.24.7.3048-3056.2004

(19) Chin M, Herscovitch M, Zhang N, Waxman DJ, Gilmore TD (2009) Overexpression of an activated REL mutant enhances the transformed state of the human B-lymphoma BJAB cell line and alters its gene expression profile. Oncogene 28: 2100-2111. doi: 10.1038/onc.2009.74

(20) Compagno M, Lim WK, Grunn A, Nandula SV, Brahmachary M, Shen Q, Bertoni F, Ponzoni M, Scandurra M, Califano A, Bhagat G, Chadburn A, Dalla-Favera R, Pasqualucci L (2009) Mutations of multiple genes cause deregulation of NF-kappaB in diffuse large B-cell lymphoma. Nature 459: 717-721. doi: 10.1038/nature07968

(21) Cong L, Ran FA, Cox D, Lin S, Barretto R, Habib N, Hsu PD, Wu X, Jiang W, Marraffini LA, Zhang F (2013) Multiplex genome engineering using CRISPR/cas systems. Science 339: 819-823. doi: 10.1126/science.1231143

(22) Curis Inc (17.01.2018) Curis announces initiation of phase 1 trial of CA-4948, a small molecule inhibitor of IRAK4 kinase in patients with lymphoma, http://investors.curis.com/2018-01-17-Curis-Announces-Initiation-of-Phase-1-Trial-of-CA-4948-a-Small-Molecule-Inhibitor-of-IRAK4-Kinase-in-Patients-with-Lymphoma, downloaded 11.03.2020

(23) Davies A, Cummin TE, Barrans S, Maishman T, Mamot C, Novak U, Caddy J, Stanton L, Kazmi-Stokes S, McMillan A, Fields P, Pocock C, Collins GP, Stephens R, Cucco F, Clipson A, Sha C, Tooze R, Care MA, Griffiths G, et al. (2019) Gene-expression profiling of bortezomib added to standard chemoimmunotherapy for diffuse large B-cell lymphoma (REMoDL-B): An open-label, randomised, phase 3 trial. Lancet Oncol 20: 649-662. doi: S1470-2045(18)30935-5

(24) Davis CA, Hitz BC, Sloan CA, Chan ET, Davidson JM, Gabdank I, Hilton JA, Jain K, Baymuradov UK, Narayanan AK, Onate KC, Graham K, Miyasato SR, Dreszer TR, Strattan JS, Jolanki O, Tanaka FY, Cherry JM (2018) The encyclopedia of DNA elements (ENCODE): Data portal update. Nucleic Acids Res 46: D794-D801. doi: 10.1093/nar/gkx1081

(25) Davis RE, Brown KD, Siebenlist U, Staudt LM (2001) Constitutive nuclear factor kappaB activity is required for survival of activated B cell-like diffuse large B cell lymphoma cells. J Exp Med 194: 1861-1874. doi: 10.1084/jem.194.12.1861

(26) Davis RE, Ngo VN, Lenz G, Tolar P, Young RM, Romesser PB, Kohlhammer H, Lamy L, Zhao H, Yang Y, Xu W, Shaffer AL, Wright G, Xiao W, Powell J, Jiang J, Thomas CJ, Rosenwald A, Ott G, Muller-Hermelink H, et al. (2010) Chronic active B-cell-receptor signalling in diffuse large B-cell lymphoma. Nature 463: 88-92. doi: 10.1038/nature08638

(27) Dekker J, Rippe K, Dekker M, Kleckner N (2002) Capturing chromosome conformation. Science 295: 1306-1311. doi: 10.1126/science.1067799

(28) Dekker J, Heard E (2015) Structural and functional diversity of topologically associating domains. FEBS Lett 589: 2877-2884. doi: 10.1016/j.febslet.2015.08.044

(29) Der CJ, Finkel T, Cooper GM (1986) Biological and biochemical properties of human rasH genes mutated at codon 61. Cell 44: 167-176. doi: 10.1016/0092-8674(86)90495-2

(30) Ding BB, Yu JJ, Yu RY, Mendez LM, Shaknovich R, Zhang Y, Cattoretti G, Ye BH (2008) Constitutively activated STAT3 promotes cell proliferation and survival in the activated B-cell subtype of diffuse large B-cell lymphomas. Blood 111: 1515-1523. doi: blood-2007-04-087734

(31) Dührsen U, Fridrik MA, Klapper W, Schmitz N (23.11.2018) Diffuses großzelliges B-Zell-Lymphom, in: DGHO Deutsche Gesellschaft für Hämatologie und Medizinische Onkologie e.V., https://www.onkopedia.com/de/onkopedia/guidelines/diffuses-grosszelliges-b-zell-lymphom/@@view/html/index.html, downloaded 11.03.2020

(32) ENCODE Project Consortium (2012) An integrated encyclopedia of DNA elements in the human genome. Nature 489: 57-74. doi: 10.1038/nature11247

(33) Farré D, Roset R, Huerta M, Adsuara JE, Roselló L, Albà MM, Messeguer X (2003) Identification of patterns in biological sequences at the ALGGEN server: PROMO and MALGEN. Nucleic Acids Res 31: 3651-3653. doi: 10.1093/nar/gkg605

(34) Fenwick C, Na SY, Voll RE, Zhong H, Im SY, Lee JW, Ghosh S (2000) A subclass of ras proteins that regulate the degradation of IkappaB. Science 287: 869-873. doi: 10.1126/science.287.5454.869

(35) Ferch U, Kloo B, Gewies A, Pfänder V, Düwel M, Peschel C, Krappmann D, Ruland J (2009) Inhibition of MALT1 protease activity is selectively toxic for activated B cell-like diffuse large B cell lymphoma cells. J Exp Med 206: 2313-2320. doi: 10.1084/jem.20091167

(36) Foulds CE, Feng Q, Ding C, Bailey S, Hunsaker TL, Malovannaya A, Hamilton RA, Gates LA, Zhang Z, Li C, Chan D, Bajaj A, Callaway CG, Edwards DP, Lonard DM, Tsai SY, Tsai MJ, Qin J, O'Malley BW (2013) Proteomic analysis of coregulators bound to ERalpha on DNA and nucleosomes reveals coregulator dynamics. Mol Cell 51: 185-199. doi: 10.1016/j.molcel.2013.06.007

(37) Gates LA, Shi J, Rohira AD, Feng Q, Zhu B, Bedford MT, Sagum CA, Jung SY, Qin J, Tsai MJ, Tsai SY, Li W, Foulds CE, O'Malley BW (2017) Acetylation on histone H3 lysine 9 mediates a switch from transcription initiation to elongation. J Biol Chem 292: 14456-14472. doi: 10.1074/jbc.M117.802074

(38) Gazumyan A, Reichlin A, Nussenzweig MC (2006) Ig beta tyrosine residues contribute to the control of B cell receptor signaling by regulating receptor internalization. J Exp Med 203: 1785-1794. doi: 10.1084/jem.20060221

(39) Gerashchenko GV, Bogatyrova OO, Rudenko EE, Kondratov AG, Gordiyuk VV, Zgonnyk YM, Vozianov OF, Pavlova TV, Zabarovsky ER, Rynditch AV, Kashuba VI (2010) Genetic and epigenetic changes of NKIRAS1 gene in human renal cell carcinomas. Exp Oncol 32: 71-75.

(40) Gibbs JB, Sigal IS, Poe M, Scolnick EM (1984) Intrinsic GTPase activity distinguishes normal and oncogenic ras p21 molecules. Proc Natl Acad Sci USA 81: 5704-5708. doi: 10.1073/pnas.81.18.5704

(41) Gilmore TD (n.d.) Target genes of NF-kB, http://people.bu.edu/Gilmore/nf-kb/target/index.html, downloaded 10.03.2020

(42) Giuliano CJ, Lin A, Girish V, Sheltzer JM (2019) Generating single cell-derived knockout clones in mammalian cells with CRISPR/Cas9. Curr Protoc Mol Biol 128: e100. doi: 10.1002/cpmb.100

(43) Gross DS, Garrard WT (1988) Nuclease hypersensitive sites in chromatin. Annu Rev Biochem 57: 159-197. doi: 10.1146/annurev.bi.57.070188.001111

(44) Guenther MG, Levine SS, Boyer LA, Jaenisch R, Young RA (2007) A chromatin landmark and transcription initiation at most promoters in human cells. Cell 130: 77-88. doi: S0092-8674(07)00681-2

(45) Guo R, Lee YT, Byrnes C, Miller J (2017) Puromycin selection confounds the RNA-seq profiles of primary human erythroblasts. Transcriptomics 05: 140. doi: 10.4172/2329-8936.1000140

(46) Hannah R, Beck M, Moravec R, Riss T (2001) CellTiter-glo™ luminescent cell viability assay: A sensitive and rapid method for determining cell viability. Promega Cell Notes 2: 11-13.

(47) Hecker M, Wagner AH (2017) Transcription factor decoy technology: A therapeutic update. Biochem Pharmacol 144: 29-34. doi: S0006-2952(17)30446-X

(48) Heintzman ND, Stuart RK, Hon G, Fu Y, Ching CW, Hawkins RD, Barrera LO, Van Calcar S, Qu C, Ching KA, Wang W, Weng Z, Green RD, Crawford GE, Ren B (2007) Distinct and predictive chromatin signatures of transcriptional promoters and enhancers in the human genome. Nat Genet 39: 311-318. doi: 10.1038/ng1966

(49) Heintzman ND, Hon GC, Hawkins RD, Kheradpour P, Stark A, Harp LF, Ye Z, Lee LK, Stuart RK, Ching CW, Ching KA, Antosiewicz-Bourget JE, Liu H, Zhang X, Green RD, Lobanenkov VV, Stewart R, Thomson JA, Crawford GE, Kellis M, et al. (2009) Histone modifications at human enhancers reflect global cell-type-specific gene expression. Nature 459: 108-112. doi: 10.1038/nature07829

(50) Huang FW, Hodis E, Xu MJ, Kryukov GV, Chin L, Garraway LA (2013) Highly recurrent TERT promoter mutations in human melanoma. Science 339: 957-959. doi: 10.1126/science.1229259

(51) Huang Q, Whitington T, Gao P, Lindberg JF, Yang Y, Sun J, Väisänen M, Szulkin R, Annala M, Yan J, Egevad LA, Zhang K, Lin R, Jolma A, Nykter M, Manninen A, Wiklund F, Vaarala MH, Visakorpi T, Xu J, et al. (2014) A prostate cancer susceptibility allele at 6q22 increases RFX6 expression by modulating HOXB13 chromatin binding. Nat Genet 46: 126-135. doi: 10.1038/ng.2862

(52) JASPAR 20 (n.d.) Detailed information of matrix profile MA0014.2 , http://jaspar.genereg.net/matrix/MA0014.2/, downloaded 12.03.2020

(53) Jiang AL, Hu XY, Zhang PJ, He ML, Kong F, Liu ZF, Yuan HQ, Zhang JY (2005) Up-regulation of NKX3.1 expression and inhibition of LNCaP cell proliferation induced by an inhibitory element decoy. Acta Biochim Biophys Sin (Shanghai) 37: 335-340. doi: 10.1111/j.1745-7270.2005.00047.x

(54) Jinek M, Chylinski K, Fonfara I, Hauer M, Doudna JA, Charpentier E (2012) A programmable dual-RNA-guided DNA endonuclease in adaptive bacterial immunity. Science 337: 816-821. doi: 10.1126/science.1225829

(55) Johnson DS, Mortazavi A, Myers RM, Wold B (2007) Genome-wide mapping of in vivo protein-DNA interactions. Science 316: 1497-1502. doi: 10.1126/science.1141319

(56) Khan A, Fornes O, Stigliani A, Gheorghe M, Castro-Mondragon JA, van der Lee R, Bessy A, Cheneby J, Kulkarni SR, Tan G, Baranasic D, Arenillas DJ, Sandelin A, Vandepoele K, Lenhard B, Ballester B, Wasserman WW, Parcy F, Mathelier A (2018) JASPAR 2018: Update of the open-access database of transcription factor binding profiles and its web framework. Nucleic Acids Res 46: D260-D266. doi: 10.1093/nar/gkx1126

(57) Khan MR, Ahmad A, Kayani N, Minhas K (2018) Expression of PAX-5 in B cell hodgkin and non hodgkin lymphoma. Asian Pac J Cancer Prev 19: 3463-3466. doi: 10.31557/APJCP.2018.19.12.3463

(58) Khurana E, Fu Y, Chakravarty D, Demichelis F, Rubin MA, Gerstein M (2016) Role of non-coding sequence variants in cancer. Nat Rev Genet 17: 93-108. doi: 10.1038/nrg.2015.17

(59) Kikuchi M, Miki T, Kumagai T, Fukuda T, Kamiyama R, Miyasaka N, Hirosawa S (2000) Identification of negative regulatory regions within the first exon and intron of the BCL6 gene. Oncogene 19: 4941-4945. doi: 10.1038/sj.onc.1203864

(60) Kimura H (2013) Histone modifications for human epigenome analysis. J Hum Genet 58: 439-445. doi: 10.1038/jhg.2013.66

(61) Knittel G, Liedgens P, Korovkina D, Seeger JM, Al-Baldawi Y, Al-Maarri M, Fritz C, Vlantis K, Bezhanova S, Scheel AH, Wolz OO, Reimann M, Moller P, Lopez C, Schlesner M, Lohneis P, Weber AN, Trumper L, German International Cancer Genome Consortium Molecular Mechanisms in Malignant Lymphoma by Sequencing Project Consortium, Staudt LM, et al. (2016) B-cell-specific conditional expression of Myd88p.L252P leads to the development of diffuse large B-cell lymphoma in mice. Blood 127: 2732-2741. doi: 10.1182/blood-2015-11-684183

(62) Kozera B, Rapacz M (2013) Reference genes in real-time PCR. J Appl Genet 54: 391-406. doi: 10.1007/s13353-013-0173-x

(63) Krappmann D, Vincendeau M (2016) Mechanisms of NF-kappaB deregulation in lymphoid malignancies. Semin Cancer Biol 39: 3-14. doi: 10.1016/j.semcancer.2016.05.002

(64) Kwasnieski JC, Mogno I, Myers CA, Corbo JC, Cohen BA (2012) Complex effects of nucleotide variants in a mammalian cis-regulatory element. Proc Natl Acad Sci USA 109: 19498-19503. doi: 10.1073/pnas.1210678109

(65) Lenz G, Davis RE, Ngo VN, Lam L, George TC, Wright GW, Dave SS, Zhao H, Xu W, Rosenwald A, Ott G, Muller-Hermelink HK, Gascoyne RD, Connors JM, Rimsza LM, Campo E, Jaffe ES, Delabie J, Smeland EB, Fisher RI, et al. (2008) Oncogenic CARD11 mutations in human diffuse large B cell lymphoma. Science 319: 1676-1679. doi: 10.1126/science.1153629

(66) Lenz G, Staudt LM (2010) Aggressive lymphomas. N Engl J Med 362: 1417-1429. doi: 10.1056/NEJMra0807082

(67) Lenz G, Wright GW, Emre NCT, Kohlhammer H, Dave SS, Davis RE, Carty S, Lam LT, Shaffer AL, Xiao W, Powell J, Rosenwald A, Ott G, Muller-Hermelink H, Gascoyne RD, Connors JM, Campo E, Jaffe ES, Delabie J, Smeland EB, et al. (2008) Molecular subtypes of diffuse large B-cell lymphoma arise by distinct genetic pathways. Proc Natl Acad Sci USA 105: 13520-13525. doi: 10.1073/pnas.0804295105

(68) Lossos IS, Alizadeh AA, Eisen MB, Chan WC, Brown PO, Botstein D, Staudt LM, Levy R (2000) Ongoing immunoglobulin somatic mutation in germinal center B cell-like but not in activated B cell-like diffuse large cell lymphomas. Proc Natl Acad Sci USA 97: 10209-10213. doi: 10.1073/pnas.180316097

(69) Lossos IS, Warnke R, Levy R (2002) BCL-6 mRNA expression in higher grade transformation of follicle center lymphoma: Correlation with somatic mutations in the 5' regulatory region of the BCL-6 gene. Leukemia 16: 1857-1862. doi: 10.1038/sj.leu.2402578

(70) Maston GA, Evans SK, Green MR (2006) Transcriptional regulatory elements in the human genome. Annu Rev Genomics Hum Genet 7: 29-59. doi: 10.1146/annurev.genom.7.080505.115623

(71) Melton C, Reuter JA, Spacek DV, Snyder M (2015) Recurrent somatic mutations in regulatory regions of human cancer genomes. Nat Genet 47: 710-716. doi: 10.1038/ng.3332

(72) Messeguer X, Escudero R, Farré D, Núñez O, Martínez J, Albà MM (2002) PROMO: Detection of known transcription regulatory elements using species-tailored searches. Bioinformatics 18: 333-334. doi: 10.1093/bioinformatics/18.2.333

(73) Mitchell S, Vargas J, Hoffmann A (2016) Signaling via the NFkappaB system. Wiley Interdiscip Rev Syst Biol Med 8: 227-241. doi: 10.1002/wsbm.1331

(74) Morin RD, Mungall K, Pleasance E, Mungall AJ, Goya R, Huff RD, Scott DW, Ding J, Roth A, Chiu R, Corbett RD, Chan FC, Mendez-Lago M, Trinh DL, Bolger-Munro M, Taylor G, Hadj Khodabakhshi A, Ben-Neriah S, Pon J, Meissner B, et al. (2013) Mutational and structural analysis of diffuse large B-cell lymphoma using whole-genome sequencing. Blood 122: 1256-1265. doi: 10.1182/blood-2013-02-483727

(75) Morton LM, Slager SL, Cerhan JR, Wang SS, Vajdic CM, Skibola CF, Bracci PM, de Sanjose S, Smedby KE, Chiu BC, Zhang Y, Mbulaiteye SM, Monnereau A, Turner JJ, Clavel J, Adami HO, Chang ET, Glimelius B, Hjalgrim H, Melbye M, et al. (2014) Etiologic heterogeneity among non-hodgkin

lymphoma subtypes: The InterLymph non-hodgkin lymphoma subtypes project. J Natl Cancer Inst Monogr 2014: 130-144. doi: 10.1093/jncimonographs/lgu013

(76) Nagel D, Spranger S, Vincendeau M, Grau M, Raffegerst S, Kloo B, Hlahla D, Neuenschwander M, Peter von Kries J, Hadian K, Dorken B, Lenz P, Lenz G, Schendel DJ, Krappmann D (2012) Pharmacologic inhibition of MALT1 protease by phenothiazines as a therapeutic approach for the treatment of aggressive ABC-DLBCL. Cancer Cell 22: 825-837. doi: 10.1016/j.ccr.2012.11.002

(77) Nakabayashi H, Hashimoto T, Miyao Y, Tjong KK, Chan J, Tamaoki T (1991) A position-dependent silencer plays a major role in repressing alpha-fetoprotein expression in human hepatoma. Mol Cell Biol 11: 5885-5893. doi: 10.1128/mcb.11.12.5885

(78) National Cancer Institute (12.04.2019) Cancer stat facts: NHL - diffuse large B-cell lymphoma (DLBCL), https://seer.cancer.gov/statfacts/html/dlbcl.html, downloaded 10.03.2020

(79) National Center for Biotechnology Information (08.03.2020) RPL15 ribosomal protein L15 [homo sapiens (human)], https://www.ncbi.nlm.nih.gov/gene/6138, downloaded 12.03.2020

(80) National Center for Biotechnology Information (09.07.2019) Reference SNP (rs) report, in: National Center for Biotechnology Information, https://www.ncbi.nlm.nih.gov/snp/rs3084709#frequency_tab, downloaded 03.04.2020

(81) New England BioLabs (n.d.) Q5® site-directed mutagenesis kit, https://www.neb.com/products/e0554-q5-site-directed-mutagenesis-kit#Product%20Information, downloaded 12.03.2020

(82) Ngo VN, Young RM, Schmitz R, Jhavar S, Xiao W, Lim K, Kohlhammer H, Xu W, Yang Y, Zhao H, Shaffer AL, Romesser P, Wright G, Powell J, Rosenwald A, Muller-Hermelink H, Ott G, Gascoyne RD, Connors JM, Rimsza LM, et al. (2010) Oncogenically active MYD88 mutations in human lymphoma. Nature 470: 115-119. doi: 10.1038/nature09671

(83) Nishimoto KP, Newkirk D, Hou S, Fruehauf J, Nelson EL (2007) Fluorescence activated cell sorting (FACS) using RNAlater to minimize RNA degradation and perturbation of mRNA expression from cells involved in initial host microbe interactions. J Microbiol Methods 70: 205-208. doi: S0167-7012(07)00126-1

(84) Nowakowski GS, Czuczman MS (2015) ABC, GCB, and double-hit diffuse large B-cell lymphoma: Does subtype make a difference in therapy selection? Am Soc Clin Oncol Educ Book: e449-57. doi: 10.14694/EdBook_AM.2015.35.e449

(85) Oeckinghaus A, Postler TS, Rao P, Schmitt H, Schmitt V, Grinberg-Bleyer Y, Kuhn LI, Gruber CW, Lienhard GE, Ghosh S (2014) kappaB-ras proteins regulate both NF-kappaB-dependent inflammation and ral-dependent proliferation. Cell Rep 8: 1793-1807. doi: S2211-1247(14)00678-0

(86) Oeckinghaus A, Ghosh S (2009) The NF-kappaB family of transcription factors and its regulation. Cold Spring Harb Perspect Biol 1: a000034. doi: 10.1101/cshperspect.a000034

(87) Oka T, Yoshino T, Hayashi K, Ohara N, Nakanishi T, Yamaai Y, Hiraki A, Sogawa CA, Kondo E, Teramoto N, Takahashi K, Tsuchiyama J, Akagi T (2001) Reduction of hematopoietic cell-specific tyrosine phosphatase SHP-1 gene expression in natural killer cell lymphoma and various types

of lymphomas/leukemias: Combination analysis with cDNA expression array and tissue microarray. Am J Clin Pathol 159: 1495-1505. doi: 10.1016/S0002-9440(10)62535-7

(88) Packham G (2008) The role of NF-kappaB in lymphoid malignancies. Br J Haematol 143: 3-15. doi: 10.1111/j.1365-2141.2008.07284.x

(89) Park SI, Park S, Lee J, Kim HE, Park SJ, Sohn J, Park YG (2016) Inhibition of cyclic AMP response element-directed transcription by decoy oligonucleotides enhances tumor-specific radiosensitivity. Biochem Biophys Res Commun 469: 363-369. doi: 10.1016/j.bbrc.2015.11.122

(90) Pasqualucci L, Trifonov V, Fabbri G, Ma J, Rossi D, Chiarenza A, Wells VA, Grunn A, Messina M, Elliot O, Chan J, Bhagat G, Chadburn A, Gaidano G, Mullighan CG, Rabadan R, Dalla-Favera R (2011) Analysis of the coding genome of diffuse large B-cell lymphoma. Nat Genet 43: 830-837. doi: 10.1038/ng.892

(91) Pekowska A, Benoukraf T, Zacarias-Cabeza J, Belhocine M, Koch F, Holota H, Imbert J, Andrau JC, Ferrier P, Spicuglia S (2011) H3K4 tri-methylation provides an epigenetic signature of active enhancers. Embo J 30: 4198-4210. doi: 10.1038/emboj.2011.295

(92) Pomerantz MM, Ahmadiyeh N, Jia L, Herman P, Verzi MP, Doddapaneni H, Beckwith CA, Chan JA, Hills A, Davis M, Yao K, Kehoe SM, Lenz HJ, Haiman CA, Yan C, Henderson BE, Frenkel B, Barretina J, Bass A, Tabernero J, et al. (2009) The 8q24 cancer risk variant rs6983267 shows long-range interaction with MYC in colorectal cancer. Nat Genet 41: 882-884. doi: 10.1038/ng.403

(93) Pridans C, Holmes ML, Polli M, Wettenhall JM, Dakic A, Corcoran LM, Smyth GK, Nutt SL (2008) Identification of Pax5 target genes in early B cell differentiation. J Immunol 180: 1719-1728. doi: 10.4049/jimmunol.180.3.1719

(94) Promega Corporation (03.2015) CellTiter-glo® luminescent cell viability assay technical bulletin, https://www.promega.de/-/media/files/resources/protocols/technical-bulletins/0/celltiter-glo-luminescent-cell-viability-assay-protocol.pdf?la=en, downloaded 24.03.2020

(95) Rada-Iglesias A, Bajpai R, Swigut T, Brugmann SA, Flynn RA, Wysocka J (2011) A unique chromatin signature uncovers early developmental enhancers in humans. Nature 470: 279-283. doi: 10.1038/nature09692

(96) Ran FA, Hsu PD, Wright J, Agarwala V, Scott DA, Zhang F (2013) Genome engineering using the CRISPR-Cas9 system. Nat Protoc 8: 2281-2308. doi: 10.1038/nprot.2013.143

(97) Rawlings DJ, Sommer K, Moreno-García ME (2006) The CARMA1 signalosome links the signalling machinery of adaptive and innate immunity in lymphocytes. Nat Rev Immunol 6: 799-812. doi: 10.1038/nri1944

(98) Richardson GM, Lannigan J, Macara IG (2015) Does FACS perturb gene expression? Cytometry A 87: 166-175. doi: 10.1002/cyto.a.22608

(99) Robinson JT, Thorvaldsdóttir H, Winckler W, Guttman M, Lander ES, Getz G, Mesirov JP (2011) Integrative genomics viewer. Nat Biotechnol 29: 24-26. doi: 10.1038/nbt.1754

(100) Rosenwald A, Wright G, Chan WC, Connors JM, Campo E, Fisher RI, Gascoyne RD, Muller-Hermelink HK, Smeland EB, Giltnane JM, Hurt EM, Zhao H, Averett L, Yang L, Wilson WH, Jaffe ES,

Simon R, Klausner RD, Powell J, Duffey PL, et al. (2002) The use of molecular profiling to predict survival after chemotherapy for diffuse large-B-cell lymphoma. N Engl J Med 346: 1937-1947. doi: 10.1056/NEJMoa012914

(101) Ryu AH, Eckalbar WL, Kreimer A, Yosef N, Ahituv N (2017) Use antibiotics in cell culture with caution: Genome-wide identification of antibiotic-induced changes in gene expression and regulation. Sci Rep 7: 7533. doi: 10.1038/s41598-017-07757-w

(102) Schmidt C, Schneller F, Fischer N, Sotlar K, Will T, Zettl F, et al. (2015) Diffus-großzelliges B-Zell-Lymphom. In: Dreyling M (editor). Maligne Lymphome - Empfehlungen zur Diagnostik, Therapie und Nachsorge., ed. 10, Zuckschwerdt, München, pp. 143-155

(103) Seeburg PH, Colby WW, Capon DJ, Goeddel DV, Levinson AD (1984) Biological properties of human c-ha-ras1 genes mutated at codon 12. Nature 312: 71-75. doi: 10.1038/312071a0

(104) Shlyueva D, Stampfel G, Stark A (2014) Transcriptional enhancers: From properties to genome-wide predictions. Nat Rev Genet 15: 272-286. doi: 10.1038/nrg3682

(105) Shuai K, Liu B (2003) Regulation of JAK-STAT signalling in the immune system. Nat Rev Immunol 3: 900-911. doi: 10.1038/nri1226

(106) Simonis M, Kooren J, de Laat W (2007) An evaluation of 3C-based methods to capture DNA interactions. Nat Methods 4: 895-901. doi: 10.1038/nmeth1114

(107) Spektrum Akademischer Verlag H (1999) Lexikon der Biologie: SNP, https://www.spektrum.de/lexikon/biologie/snp/61937, downloaded 15.04.2020

(108) Sultan S, Baloch N, Ahmed ZA, Irfan SM, Parveen S (2018) Pattern of bone marrow involvement in non hodgkin's lymphoma classified according to WHO classification: Report of a developing country pakistan. J Lab Physicians 10: 17-20. doi: 10.4103/JLP.JLP_9_17

(109) Sun S (2011) Non-canonical NF-κB signaling pathway. Cell Res 21: 71-85. doi: 10.1038/cr.2010.177

(110) Sun S (2017) The non-canonical NF-κB pathway in immunity and inflammation. Nat Rev Immunol 17: 545-558. doi: 10.1038/nri.2017.52

(111) Sur I, Taipale J (2016) The role of enhancers in cancer. Nat Rev Cancer 16: 483-493. doi: 10.1038/nrc.2016.62

(112) Swerdlow SH, Campo E, Harris NL, Jaffe ES, Pileri SA, Stein H, et al. (2017) Diffuse large B-cell lymphoma, NOS. In: WHO (editor). WHO Classification of Tumours of Haematopoietic and Lymphoid Tissues., ed. 4, International Agency for Research on Cancer, Lyon, France, pp. 291-297

(113) Tago K, Funakoshi-Tago M, Sakinawa M, Mizuno N, Itoh H (2010) KappaB-ras is a nuclear-cytoplasmic small GTPase that inhibits NF-kappaB activation through the suppression of transcriptional activation of p65/RelA. J Biol Chem 285: 30622-30633. doi: 10.1074/jbc.M110.117028

(114) ThermoFisher Scientific (03.2009) 260/280 and 260/230 ratios, http://hpc.ilri.cgiar.org/beca/training/IMBB_2015/lectures/NanoDrop.pdf, downloaded 12.03.2020

(115) Thieblemont C, Tilly H, Gomes da Silva M, Casasnovas RO, Fruchart C, Morschhauser F, Haioun C, Lazarovici J, Grosicka A, Perrot A, Trotman J, Sebban C, Caballero D, Greil R, van Eygen K, Cohen AM, Gonzalez H, Bouabdallah R, Oberic L, Corront B, et al. (2017) Lenalidomide maintenance compared with placebo in responding elderly patients with diffuse large B-cell lymphoma treated with first-line rituximab plus cyclophosphamide, doxorubicin, vincristine, and prednisone. J Clin Oncol 35: 2473-2481. doi: 10.1200/JCO.2017.72.6984

(116) Thompson JE, Phillips RJ, Erdjument-Bromage H, Tempst P, Ghosh S (1995) IκB-β regulates the persistent response in a biphasic activation of NF-κB. Cell 80: 573-582. doi: 10.1016/0092-8674(95)90511-1

(117) Tilly H, Gomes da Silva M, Vitolo U, Jack A, Meignan M, Lopez-Guillermo A, Walewski J, André M, Johnson PW, Pfreundschuh M, Ladetto M (2015) Diffuse large B-cell lymphoma (DLBCL): ESMO clinical practice guidelines for diagnosis, treatment and follow-up. Ann Oncol 26: v116-v125. doi: 10.1093/annonc/mdv304

(118) Tolhuis B, Palstra RJ, Splinter E, Grosveld F, de Laat W (2002) Looping and interaction between hypersensitive sites in the active beta-globin locus. Mol Cell 10: 1453-1465. doi: S1097-2765(02)00781-5

(119) Turvey SE, Durandy A, Fischer A, Fung SY, Geha RS, Gewies A, Giese T, Greil J, Keller B, McKinnon ML, Neven B, Rozmus J, Ruland J, Snow AL, Stepensky P, Warnatz K (2014) The CARD11-BCL10-MALT1 (CBM) signalosome complex: Stepping into the limelight of human primary immunodeficiency. J Allergy Clin Immunol 134: 276-284. doi: 10.1016/j.jaci.2014.06.015

(120) van den Hoff MJ, Moorman AF, Lamers WH (1992) Electroporation in 'intracellular' buffer increases cell survival. Nucleic Acids Res 20: 2902. doi: 10.1093/nar/20.11.2902

(121) Wang H, Zhao L, Li K, Ling R, Li X, Wang L (2006) Overexpression of ribosomal protein L15 is associated with cell proliferation in gastric cancer. BMC Cancer 6: 91. doi: 10.1186/1471-2407-6-91

(122) Weinhold N, Jacobsen A, Schultz N, Sander C, Lee W (2014) Genome-wide analysis of noncoding regulatory mutations in cancer. Nat Genet 46: 1160-1165. doi: 10.1038/ng.3101

(123) Yong K, Cavet J, Johnson P, Morgan G, Williams C, Nakashima D, Akinaga S, Oakervee H, Cavenagh J (2015) Phase I study of KW-2478, a novel Hsp90 inhibitor, in patients with B-cell malignancies. Br J Cancer 114: 7-13. doi: 10.1038/bjc.2015.422

(124) Younes A, Sehn LH, Johnson P, Zinzani PL, Hong X, Zhu J, Patti C, Belada D, Samoilova O, Suh C, Leppa S, Rai S, Turgut M, Jurczak W, Cheung MC, Gurion R, Yeh SP, Lopez-Hernandez A, Duhrsen U, Thieblemont C, et al. (2019) Randomized phase III trial of ibrutinib and rituximab plus cyclophosphamide, doxorubicin, vincristine, and prednisone in non-germinal center B-cell diffuse large B-cell lymphoma. J Clin Oncol 37: 1285-1295. doi: 10.1200/JCO.18.02403

(125) Zelenetz AD, Salles G, Mason KD, Casulo C, Le Gouill S, Sehn LH, Tilly H, Cartron G, Chamuleau MED, Goy A, Tam CS, Lugtenburg PJ, Petrich AM, Sinha A, Samineni D, Herter S, Ingalla E, Szafer-Glusman E, Klein C, Sampath D, et al. (2019) Venetoclax plus R- or G-CHOP in non-hodgkin lymphoma: Results from the CAVALLI phase 1b trial. Blood 133: 1964-1976. doi: 10.1182/blood-2018-11-880526

6 Acknowledgements

I am grateful to Prof. Dr. Frank Rosenbauer for giving me the opportunity to emerge into the challenging field of science and for his supervision during my time at the laboratory.

Furthermore I would like to thank Dr. Andrea Oeckinghaus for her constantly open door, her advice and supervision of my project and for always succeeding at keeping my motivation up.

Many thanks go to the whole AG Rosenbauer and AG Oeckinghaus and everyone else at the institute for their continuous support and cooperativeness, teaching of unknown methods and patience for my many questions. I especially want to thank Alexander Tönges for helping me to get familiar with laboratory work as well as his preliminary work and for providing computational analyses for the project.

I would like to thank my second supervisor Prof. Dr. Wolfgang Hartmann for his time and support and Prof. Dr. Georg Lenz for providing the DLBCL cell lines for our project.

I acknowledge the ENCODE Consortium and the ENCODE production laboratories for generating the particular datasets**.**

I want to thank the „Medizinerkolleg Münster“ for their financial support and instructional seminars.

I thank my friends and my boyfriend for their endless support and creativity in keeping my mood up and Trevor Scott for proof-reading my thesis.

Last but not least a huge thanks to my parents for the emotional support and coddling me up after difficult times.

8 Appendix

8.1 Figures

8.2 Tables